

Founded 1925
Incorporated
by Royal Charter 1961

*To promote the advancement
of radio, electronics and kindred
subjects by the exchange of
information in these branches
of engineering*

The Radio and Electronic Engineer

The Journal of the Institution of Electronic and Radio Engineers

JAMES CLERK MAXWELL 1831-1879

The role of James Clerk Maxwell as the father of radio science is well known and his work has been honoured by this Institution with the establishment in 1951 of the Clerk Maxwell Memorial Lectures. Since 1945 a senior premium awarded by the Institution has also borne his name.

Maxwell was born on 13th June 1831 in Edinburgh and this year therefore marks the 150th anniversary of his birth. His early life was spent at Glenlair, Kirkcudbrightshire, and it was there he was buried after his death in Cambridge on 5th November 1879 at the age of forty-eight years. He entered Edinburgh University in 1847 and after three years went on to Cambridge, becoming a student at Trinity College and passing the mathematical tripos with distinction in 1854.

For the next two years Maxwell was at Cambridge, lecturing in hydrostatics and optics in which he carried out many experiments, and 'working away at electricity'. In 1856 he was appointed to the Chair of Natural Philosophy at Marischal College, Aberdeen where he remained until 1868 when he was appointed to the Chair of Natural Philosophy at King's College, London. During the next five years he worked mainly on colour but also laid the foundations for his later, great work, the 'Treatise on Electricity and Magnetism'. From 1865 he was in retirement at Glenlair and apart from occasional special lectures and acting as examiner for the mathematical tripos at Cambridge, his main energies were devoted to his 'Treatise' which was published in 1873.

Physics at Cambridge was on the threshold of great changes at this time, and in 1870 the Duke of Devonshire, then Chancellor of the University, offered to build and furnish a Physical Laboratory. In 1871 Maxwell was appointed to the new Chair of Experimental Physics and designed and supervised the erection of the new laboratory which was formally opened in June 1874.

For the next four years, Maxwell's most important and continuing work was superintending experimental work in the Cavendish Laboratory. His last public lecture, the Rede Lecture at Cambridge in 1878, was entitled 'On the Telephone', the invention of which he considered to be a 'material symbol of the widely separated departments of human knowledge', and he spoke of the great benefits which could result from the cross-fertilization of the sciences. In a fine tribute on the occasion of the centenary of his birth, Max Planck said of him 'It was his task to build and complete the classical theory, and in so doing he achieved greatness unequalled. His name stands magnificent on the portal of classical physics, and we can say this of him: by his birth James Clerk Maxwell belongs to Edinburgh, by his personality he belongs to Cambridge, by his work he belongs to the whole world.'

F.W.S.

The 10th Clerk Maxwell Memorial Lecture, entitled 'The Complete Physicist', was given at the recent Institution Conference in Leeds by Professor R.V. Jones, C.B., F.R.S., who held the Chair of Natural Philosophy at the University of Aberdeen from 1946 until his retirement this year. The lecture, which assesses Maxwell's many contributions to science, will be published in the November/December 1981 issue of *The Radio and Electronic Engineer*.

Letters to the Editor

From: **B. Priestley**, B.Sc., C.Eng., M.I.E.R.E.
A. H. Harrold (Graduate)
G. E. Smythe (Associate)
T. Lomas, E.R.D., Dip.E.E., C.Eng., M.I.E.E.,
M.I.E.R.E.

Oscillator Design

I was gratified to note from the May issue of *The Radio and Electronic Engineer* (p. 203) that others share my concern over the state of oscillator design, and I would like to add the following comments.

First to Mr Mitson: I did not refer solely to oscillators produced for biological telemetry although I did include some of the horrible examples sold to unsuspecting biologists by so-called engineers. If this makes a biologist feel he can do no worse himself, it underlines the need for liaison indicated by Mr Mitson (plus a gentle pointer on the mis-use of the term engineer?).

Secondly to Messrs Kentley and Rogers: Although the quartz crystal does complicate oscillator design, the basic principles are exactly the same for any sinusoidal oscillator and it is these which are glossed over. If additional guidance is available in industry it can only be used over this foundation. (Personally I have found the attitude of crystal manufacturers to vary widely from 'We consider this information will not help you so we won't tell you', to the very friendly and helpful.)

However, since first writing I have discovered it is now possible to qualify in electronics without any knowledge of electromagnetic field theory! (IERE Education Committee please note!) In such circumstances we seem to be fighting a losing battle suggesting that engineers should learn basic principles rather than be programmed to fill a slot.

B. PRIESTLEY

43 Raymond Road,
Langley, Slough,
Berkshire SL3 8LN
15th May 1981

[The Education and Training Committee is well aware of the present trend towards modifying qualifications and has given it much thought on several recent occasions. Basically the problem is that a three-year degree course is not long enough in which to cover every subject that might be considered essential. But the Committee is not always happy about what has been sacrificed as a consequence in some courses.—EDITOR.]

Multi-disciplinary Engineering in the Process Industries

What a pleasant breath of fresh air greeted me as I opened my journal in June! There on page 255 was an article from kindred spirits who have at last recognized the needs of the process industry. I refer to the brief paper 'Multi-disciplinary engineering in the process industries'.

Having started my working life in the electronics industry, gaining HNC and endorsements on a day-release basis, I followed the process instrumentation route into the process industry. I have over the years worked for both contractors and end-users and now I have my own process control engineering design company.

The need for multi-discipline knowledge is paramount in this field of engineering, much of which can only be gained by bitter experience. The engineers who work in this sector, and I am proud to be amongst them, have to satisfy very rigorous requirements before being able to follow this sometimes frustrating but always satisfying way of life. These are briefly:

1. A sound technical education—not necessarily a degree but unfortunately this now seems to be the minimum.
2. A sound practical approach to engineering, for what you design has to work and withstand all manner of environmental abuse.
3. An ability to communicate with a full cross-section of people from directors and managers to skilled and unskilled artisans—without this ability you will not get off base 1.
4. A willingness, albeit sometimes reluctantly, to go out onto site in all weathers at all time of the day or night—don't forget this is what engineering is all about.
5. Above all other criteria, the ability to understand and appreciate the requirements and difficulties of engineers of all disciplines, and a willingness to learn from them as they learn from you—there's no place for prima donnas on site, teamwork is the key.

Much of what I have listed above is good sound common sense and it is this area of our engineers training that needs a lot of attention. I, on reflection, consider myself fortunate that I studied on a part-time basis as this permitted me to work alongside people at shop-floor level during the most informative years of my apprenticeship. I feel many graduates today have missed out on this experience and whilst they may be the managers to tomorrow they may never gain the 'common touch'—a bridge which must be strong for our nation's success in the future.

So it's back to our academics to appreciate that not all engineering is carried out in laboratories or factories with clearly defined and narrow bands of development, and it's back to our Institutions to recognize the vast number of sound practical engineers, who may not be academics, but without their foresight and abilities there would not be the need for research and development as we know it today.

A. H. HARROLD

'Corner House'
Forest Edge Road,
Ringwood,
Hampshire BH24 3DF
10th June 1981

The 'parting shot' in the letter from Mr. A. C. Evans (June 1981, p. 258) caused me to reflect that his remark about the paucity of correspondence in the journals of the learned Institutions is not true of other publications such as *Wireless World*.

Is it perhaps the case that the majority of engineers can spare insufficient time from their immediate problems fully to evaluate such erudite contributions (in the issue cited all the papers come from Research Establishments or Universities) to the extent necessary to comment on them, or even, dare one suggest, to understand the more specialized papers? That they are valuable contributions to the state of the art no one doubts but they seem not to inflame the passions quite as much as suggestions that a pair of PX 4's in class A push-pull may out perform any of these modern transistor output stages, or that Essen may supplant Einstein.

Correspondence seems to thrive on controversy and this often throws up interesting points that otherwise might not come to light. Perhaps then you could start by inviting suggestions for technical topics which are open to argument,

such as, 'A study of the optimum frequency and mode for an open-channel (c.b.) service in the European Common Market'.

G. E. SMYTHE

9 Camborne Road,
Sutton,
Surrey SM2 6RJ
11th June 1981

I am writing to say how very much I sympathize with the views expressed in the article 'Multi-disciplinary engineering in the process industries' in the June issue of the Journal. There is a clear and imperative need in any technology based business or industry (I would suggest not only in the process industries) for people with a thorough grounding in technology plus an appreciation of the many other important facets of business

e.g. marketing, sales, finance, delivery, quality, etc., if the business is to survive and thrive in today's highly competitive world. This is not to say that there will not always be a need for specialists but rather that the very survival of business depends upon those who can take a comprehensive view of business opportunities and threats. I would, indeed, question whether an engineer without an understanding of business issues other than technology can properly be regarded as a professional engineer. In drawing attention to the need for engineers to be trained in other than a single discipline the article has done a good service.

T. LOMAS

21 Clarence Road
St. Albans
Herts AL1 4NP
24th June 1981

Announcements

Back copies of the Journal

Because of exceptional calls for some of this year's issues of *The Radio and Electronic Engineer*, the Institution's stocks have become depleted and difficulty is anticipated in fulfilling future new subscriptions for 1981. Any member who has no further need for his or her copies is therefore invited to send them to the Publications Department at 99 Gower Street. The issues required are:

February, March, April, June 1981

and any of these will be most welcome.

Stocks of certain earlier issues are also exhausted notably the following:

1977 January/February, March, April, August, September

1979 February

1980 January/February, March, July, August

These are needed to meet orders from libraries for complete back sets for binding. The Institution will gladly refund postage.

Subscriptions for 1982

The subscription rates to non-members and libraries for *The Radio and Electronic Engineer* for 1982 will be as follows:

	Annual Subscription	Single issue
UK and Ireland	£38.00	£3.50
Overseas	£43.50	£4.00
North and South America	\$92.00	\$8.00

Correction

In the paper 'Integrated optics, a tutorial review', published in the July/August 1981 issue of *The Radio and Electronic Engineer*, the following correction should be made.

Page 404, Sect 5.4, The final sentence in the first paragraph *should read*: This is the principle governing positive photoresists but, by suitable choice of polymer-solvent systems, a negative resist can be used in which the incident light beam can be employed to indicate polymerization of the deposited monomer.

Standard Frequency and Time Service

(Communication from the National Physical Laboratory)

Relative Phase Readings in microseconds

NPL—Station
(Readings at 1500 UT)

June 1981	MSF 60 kHz	GBR 16 kHz	Droitwich 200 kHz*
1	1.4	18.1	61.7
2	1.4	18.5	61.9
3	1.4	17.1	62.1
4	1.5	18.6	62.3
5	1.4	18.1	62.5
6	1.6	17.8	62.8
7	1.6	18.1	63.0
8	1.6	17.8	63.3
9	1.6	18.3	63.6
10	1.6	17.7	63.8
11	1.6	16.4	64.1
12	1.4	15.8	64.3
13	1.2	16.1	64.5
14	1.2	16.1	64.7
15	1.3	14.1	64.9
16	1.2	17.1	65.1
17	1.2	16.4	65.3
18	1.2	16.4	65.6
19	1.2	16.3	65.8
20	1.2	16.3	66.0
21	1.2	16.3	66.3
22	0.9	16.7	66.5
23	1.1	16.7	66.6
24	1.1	16.8	66.6
25	1.1	16.3	66.9
26	1.1	16.9	67.1
27	1.1	16.3	67.3
28	1.1	16.3	67.6
29	0.9	16.4	67.7
30	0.9	16.2	68.0

Notes: (a) Relative to UTC scale ($UTC_{NPL} - Station = +10$ at 1500 UT, 1st January 1977).

(b) The convention followed is that a decrease in phase reading represents an increase in frequency.

(c) 1 μ s represents a frequency change of 1 part in 10^{11} per day.

* It may be assumed that the satellite stations on 200 kHz at Westerglen and Burghhead will follow the day to day changes in these phase values.

Function Generator Review

During recent months, three leading companies have introduced new function generators. Although each has a different declared purpose, brief notes of their features are interesting as giving an insight into current practice.

A new multi-purpose waveform generator, the 2123 has been launched by **Marconi Instruments**. This is a portable and highly versatile instrument, suitable for use in educational establishments, laboratories, production and maintenance areas. It costs £215 (excl. V.A.T.)

The 2123 produces sine, square, and triangular waves at frequencies between 0.003 Hz and 200 kHz, with ramp generation between 0.003 Hz and 20 kHz. Source impedance is 60 Ω on all functions, with variable output to a maximum of 10 V p-p, calibrated into a 600 Ω load. Two auxiliary outputs enable a triangular wave to trigger an oscilloscope sweep, and TTL compatible square wave to supply up to 20 standard loads.



Marconi Instruments multi-purpose waveform generator 2123

To simplify measurement of frequency response in amplifiers and filters, the 2123 is fitted with an internal logarithmic sweep, down to one thousandth of the maximum frequency displayed on the dial.

The frequency can be set by seven range pushbuttons on the front panel, in conjunction with a multi-turn potentiometer dial with three-digit read-out. Alternatively, the frequency may be controlled by application of a direct voltage (v.c.f.) to rear panel sockets; this is particularly useful for users of control or automatic systems.

A high level of cost-effective performance is claimed for a new log sweep function generator announced by **Racal-Dana Instruments**. The Exact 500SL function generator, for which Racal-Dana Instruments is sole UK distributor, has a



Exact 500SL function generator

frequency range of 0.005–5 MHz, with many advanced high-performance features, and is competitively priced at less than £250.

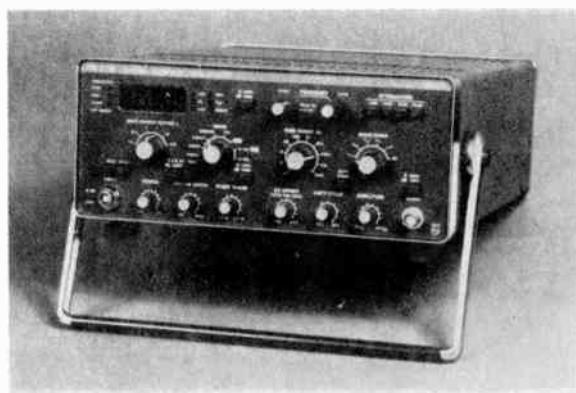
The generator provides a haversine mode, low distortion sine waves (0.5%), highly linear triangles—greater than 99%—and fast rise and fall square waves of less than 40 ns. Output amplitudes are 20 V peak-to-peak open circuit—10 V peak-to-peak into 50 Ω —and may be attenuated up to 40 dB using the variable amplitude control and the low output socket. A d.c. offset control allows adjustment of waveform offset up to +10 V. The d.c. offset control has a detented off position when no offset is desired.

Frequency may be varied manually with the multiplier control, externally via a v.c.f. input, or internally with a built-in sweep. A pushbutton selects either linear or logarithmic frequency variation.

A lockout mode is set on release of the button. Sine and triangle signals will lock at zero volts, and the square and haversine signals will lock at their negative peaks. An external or manual trigger will produce one cycle of the selected waveform which stops at its normal lockout level. When the gate pushbutton is depressed, the external or manual signal will cause the generator to run until the signal goes low or the manual pushbutton is released.

In addition to high, low, and v.c.f. inputs, the 500SL features a TTL compatible sync output, a $V:f$ (voltage proportional to frequency) output, and a sweep output. It is housed in a rugged aluminium box providing good e.m. screening and weighs 2.27 kg (5lb).

A new top-level function generator has been added to **Philips'** wide range of low frequency equipment, supplied in the UK by Pye Unicam of Cambridge. It is the PM 5134, a versatile and sophisticated research-level function generator which covers a wide 20 MHz bandwidth and provides sine, square and triangular waveforms as well as positive and negative going pulses and d.c.



Philips research-level function generator—PM5134

Normal or crystal-controlled operation is possible—the latter including a frequency-lock facility and giving accuracies of ± 5 parts in 10^6 . Single and burst modes are also provided. Versatile sweep facilities allow internal or external single or continuous sweep with independent controls for start and stop frequencies.

Other features of the generator include amplitude and frequency modulation, internally or externally, with a.m. depth adjustable from 0 to 100% and f.m. from 0 to 10%. The instrument produces a high 20 V peak-to-peak output (10 V peak-to-peak pulses) with stepped and variable attenuation. Output impedance is pushbutton selectable to 50 or 600 Ω .

A three-and-a-half digit l.e.d. read-out displays output frequency and open-circuit output voltage. There are also separate l.e.d.s indicating frequency and voltage ranges, sweep modes and setting errors. The 1 MHz to 20 MHz frequency range is covered in ten linear sub-ranges with separate coarse and fine controls. Attenuation up to 60 dB is incorporated in calibrated steps of 3, 6, 10 and 20 dB with variable attenuation up to 20 dB. D.c. offset is available from -5 to +5 V and the duty cycle can be varied from 10 to 90%.

Very stable and accurate output signals can be obtained using the crystal-controlled mode. A crystal lock position is included for repetitive and other high accuracy work. This facility is also available for a.m. operation.

Sweep mode operation can be started either manually or electronically by remote control. The sweep period is continuously adjustable from 5 ms to 100 s and there are both hold and reset facilities. As with single-cycle and burst signals, the start phase is fully adjustable from -90° to $+90^\circ$.

The PM 5134 is designed for a wide range of applications in high level education and industrial research and development. It is a robust instrument, its strong metal case giving full electrical screening and good mechanical protection. It costs £1100.

A Digital Television Studio Standard

The Technical Committee of the European Broadcasting Union (EBU) has agreed to propose a set of technical parameters as a digital television studio standard, in the hope that these will be adopted throughout the world. The decision is seen as a watershed in broadcasting technology.

The 1960s left the world with a diversity of colour systems (PAL, SECAM, NTSC) and these will be used for broadcasting to the public for many years to come. Existing receivers will, therefore, not become obsolete in the foreseeable future.

However, in the field of television programme production, digital technology offers the potential for considerable improvements in facilities, picture quality, and many other advantages. An agreed worldwide digital standard in this area would mean less expensive equipment, because of the economies of scale, and benefit international programme exchange. It would have important financial advantages for users and manufacturers, lead to improvements in the technical quality of programmes shown in a country with a different television system from the originating country, and assist the international exchange of technical information on television production.

In order to consider not only the requirements for the 625-line television standards used in Europe, but also those of the regions where a 525-line standard is used, the EBU has coordinated its studies with the Society of Motion Picture and Television Engineers in North America.

After considerable discussion, the EBU proposes that the digital standard should not be based on the PAL, SECAM or NTSC systems, but instead on a principle technically known as 'component coding' with a particular set of parameters that should apply both in countries using 525-line and 625-line television standards.

The EBU is proposing a parameter set known as

'13.5:6.75:6.75'. By popular convention, this describes a component-coded digital television system with a luminance signal sampled at a frequency of 13.5 MHz, and the two colour-difference signals sampled at a frequency of 6.75 MHz. It is hoped that these parameters will be applicable to both 525-line and 625-line television systems, and hence that the number of samples per television line will then be very similar. Because of the different field rates, the number of samples per picture, however, will be different.

The EBU proposal will be submitted to the forthcoming Final Meetings of the CCIR Study Groups in September 1981 in Geneva, Switzerland, in the hope that it will obtain worldwide support.

The need for a worldwide standard in this field was the subject of a recommendation by all unions at the 3rd World Conference of Broadcasting Unions held in Tokyo in 1980 and already there are positive indications of support for the EBU proposal from several of the other unions. In particular, the OTI (Organizaçion de la Television Iberoamericana) has already conveyed its support to the EBU for the proposal. This is particularly noteworthy because both 525-line and 625-line countries exist in the OTI area. Encouraging reactions have also come from unions in North America, NANBA (North American National Broadcasters Association) and in Africa, URTNA (Union of National Radio and Television Organizations of Africa).

The EBU Technical Committee, being the consultative engineering body of the EBU, has submitted its views to the Union's Administrative Council, and the proposal was expected to become the subject of an official EBU policy statement after the meeting of the EBU Administrative Council, scheduled for 22nd-25th May 1981.

Members' Appointments

CORPORATE MEMBERS

Cdr D. G. Edwards, RN (Ret) (Fellow 1964, Member 1950) who recently retired as Senior Reliability Engineer with the Ministry of Defence, Navy Department, has taken up consultancy work in the reliability and quality assurance field.

E. R. Friedlaender (Fellow 1944) is now Deputy Mayor of the London Borough of Brent where he has been a councillor since 1971. After coming to the UK in 1936 he was a specialist on design and manufacture of magnetic dust core components while before his retirement in 1973 he was initially a patent consultant and later a freelance industrial journalist working with European technical magazines.

Vice Admiral Sir Philip Watson, K.B.E., M.V.O. (Fellow 1967) has recently been appointed Chairman of Marconi Radar Systems. For the past three years Sir Philip has been the Naval and Defence Affairs Adviser to GEC Marconi and a director of the Marconi International Marine Company.

Cdr A. C. Cowin, M.Sc., RN (Ret) (Member 1966, Graduate 1961) has taken up a Civil Service appointment as an Electrical Engineer with the Defence Intelligence Staff of the Ministry of Defence. Cdr Cowin has served on the Membership Committee of the Institution since 1980.

D. R. Hill, M.Phil. (Member 1980) has joined H. R. Smith (Microwaves) of Eynsham, Oxfordshire. After setting up new premises for the Company at Kingsland, Herefordshire, he will be concerned with research, design and development of microwave components and subsystems,

notably stripline and microstrip antennas. He was previously Principal Antenna Engineer with Southern Microwave Laboratories, Hayling Island, Hants.

M. Hounsell (Member 1971) has been appointed Manager, Programme Services and Engineering, South, with BBC Television. He joined the BBC in 1963 and worked in Television Networks at the Television Centre in London. Since 1975 Mr Hounsell has been Senior Television Engineer at Plymouth.

J. W. B. McIlwraith (Member 1956, Graduate 1952) who was Chief Telecommunications Officer, Airports and Airways Aids, with the National Air Traffic Services at Liverpool, is now Director of Telecommunications (Projects) based in London.

Lt Cdr P. Nightingale, RN (Member 1972, Graduate 1967) has just taken up a two-year appointment in the Bahamas as Training Design Officer with the Bahamian Defence Force.

B. W. Potter (Member 1969, Graduate 1964) has been appointed Manager, Programme Services and Engineering, East with the BBC. A member of the Corporation since 1960, he has held appointments with the Communications Department in various regions, the last of these being Communications Manager at Manchester since 1979.*

G. Salter (Member 1964) who has been with the BBC since 1943, latterly as Head of Programme Services and Engineering, Wales, has left the Corporation and taken up a post as Studio Technical Systems Advisor in the Network Operations and Maintenance

Department of the Independent Broadcasting Authority at Crawley Court.*

W. A. M. Smith (Member 1969) has retired from Cable and Wireless after twenty seven years of service with the company. Mr Smith has spent the last fifteen years in Hong Kong, his last appointment being Deputy General Manager and Divisional Manager, Telecommunications Service and Marketing.

W. St John White (Member 1970, Associate 1947) who joined the Decca Navigator Company in 1946 as a Development Engineer following wartime service with the Telecommunication Research Establishment, has been appointed to the board of Racal-Decca. Since 1969 he has been a director of Decca Navigator Company responsible for marketing of avionic systems.

S. R. Tumoe (Member 1973) has been appointed Director of Telecommunications in the Sierra Leone Posts & Telecommunications Department. He was formerly senior engineer and head of the Network Planning Division.

P. R. Thorogood (Member 1971) who has been with Cable and Wireless at Hong Kong since 1980, has been transferred to the post of Divisional Manager, Engineering of Bahrain Telecommunications Company.

NON-CORPORATE MEMBERS

Sir Kenneth Corfield F. Eng., F.I. Mech. E. (Companion 1976), who is Chairman and Managing Director of Standard Telephones and Cables, has been awarded an Honorary Doctorate of Science by the City University. Sir Kenneth's appointment as Chairman-designate of the new Engineering Council was announced on July 30th.

* *Editorial Note* Incorrect details of the appointments held by these Members were printed in the June issue of the Journal. Apologies are extended to the Members concerned and to readers for any embarrassment or confusion this caused.

Obituary

The Institution has learned with regret of the deaths of the following members.

Derek Vere Staynor, M.B.E. (Member 1959) of Boreham Wood, Hertfordshire, died on 15th May 1981, aged 56. Born and educated in India, Mr Staynor served with the Royal Air Force as an Instructor Mechanic during the war and worked initially for four years as an Inspector in charge of instruments with Orient Airways at Karachi Airport. He then joined Field Aircraft Services, Bovingdon becoming Chief Inspector. Since 1957 he had been with Microwave and Electronics Division of Elliott Brothers, London. He was appointed M.B.E. in the 1971 New Year Honours List.

Edwin Charles Stevenson (Member 1961) of Wokingham, Berkshire, died recently, aged 50. Following National Service as an Air

Radar Mechanic with the Royal Air Force, Mr Stevenson worked for some two years with the Ministry of Aviation Inspectorate of Electrical and Mechanical Engineering before moving in 1955 to General Radiological as a Senior Electronics Test Engineer. From 1957-60 he was Assistant Development Manager and Project Engineer with the Multitone Electric Company. In 1960 he joined Sangamo Weston in Enfield.

Brian John Swainson (Member 1961, Graduate 1959) of Southport died on 10th November 1980, aged 46. Following National Service with the Royal Air Force, Mr Swainson joined the Automatic Telephone and Electric Company, Liverpool as Telecommunications Engineer in 1956. He remained with the company, subsequently Plessey Telecommunications, until the time of his death. For a number of years Mr Swainson was Honorary Secretary of the Institution's Merseyside Section.

Eric Victor Taylor (Member 1964, Student 1960) of Hutton, Essex, died on 17th March, aged 48. Mr Taylor undertook an apprenticeship with Kelvin Hughes from 1946-51 and subsequently worked in the Marine Radar Laboratory as a Development Project Engineer. In 1960, following part-time study at East Ham College of Technology, he gained his HNC in electrical engineering with endorsements.

Major Arthur Stanley Tate, R Sigs (Ret) (Member 1943) of Rainham, Kent, died in November 1980, aged 82. Major Tate joined the Royal Signals in 1916 and in 1929 was promoted to Foreman of Signals. In 1941 he was granted a commission and was for some time an Inspecting Officer for electrical and mechanical equipment. After leaving the army, he continued with the Inspectorate until his retirement in 1963.

New Books Received

The following books which have been received recently have been placed in the Institution's Library and may be borrowed by members resident in the British Isles.

Design of Continuous and Digital Electronic Systems

GORDON J. A. BIRD (*EMI Electronics*)
McGraw-Hill, Maidenhead, 1980.
19 x 25.5 cm. 408 pages. £20.

CONTENTS: Transform theory. System analysis. Filter transfer functions. The transient response of filters. Feedback and root locus. Active filters. Phase locked loops. The z transform. Sampled data systems. Computer simulation. Digital filters.

Intended both for practising engineer and student this book deals with the methods of solving practical problems in electronic engineering through the use of transform theory and the concept of poles and zeros. Covers three broad areas: Basic theory and filter applications; Feedback theory and applications; Digital theory and applications.

Solid State Radio Engineering

HERBERT L. KRAUSS, CHARLES W. BOSTIAN
(*Virginia Polytechnic Institute and State University*) and FREDERICK H. RAAB
(*Austin Company*). Wiley, New York,
1980. 17 x 23.5 cm. 534 pages. £12.

CONTENTS: Radio communication systems. Electrical noise. Resonant circuits and impedance transformation. Small-signal high-frequency amplifiers. Sinewave oscillators. Phase-locked loops. Mixers. Modulation. Amplitude modulation receivers. F.m. and p.m. receivers. Television receivers. Linear power amplifiers. Tuned power amplifiers. High-efficiency power amplifiers. C.w., f.m. and a.m. transmitters. Single-sideband transmitters.

In its analysis and design of r.f. electronic circuits, this book reflects the developments of the past decade which have initiated an unprecedented growth in the use of analogue radio systems for personal and business voice communications. The book is intended to be both a reference for the working engineer and a textbook for senior level students in electrical engineering and electrical technology.

Analog Signal Processing and Instrumentation

ARIE F. ARBEL (*Haiifa Institute of Technology*). Cambridge University Press,
1980. 16 x 23 cm. £27.50. 440 pages.

CONTENTS: Basic and feedback amplifiers. Transducers. Analog signal conditioning. Analog signal measurement in the time domain. Digital-to-analog converters. Analog-to-digital conversion techniques. Converters, selected topics. Data acquisition systems. Estimation of statistics of waveforms and events. Signal enhancement. Computer aided design.

Intended for the electronic system designer who utilizes readily available integrated

circuit modules. Most of the material grew out of a course taught by the author at the Technion-Israel Institute of Technology.

Handbook of Rectifier Circuits

G. J. SCOLES (*formerly English Electric Valve Company*). Ellis Horwood, Chichester,
1980. 15 x 23.5 cm. 235 pages. £22.

CONTENTS: Rectifying devices. Half-wave, full-wave and bridge. Three-phase rectifier bridges having an output frequency of 12 times the mains frequency. Voltage multiplying bridges. Biphas voltage-multipliers. Single-phase/three-phase hybrid circuits. Double-input circuits. Capacitively-coupled, double-driven rectifier circuits. Partial-bridges. Half-voltage circuits. Hammer circuits and anvil circuits. Double-output rectifier circuits. Constant-current techniques. Voltage control by grids and gates. Techniques for generating ultra-high voltages. Multi-stage voltage-multiplying circuits. The tuned-bridge rectifier and its application to voltage-multiplying circuits. Switched, tuned, voltage-multiplier circuits. Further possible multiplying circuits. Three-phase transformer connection, mainly for bridge rectifier circuits. Simple smoothing circuits. The switching of transformers. Circuit component rating.

The handbook first describes the relatively few rectifier circuits in common use and then shows how these can be combined and adapted so as to produce a large number of 'brand new' circuits of wide application wherever rectified power supplies are required.

Electronic Devices

F. R. CONNOR. Edward Arnold, London,
1980. 13.5 x 21.5 cm. 121 pages. £3.95.
(Paper bound).

CONTENTS: Atomic theory. Semiconductor theory. Solid-state devices. Electron dynamics. Vacuum devices.

An introductory book on electronic devices it endeavours to present the basic ideas of both vacuum and solid-state devices.

Many worked examples from past examination papers are provided to illustrate the application of the fundamental theory.

Electromagnetism and its Applications—An Introduction

B. BOLTON (*University of Bath*). Van Nostrand Reinhold, Wokingham, 1980.
21 x 29 cm. 156 pages. £10 (clothbound)
£4.50 (paperback).

CONTENTS: Static electricity or when to keep your shirt on. Charges and forces. Electrostatic copiers and chimneys that don't smoke. Electric field strength and potential energy. Electric potential difference. Lightning, kugelblitz and when to stand on one leg. Gauss'

law. Motors and rockets. The effect of dielectric materials on the electrostatic field. Tracking, treeing and bushings. Capacitance. Charge-coupled devices. Energy in electrostatic systems. Electrostatic generators. Diagnostic test. The magnetic field. Navigators all at sea. Magnetic flux density. The free-space constants. The effect of iron on the steady magnetic field. Bubble and squeak. Ampere's circuital law. This is your local displacement current—here is the news. Magnetic circuits. Some small machines. Permanent magnets. Do, do, do, do, do you remember? The Biot-Savart law. Electromagnetic induction. The new ice age. Mutual and self inductance. Energy storage in the magnetic field. Machinery. The transformer. More about the transformer. Hysteresis and eddy-current loss. And finally, Maxwell.

This textbook covering the basic principles of electromagnetism is for first year undergraduates and students on diploma courses. The chapter headings, quoted above, indicate the informal approach.

Radar Anti-jamming Techniques

Edited by M. V. MAKSMOV. Artech House
Dedham, MA 1979. 15.5 x 23.5 cm. 421
pages. £29.

CONTENTS: Natural radio interference Man-made radio interference Mutual interference and electromagnetic compatibility of electronic systems. General description of radio interference control techniques Protection of receivers from overloads and cancellation of radio interference. Spatial, polarization, frequency and phase selection. Time and amplitude selection. Functional, structural and combined selection. Combined coordinate sensors.

Translated from the Russian, this book by a group of Soviet electronic engineers is intended primarily for those engaged in the development and operation of various kinds of electronic equipment. It may also serve as a textbook for students of advanced radio engineering courses. Methods of protecting radio systems from radio interference are described in detail and wide attention is devoted to methods of protecting systems from jamming.

Handbook of Microcircuit Design and Application

DAVID F. STOUT (*Ford Aerospace & Communications Corporation*). McGraw-Hill, New York, 1980. 15.5 x 24 cm. 499 pages.
£18.20.

CONTENTS: Introduction to microcircuits. Digital families. Combinational circuits. Flip-flops and shift registers. Read-write random-access memories. Read-only memory devices. Data-word sorting and checking. Sequential circuits. Digital signal generation. Serial communications microcircuits. Parallel communications microcircuits. BCD circuits. The microprocessor and the microcomputer. Microprocessor controlled A/D converters. Microcomputer-based traffic systems. Keyboard scanner circuits. Application for the 6800 microprocessor: A polyphonic music synthesizer. Special purpose LSI circuits. Operational amplifiers. Active filters. Regulators. Nonlinear analog microcircuits. Analog signal generation. Sampling and

multiplexing circuits. Analog-to-digital converters. Digital-to-analog converters. Phase-locked-loop circuits.

A comprehensive handbook to help solve problems relating to the design and application of most classes of digital and analogue circuits.

Radar Electronic Counter-countermeasures

STEPHEN L. JOHNSTON (Editor). Artech House, Dedham, MA, 1980. 21 x 27.5 cm. 546 pages. £29.

CONTENTS: Introduction to radar electronic counter-countermeasure. General ECCM. ECCM in the transmitter. ECCM in the antenna. ECCM in the Antenna: Sidelobe blanker/canceller. ECCM in the receiver (general). ECCM in the receiver signal processor. ECCM in the system, operational, and other ECCMs. ECM/CCM, ECCM efficacy, simulation and analysis.

These 52 reprints cover a time span from 1946 to 1978. About one-third are by non-US authors from Chile, Denmark, Germany, India, Italy, Japan, Netherlands, Sweden and including several from the United Kingdom. Five papers were originally presented at the 1978 Military Microwaves conference in London.

Electrical Interference in Electronic Systems: Its Avoidance within High-voltage Substations and Elsewhere

R. E. MARTIN (Consultant). Research Studies Press, Forest Grove, OR, 1979. 14.5 x 22 cm. 198 pages. £11.30.

CONTENTS: Interference ingress. Interference measurements in substations. Susceptibility of computers to interference. Susceptibility of solid-state circuits to noise and to damage. Typical values of attenuation required. Check list of desirable precautions. Test specifications and methods.

Intended to be used in conjunction with other documents to facilitate interference immunization by isolation, screening, filtering, earthing and layout design for electronic systems in electrically noisy environments. It deals particularly with the use of electronic equipment in high-voltage electricity substations and outlines the way in which harmful interference may enter the electronic systems as well as indicating appropriate measures for the control of the effect of such interference. It is not concerned with interference effects external to the station.

A Retrospective Technology Assessment: Submarine Telegraphy—The Transatlantic Cable of 1866

V. T. COATES and B. FINN (National Museum of History and Technology). San Francisco Press, (547 Howard Street, San Francisco 94105 USA.) 1979. 17 x 25 cm. 264 pages. \$8.50.

A methodological study on a remarkable technological development of its time namely the introduction of submarine cables with particular reference to the transatlantic cables of the 1860s. Submarine cables are shown to have brought about significant changes in many institutions ranging from shipping and commerce to diplomacy and military organizations.

The Engineering of Microprocessor Systems. Guidelines on System Development

Electrical Research Association, Leatherhead, Surrey. Pergamon, Oxford, 1979. 21 x 29.5 cm. 175 pages. £7.00.

CONTENTS: A guide to the jargon. The significance of microprocessors for industry. Choosing the right technology. Selecting the microprocessor. The development process. Setting up the development laboratory.

The book is primarily for managers and other users who have the responsibility for microprocessor system developments but who may lack direct experience in this field.

Handbook for Radio Engineering Managers

J. F. ROSS (Registered Professional Engineer in Australia). Butterworths, London, 1980. 16 x 24 cm. 947 pages. £35.

CONTENTS: Management and organization. Engineering economy. Safety practice. Fires in radio installations. Environmental aspects in radio engineering. Specification and contract administration.

Designed to help anyone associated with the management of radio projects, services and facilities from the large complex radio stations and networks down to the small station. It describes managerial factors and aspects associated with the design, installation, commissioning, operation and maintenance of radio engineering services and facilities with particular emphasis on efficiency, productivity, budgeting, organization, safety practice and environmental obligations.

The VDT Manual

A. CAKIR (Technical University of Berlin), D. J. HART (Inca-Fiej Research Association) and T. F. M. STEWART (University of Loughborough). IFRA, Darmstadt, 1979. 21 x 29.5 cm. 250 pages.

CONTENTS: VDT basics. Light, vision and the optical characteristics of visual displays. Ergonomic requirements for vdt's. Ergonomic requirements for vdt workplaces. The health, safety and organizational aspects of working with vdt's.

Despite the vast amount of literature on computers, little has been written about the people who use them and the conditions under which they are used. It sets out to analyse the ergonomic, health and safety aspects of working with visual display terminals.

Experimenter's Guide to Solid State Electronics Projects

ALFRED W. BARBER. Parker Publishing Company, New York, 1980. 16 x 23 cm. 214 pages. £9.70.

CONTENTS: Experimenting with crystal detectors, diodes and rectifiers. Projects and experiments with transistors. Building and experimenting with solid state power supplies. Experimenting with silicon controlled rectifiers and triacs. Building photo detectors, photo couplers and optical fibre devices. Experimenting with solar cells. Experimenting with field effect transistors. Project: build your own experimental laboratory. Experimenting with linear integrated circuits.

A collection of easy-to-follow electronics projects and tests for experiments with solid-

state devices such as solar cells, fibre optics, l.e.d.s and both linear and digital i.c.s.

The Art of Electronics

PAUL HOROWITZ (Harvard University) and WINFIELD HILL (Sea Data Corporation). Cambridge University Press, 1980. 17.5 x 25 cm. 716 pages. £35 (Hard covers), £12.50 (Paperback)

CONTENTS: Transistors. Feedback and operational amplifiers. Active filters and oscillators. Voltage regulators and power circuits. Field-effect transistors. Precision circuits and low-noise techniques. Digital electronics. Digital meets analog. Minicomputers. Microprocessors. Electronic construction techniques. High-frequency and high-speed techniques. Measurements and signal processing.

A text/reference book that emphasizes electronic circuit design techniques and scientific measurements. It begins at a level suitable for those with no previous experience in electronics and takes the reader through to a reasonable level of design proficiency.

The Microelectronics Revolution

TOM FORESTER (Editor). Basil Blackwell, Oxford, 1980. 15.5 x 23.5 cm. 589 pages.

CONTENTS: The microelectronics revolution. Economic and social implications. The micro-electronic age.

The aim of the book is to bring together natural and social scientists in a positive way on a uniquely important topic. The contributors, all experts in their fields, explain in turn the origins and nature of microelectronics and the increasing use of microprocessors in everyday products. It details the impact of the new technology on society, the consequences for employment and the implications for industrial relations.

Broadcasting—An Introduction

JOHN R. BITTNER (DePauw University). Rustic Hall, Englewood Cliffs NJ, 1980. 18 x 23.5 cm. 508 pages. £10.35 (cloth).

CONTENTS: Broadcasting as mass communication. The beginning of wireless. The development of modern radio and television. Radio waves and the spectrum. Broadcasting's use of microwaves and satellites. Cable. Networks and syndication. Educational and public broadcasting. Television in business and industry. International broadcasting. Early attempts at government control. The Federal Communications Commission. Control of broadcast programming. Regulation station operations. Cable, satellites and future perspectives. Advertising and economics. Broadcast ratings. The research process. The broadcast audience: approaches to studying effects. Using the library to learn about broadcasting.

The book is designed for use in single term introductory broadcasting courses in the US, being directed toward students who aspire to be either 'responsible consumers of broadcasting in society' or practising professionals in broadcasting or related fields. The book covers mainly the Northern American continent but it will provide interesting reading for the British student. This is despite the fact that the only reference to J. Logie Baird is in connection with his experiments in video recording and it completely ignores the BBC's broadcasting of television in 1936, and indeed until after the War!

Microprocessor-based digital filters

R. J. SIMPSON, B.Tech, M.Sc., Ph.D.,
C.Eng., F.I.E.E.*

and

T. J. TERRELL, M.Sc., Ph.D., C.Eng., M.I.E.E.*

SUMMARY

The concepts of microprocessor-based digital filter implementation are presented via a case study of a low-pass filter designed using the bilinear z -transform method. Implementation aspects associated with an 8-bit general-purpose microprocessor-based realization and a single-chip signal processor are discussed and results included.

* Systems and Instrumentation Division, Preston Polytechnic, Preston, PR1 2TQ

1 Introduction

A digital filter may be thought of as being simply the equivalent of an analogue filter implemented using a digital processor. It may, however, have a number of advantages in many applications, namely:

It does not drift.

It can handle low frequency signals.

Frequency response characteristics can be made to approximate closely to the ideal.

It can be made to have no insertion loss.

Linear phase characteristics are possible.

Adaptive filtering may be achieved.

Digital word-length may be specified by the designer.

The digital processor used for filter implementation may take the form of hardwired dedicated hardware, or a minicomputer system, or a microprocessor-based system. The latter form has relative merits of low cost, small physical size and programmability, and consequently discussion of practical implementation will be restricted to microprocessor-based systems.

Realization of a digital filter requires an algorithm (linear difference equation) for calculating the discrete-time values used for the filtering process. There are a number of established design methods for deriving the required linear difference equation via the corresponding z -plane representation of the digital filter transfer function.¹⁻⁷ The approach may involve the selection or derivation of a suitable transfer function, $G(s)$, corresponding to an analogue filter which meets the appropriate specification. The digital filter transfer function $G(z)$ is then derived from knowledge of $G(s)$, using an s -plane to z -plane mapping.

In some digital filter designs an objective may be to achieve a time-domain specification, in which case the time response of the analogue filter is used as the basis for deriving $G(z)$. This method is suitable if the digital filter is required to have the same impulse-response or step-response as the prototype analogue filter $G(s)$. That is, the s -plane to z -plane mapping is achieved via the corresponding impulse invariant⁸ or step invariant⁹ design methods. A point to note is that for the step invariant design method, if the analogue prototype filter has fast rise-time and short settling time, these characteristics will be preserved in the digital filter. It should also be noted that for both methods, the frequency response characteristic of $G(z)$ may not match that of $G(s)$, the closeness of the match depends upon the frequency response of $G(s)$ being adequately bandlimited.

However filters are often specified in terms of frequency response characteristics and in many digital filter designs these are the main considerations. Consequently time-invariant design methods are generally not satisfactory in such cases.

An s -plane to z -plane mapping, which is characteristically bandlimiting in its action, is the

bilinear z -transform.¹⁰ This method is easy to apply because it is simply a matter of substituting a function of z for each Laplace operator s appearing in $G(s)$. This is a common approach to digital filter design and $G(s)$ may be based on prototype Butterworth, Chebyshev, elliptic or Bessel analogue filters which have the desired frequency-domain characteristics.

It is therefore appropriate to introduce the concepts of digital filter design via an illustrative example involving a 2nd-order Butterworth filter, which is mapped to the z -plane using the bilinear z -transform method.

2 Illustrative Design Example

The transfer function of the normalized 2nd-order Butterworth low-pass filter is given by equation (1):

$$G(s) = \frac{1}{s^2 + \sqrt{2}s + 1} \tag{1}$$

Let the specification for the digital filter be: low-pass digital filter cut-off frequency, $f_{cd} = 100$ Hz, sampling period, $T = 1.6$ ms. ($f_s = 1/T = 625$ Hz). The transfer function given by equation (1) may be denormalized using the relationships given in Table 1. In this example we replace s by s/ω_{ca} in equation (1), where ω_{ca} is the radian cut-off frequency of $G(s)$, thus yielding

$$G(s) = \frac{1}{\left(\frac{s}{\omega_{ca}}\right)^2 + \frac{\sqrt{2}s}{\omega_{ca}} + 1} \tag{2}$$

The transfer function given by equation (2) may now be mapped from the s -plane to the z -plane using the bilinear z -transformation. However a non-linear frequency distortion is produced by the bilinear z -transform. This warping must be taken into account in the design process by pre-warping the s -plane frequency scale. To achieve this the cut-off frequency of the denormalized prototype analogue filter is calculated using equation (3)

$$\omega_{ca} = \frac{2}{T} \tan\left(\frac{\omega_{cd}T}{2}\right) \tag{3}$$

where ω_{ca} is the radian pre-warped cut-off frequency of

$$G(z) = \frac{472243.84}{\left\{1250\left(\frac{z-1}{z+1}\right)\right\}^2 + \left\{971.85 \times 1250\left(\frac{z-1}{z+1}\right)\right\} + 472243.84} \tag{6}$$

which simplifies to

$$G(z) = \frac{z^2 + 2z + 1}{6.88z^2 - 4.62z + 1.74}$$

To transform from normalized low-pass to:	Substitute for s
low-pass	s/ω_{ca}
high-pass	ω_{ca}/s
bandstop	$s(\omega_{cau} - \omega_{cal})/(s^2 + \omega_{cal} \cdot \omega_{cau})$
bandpass	$(s^2 + \omega_{cal} \cdot \omega_{cau})/s(\omega_{cau} - \omega_{cal})$

ω_{cau} = upper transition radian frequency, ω_{cal} = lower transition radian frequency

the denormalized analogue filter, ω_{cd} is the specified radian cut-off frequency of the digital filter, and T is the sampling period in seconds. Substituting the specified parameters in equation (3) yields

$$\omega_{ca} = \frac{2}{1.6 \times 10^{-3}} \tan\left(200\pi \times \frac{1.6 \times 10^{-3}}{2}\right) = 687.2 \text{ rad/s}$$

The next step in the design is to substitute this value of ω_{ca} in equation (2), thereby producing the pre-warped transformed transfer function, $G(s)_{pwt}$, thus

$$G(s)_{pwt} = \frac{1}{\left(\frac{s}{687.2}\right)^2 + \frac{\sqrt{2}s}{687.2} + 1}$$

$$G(s)_{pwt} = \frac{472243.84}{s^2 + 971.85s + 472243.84} \tag{4}$$

For the bilinear z -transform we use the substitution

$$s = \frac{2}{T} \left(\frac{z-1}{z+1}\right)$$

and for the specified value of T this gives

$$s = 1250 \left(\frac{z-1}{z+1}\right) \tag{5}$$

Substituting equation (5) in equation (4) gives $G(z)$, i.e.

Having derived the transfer function, $G(z)$, for the digital filter, it is necessary to establish the location of its poles (roots of the denominator polynomial: equation (6)), and for stability, ensure that they lie within

the unit circle in the z -plane. In this example the poles of $G(z)$ are a complex conjugate pair at $z = 0.336 \pm j0.374$, these lie within the unit circle, thereby yielding a stable filter.

It is also appropriate at this stage to check the filter frequency response characteristic, $G(e^{j\omega T})$. This is achieved by substituting $e^{j\omega T}$ for z in equation (6) giving

$$G(e^{j\omega T}) = \frac{(\cos 2\omega T + 2 \cos \omega T + 1) + j(\sin 2\omega T + 2 \sin \omega T)}{(6.88 \cos 2\omega T - 4.62 \cos \omega T + 1.74) + j(6.88 \sin 2\omega T - 4.62 \sin \omega T)} \quad (7)$$

The magnitude $|G(e^{j\omega T})|$ and phase $\angle G(e^{j\omega T})$ characteristics were evaluated at several frequencies in the range 0 to 400 Hz, and the results are shown in Fig. 1. For comparison the frequency response characteristics $|G(j\omega)|$ and $\angle G(j\omega)$ of the denormalized prototype analogue filter are included. These were achieved by substituting $j\omega$ for s in equation (2), thus yielding for a value of f_{ca} equal to 100 Hz

$$G(j\omega) = \frac{394784.2}{(394784.2 - \omega^2) + j888.6 \omega}$$

The results in Fig. 1 show that up to the filter cut-off frequency the digital and analogue filter characteristics are closely matched. However for values of frequency approaching $f_s/2$ Hz there are significant errors, and indeed beyond $f_s/2$ aliasing occurs. The characteristics of $G(z)$ are dependent upon the sampling period, T , and the

matching of $G(z)$ to $G(s)$ may be improved by decreasing T if practicable. The direct form of realization of an n th-order digital filter may be expressed as equation (8):

$$G(z) = \frac{\sum_{i=0}^l a_i z^{-i}}{1 + \sum_{i=1}^m b_i z^{-i}} = \frac{Y(z)}{X(z)} \quad (8)$$

where $m > l$ for realizability

Since z^{-d} implies a time delay equal to d sampling instants, it follows that the corresponding linear difference equation may be written as

$$y(n)T = \sum_{i=0}^l a_i x(n-i)T - \sum_{i=1}^m b_i y(n-i)T \quad (9)$$

Converting equation (6) to the corresponding linear difference equation form, gives equation (10):

$$y(n)T = 0.145x(n)T + 0.291x(n-1)T + 0.145x(n-2)T + 0.671y(n-1)T - 0.253y(n-2)T \quad (10)$$

In Section 3 two forms of microprocessor system implementation of the filter are discussed.

3 Microprocessor Implementation

The processor word length required to maintain stability, assuming truncation rather than rounding of the filter coefficients, may be determined using the method reported by Kuo and Kaiser.¹¹

They showed that for an n th-order filter having distinct poles at $(\cos \omega_k T - j \sin \omega_k T)$, where k is an integer in the range $n \geq k \geq 1$, the number of processor bits, w , must be

$$w = \text{smallest integer exceeding} \left\{ -\log_2 \left[\frac{5\sqrt{n}}{2^{n+2}} \prod_{k=1}^n (\omega_k T) \right] \right\} \quad (11)$$

Evaluating equation (11) for the complex conjugate poles obtained from equation (6), yields $w = 2$. This is not a surprising result considering that the poles are located well away from the circumference (stability boundary) of the unit circle. There is no guarantee that with this value of w the filter will meet its specified frequency response characteristic. Generally, a rule-of-thumb is employed whereby normally four or five bits are added to w in order to take account of quantization and computational errors. This suggests that for this example it may be appropriate to consider implementation using an 8-bit wordlength.

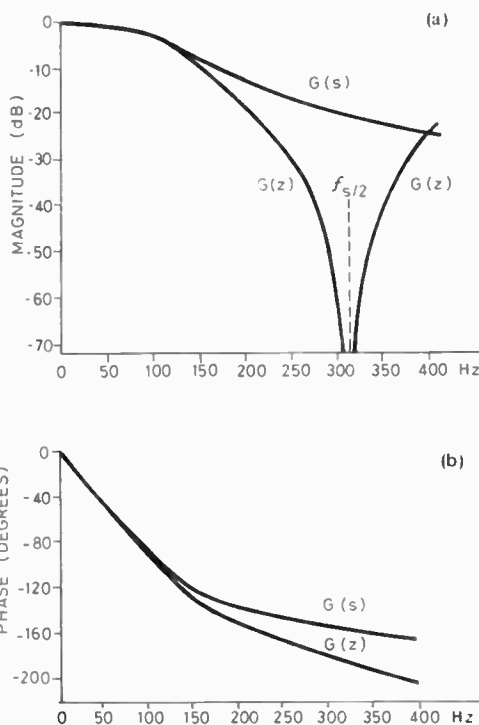


Fig. 1. (a) Amplitude/frequency response for $G(s)$ and $G(z)$.
(b) Phase/frequency response for $G(s)$ and $G(z)$.

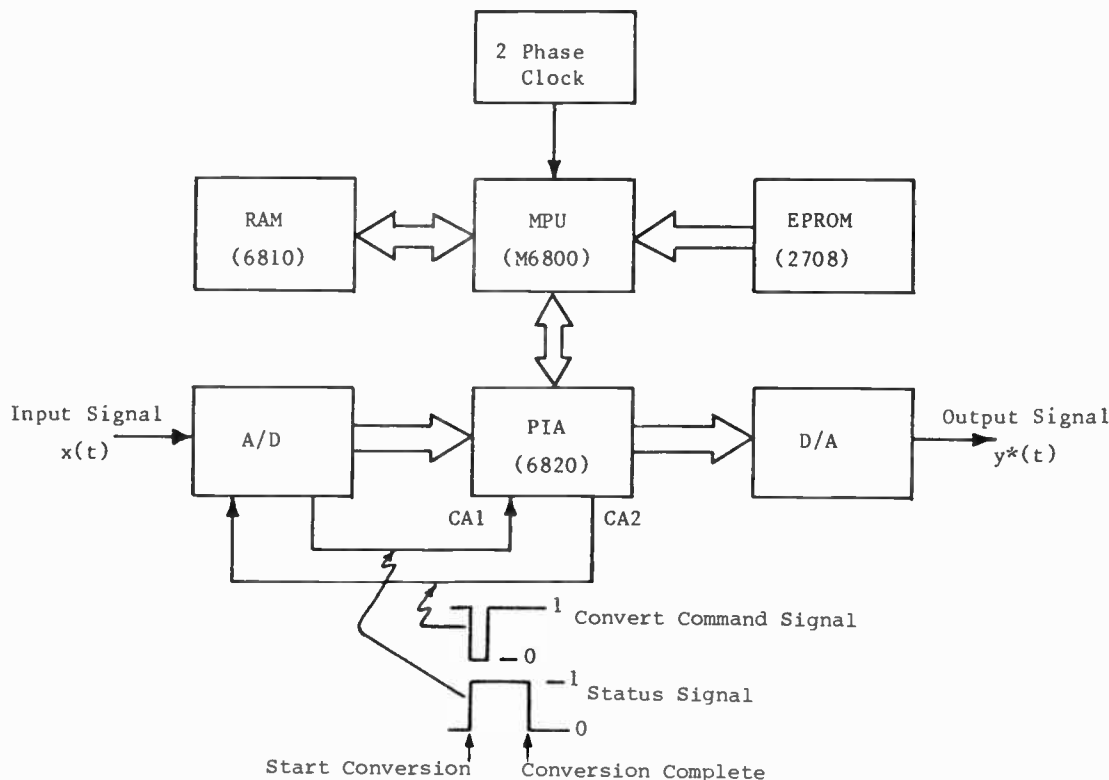


Fig. 2. Block diagram of 8-bit microprocessor system.

A typical 8-bit microprocessor-based digital filter configuration is shown schematically in Fig. 2. The flowchart for the filter implementation is shown in Fig. 3.

In computing $y(n)T$ (eqn. (9)) the product terms in the equation involve evaluating the multiplication of two 8-bit binary numbers, thereby producing a 16-bit result which would normally be rounded or truncated and represented by the most significant 8-bits. This obviously introduces computational errors which may degrade the filter performance. In the design example, discussed in Section 2, with 8-bit representation, the rounding or truncation effect is insignificant because the poles of the filter are located well away from the circumference of the unit circle, and a considerable change in the representation of the product terms would be required to cause a significant degradation of the filter frequency characteristics.

The multiplication may be achieved using a software subroutine or a hardware multiplier, the latter being generally faster in operation when compared with the software subroutine. However, today the cost/bit of r.o.m. (or e.p.r.o.m.) is not a serious limitation to the digital filter designer, and consequently the look-up table method of implementation has the advantage of relatively fast operating speed, and it is easily programmed.

The practical results shown in Figs. 4 and 5 were obtained from an M6800-based realization of the second-order low-pass digital filter. Figure 4 shows the digital filter waveforms and Fig. 5 is a spectral analysis of

the output signal, which illustrates the low-pass characteristic and aliasing effects.

In terms of chip count the microprocessor-based digital filter system shown in Fig. 2 may be reduced by replacing the 6800 m.p.u., 6810 r.a.m. and 2-phase clock circuit by a 6802 m.p.u., which has an integral clock and r.a.m. In contrast, for some practical applications, the system may need expanding to provide a multiplexed input and/or a multiplexed output.

An alternative form of realization may be achieved using the single-chip Intel 2920 signal processor.^{1,2} This n.m.o.s. chip has 'on board' sample-and-hold circuits and d/a and a/d converters. It has its own e.p.r.o.m., scratch pad memory and special instruction set for signal processing. The functional block diagram of the 2920 is shown in Fig. 6.

Under program control, one of four possible inputs is selected and then sampled and held, and the signal is then converted linearly to a digital word with up to 9-bits of resolution (includes sign-bit). An internal digital to analogue register (DAR) accumulates the digital word until the conversion is complete, giving the required $x(n)T$. The word is then loaded into the scratch pad memory to be used in the subsequent evaluation of $y(n)T$. The DAR is also used to drive the d/a converter to any of eight analogue outputs via the output demultiplexer and sample-and-hold amplifiers. An interesting feature is that the analogue and digital operations can be executed simultaneously, and consequently this results in a relatively short instruction

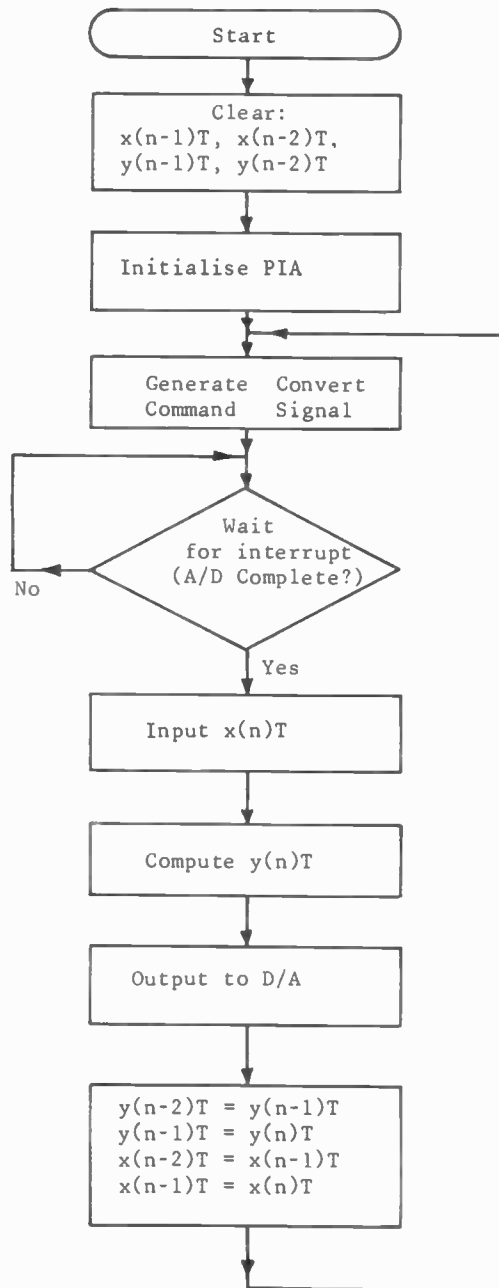


Fig. 3. Flowchart for M6800-based digital filter.

set, particularly suited to digital signal applications.

It should be noted that in comparison with the 8-bit microprocessor-based filter having a sampling time of 1.6 ms, the Intel 2920 can sample approximately ten times faster, thereby increasing the baseband of the input signal.

A 2920 realization of the low-pass digital filter, with $T = 0.192$ ms, has been achieved and the results compare favourably with those shown in Figs. 4 and 5. It is outside the scope of this paper to present details of the program development and the corresponding assembly language listing—however readers requiring further information are encouraged to contact the authors.

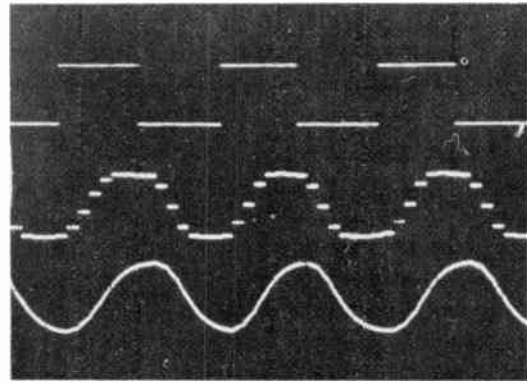


Fig. 4. Waveforms for M6800-based filter:
(a) input signal, $x(t)$;
(b) output signal from d/a converter, $y^*(t)$; and
(c) output from reconstruction filter, $y(t)$.

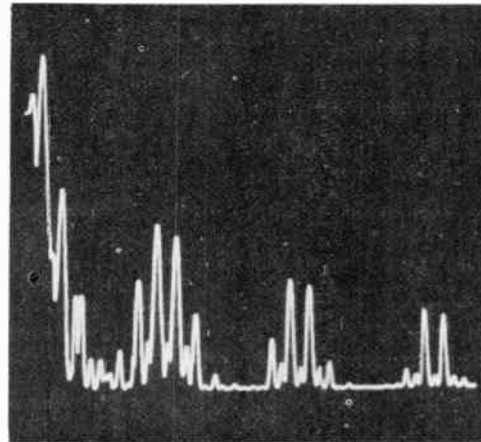


Fig. 5. Results of spectrum analysis carried out on the 2nd-order Butterworth low-pass filter

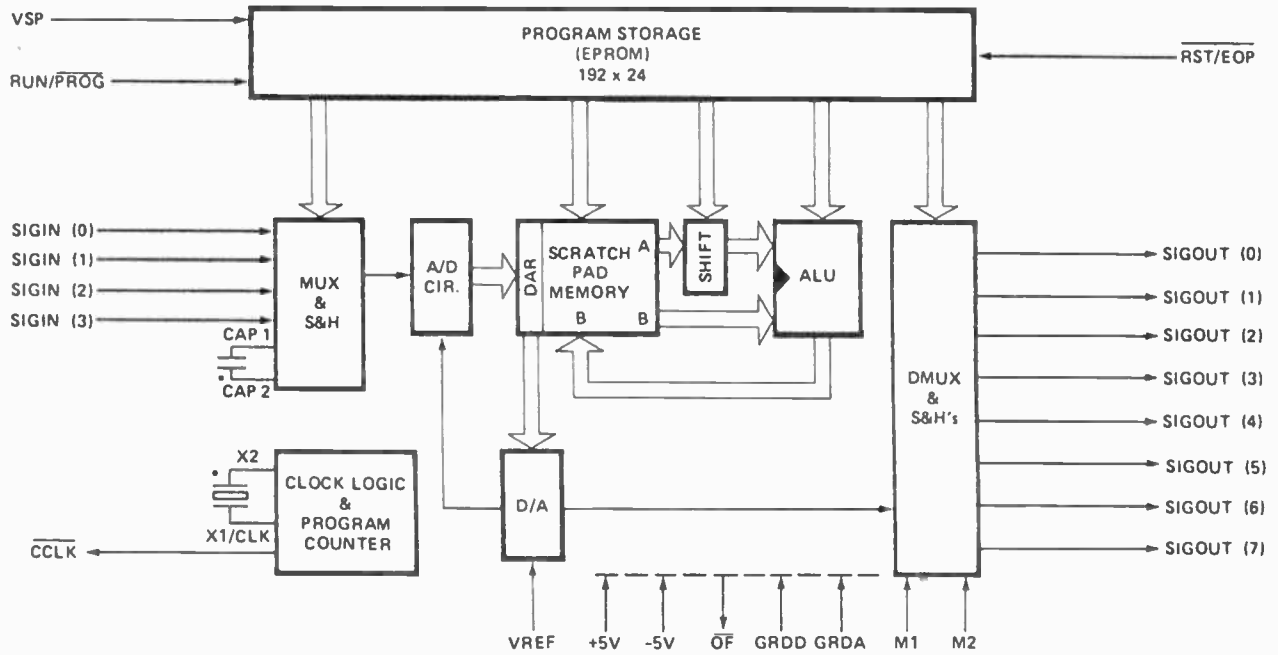
Spectrum analyser settings:
vertical scale—10 dB/cm
horizontal scale—100 Hz/cm
bandwidth—10 Hz.

4 Concluding Remarks

This paper has attempted, by using a relatively simple case study, to illustrate the main characteristics of a digital filter implementation using microprocessor-based systems. It has been shown that a general-purpose 8-bit processor, with the necessary peripheral signal conditioning elements, operated satisfactorily. In comparison the single-chip 2920 signal processor implements the desired filtering action, but has an added advantage of requiring less hardware. Furthermore the 2920 can easily deal with multiplexed input signals, and offer demultiplexed output signals. Undoubtedly the 2920 offers designers an opportunity to develop single-chip signal processing systems.

5 References

- 1 Rader, C. M. and Gold, B., 'Digital filter design in the frequency domain', *Proc. IEEE*, 55, pp. 149-71, 1967.
- 2 Rabiner, L. R. and Gold, B., 'Theory and Application of Digital Signal Processing' (Prentice-Hall, Englewood Cliffs, N.J., 1975).
- 3 Gold, B. and Rader, C. M., 'Digital Processing of Signals' (McGraw-Hill, New York, 1969).



*EXTERNAL COMPONENTS

Fig 6. Intel 2920 block diagram. (Courtesy Intel Corp.)

4 Bogner, R. E. and Constantinides, A. G., 'Introduction to Digital Filtering' (Wiley, New York and London, 1975).

5 Antoniou, A., 'Digital Filter Analysis and Design' (McGraw-Hill, New York, 1979).

6 Oppenheim, A. V. and Schaffer, R. W., 'Digital Signal Processing' (Prentice-Hall, Englewood Cliffs, N.J., 1975).

7 Terrell, T. J., 'Introduction to Digital Filters' (Macmillan, London, 1980).

8 Kaiser, J. F., 'Design methods for sampled data filters', Proc. 1st Allerton Conf. on Circuit System Theory, pp. 221-36, 1963.

9 Terrell, T. J. and Simpson, R. J., 'A step-invariant design method for high-pass digital filters', *Intl J. Elect. Engng Educ.*, 17, pp. 335-42, 1980.

10 Tustin, A., 'A method of analysing the behaviour of linear system in terms of time series', *J. Instn Elect. Engrs*, 94, Part IIA, pp. 130-42, 1947.

11 Kuo, F. F. and Kaiser, J. F., 'System Analysis by Digital Computer' (Wiley, New York, 1966).

12 '2920 Analog Signal Processor Design Handbook'. Intel Corp., 1980.

Manuscript first received by the Institution on 12th November 1980 and in revised form on 13th March 1981 (Paper No. 2004/CC345)

Pseudo-linear operation of second-order phase-locked loops

J. E. ALLOS, Ph.D., C.Eng., F.I.E.R.E.,*

S. R. AL-ARAJI, Ph.D.,
C.Eng., M.I.E.E., M.I.E.R.E.*

and

E.H. EZZET, B.Sc., M.Sc.*

SUMMARY

This paper defines a region of operation, calling it the pseudo-linear region, where a phase-locked loop (p.l.l.), behaves essentially in a linear manner. The results obtained for a loop with an active second-order filter suggest a very simple empirical definition for this region as a function of the parameters of the loop (ξ and ω_n), and classifies the regions of operation of the p.l.l., linear, pseudo-linear, non-linear and cycle slipping.

* Department of Electrical Engineering, College of Engineering, Baghdad University, Iraq.

1 Introduction

The phase-locked loop (p.l.l.) which is incorporated in one way or another in most up-to-date communication systems has been extensively studied, either in the region where it is in the process of acquiring lock and is therefore cycle slipping,¹ or as a linear system.²

In actual fact the linear analysis is not really valid except for very small phase error, say less than 5 degrees, putting a severe limitation on the usefulness of such analysis. This leaves out what probably is the most important region of operation of the p.l.l., i.e. when it is in lock, but having large phase errors. This paper defines a region, calling it the pseudo-linear region, where the behaviour of the loop, although non-linear, approximates closely to the linear model. The definition is based on one of the parameters of the transient response of the loop, namely the settling time, which in most applications is the parameter of greatest interest. If the frequency of the input to the loop is suddenly changed, the frequency of the output will try to track the input. The settling time is that necessary for the output frequency to reach, and remain within, $\pm 2\%$ of the frequency change from the frequency of the input. For small changes in frequency, the loop is linear, and the settling time is constant. For greater steps in frequency, the loop exhibits non-linear behaviour, and the settling time increases until a certain step value reached or exceeded, when the loop loses lock and begins to cycle slip and the settling time increases very sharply. (This is shown clearly in Fig. 6.) The pseudo-linear region is defined as that region where the settling time does not increase by more than 10% of its value for the linear model. This puts an upper bound on the step of frequency which may be applied (360 rad/s in Fig. 6). The pseudo-linear region was studied for a second-order loop with active filter which is the optimum estimate³ for a step of frequency, and is thus most widely used, together with the second-order loop with the passive filter, which anyway approximates quite closely to it.⁴ Due to the non-linear nature of the problem, an exact analysis is not possible. The response of the non-linear loop was solved on a digital computer, using the Runge-Kutta method, and the pseudo-linear region is described in terms of the natural frequency (ω_n) and the damping ratio (ξ). A very simple empirical relationship was obtained relating the frequency step with ω_n and ξ . This enables the designer to choose his parameters so as to stay in the pseudo-linear region, where the loop may be considered approximately linear. These results tie in with an empirical formula recently given by Gardner⁵ for the frequency step at which cycle slipping begins, and thus the regions of operation of the p.l.l. are clearly classified as shown in Fig. 9.

2 Theoretical Background

The block diagram of a p.l.l. in lock is shown in Fig. 1, where:

$$\text{Input } f_i(t) = A_1 \sin(\omega t + \varphi_1)$$

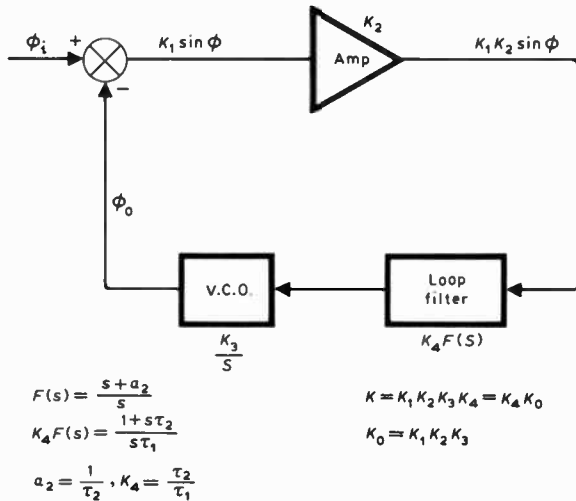


Fig. 1. Block diagram of the phase-locked loop circuit.

Output $f_o(t) = A_2 \sin\left(\omega t + \frac{\pi}{2} + \varphi_o\right)$

and

$$\varphi = \varphi_i - \varphi_o.$$

The filter shown is active and the loop is second order⁴, i.e. the d.c. gain of the loop is theoretically infinite.

The equation describing the system is then

$$\ddot{\varphi} + (K \cos \varphi)\dot{\varphi} + K a_2 \sin \varphi = \ddot{\varphi}_i. \quad (1)$$

This is a non-linear differential equation in φ . If φ is very small, then it can be reduced to

$$\ddot{\varphi} + K\dot{\varphi} + K a_2 \varphi = \ddot{\varphi}_i. \quad (2)$$

2.1 Linear Analysis

Equation (2) describes the linear model of the p.l.l., where the output of the phase detector in Fig. 1 becomes $K_1 \varphi$ instead of $K_1 \sin \varphi$ and its solution in the time domain for a unit step input in frequency can be shown to be:

$$\Delta\omega = \frac{e^{-\xi\omega_n t}}{\delta} (\delta \cos \delta t - \xi\omega_n \sin \delta t) \quad (3)$$

where $\Delta\omega$ is the error frequency between input and output.

$$\begin{aligned} \omega_n &= \sqrt{K a_2} \\ \xi &= \frac{K}{2\omega_n} \\ \delta &= \omega_n \sqrt{1 - \xi^2}. \end{aligned}$$

The root locus can be very useful in the linear analysis of a p.l.l.⁴ The open-loop transfer function of the loop is given by $K(s+a_2)/s^2$ and the root locus is shown in Fig. 2, which is a circle of centre $-a_2$, and radius a_2 . The

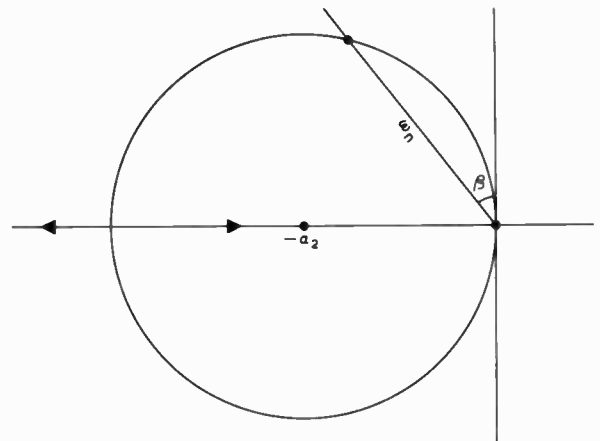


Fig. 2. Root locus plot of the p.l.l. with active second-order filter.

value of K determines the position of the closed-loop poles:

$$\begin{aligned} s &= -\frac{K}{2} \pm j\frac{1}{2}\sqrt{4a_2 K - K^2} \\ &= -a \pm jb, \end{aligned} \quad (4)$$

where

$$a = \frac{K}{2}, \quad b = \frac{1}{2}\sqrt{4a_2 K - K^2}$$

and

$$\begin{aligned} \omega_n &= \sqrt{a^2 + b^2} = \sqrt{K a_2} \\ \xi &= \sin \beta = \frac{a}{\omega_n} = \frac{K}{2\omega_n}. \end{aligned}$$

The settling time T_s is the time necessary for $\Delta\omega$ in equation (3) to remain within ± 0.02 . Since it is quite laborious to obtain T_s from equation (3), quite frequently it is evaluated with a good degree of approximation (for $\xi = 0.707$) as:⁶

$$T_s = \frac{4}{a}.$$

Figure 3 is a plot of T_s versus ξ for $\omega_n = 100\sqrt{2}$ rad/s for the exact value of T_s .

2.2 Non-linear Analysis

If the frequency step applied is large, the linear analysis given above no longer holds, and a solution of equation

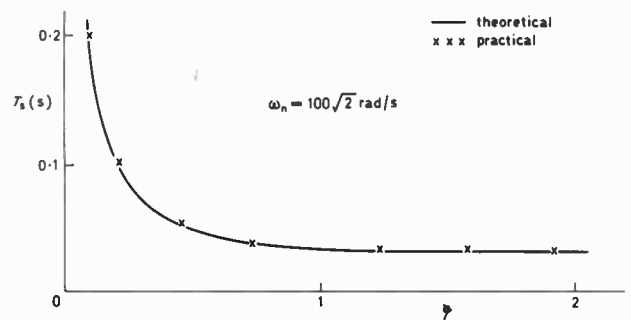


Fig. 3. Plot of settling time versus damping factor (ξ) for the linear p.l.l.

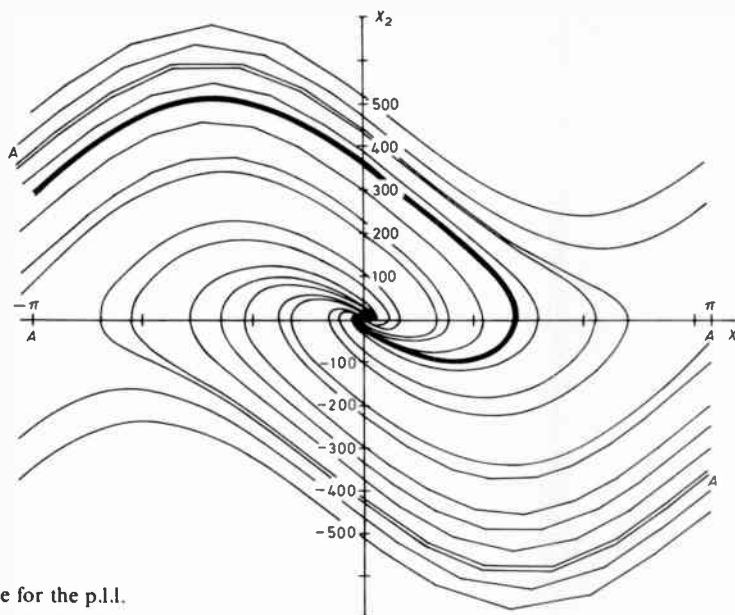


Fig. 4. Trajectories in the phase plane for the p.l.l.

(1) becomes necessary. Since it is a non-linear differential equation, an exact solution is not possible. Trajectories in the phase plane⁷ can be obtained, and Fig. 4 shows such a trajectory. However, it is not easy to obtain the settling time from such a trajectory, since time is an implicit variable in the phase plane. To obtain a definition for the pseudo-linear region, equation (2) was solved on an IBM 1130 digital computer, using the Runge-Kutta method, for different values of input step in frequency, and for different values of ξ and ω_n (and thus different values of K and a_2). From the solution, it was possible to obtain T_s as defined in Section 2.1. Figure 5 shows a plot of T_s versus input frequency step value for one value of ω_n . It is a family of curves, each curve for one value of ξ . Similar data were obtained for

$\omega_n = 50, 50\sqrt{2}, 100, 100\sqrt{2}, 200, 200\sqrt{2},$
and 400 rad/s.

3 Pseudo-linear Region

The pseudo-linear region denotes that region where the behaviour of the p.l.l., although not exactly linear, can be approximated to that of the linear model. Since non-linearity exhibits itself in the transient response of the loop, one of the parameters⁴ of the transient response must be chosen for a measure of linearity. The settling time is the obvious parameter to choose since it is the parameter normally of greatest interest. It is expected that similar results will be obtained if any of the other parameters are chosen, e.g. peak time or maximum per unit overshoot.

The loop is defined as pseudo-linear when its settling time is not greater by more than 10% than the settling time of the linear model. This requires that the input frequency step should not exceed a certain value y , which is then a function of ξ and ω_n . Figure 6 shows a plot of T_s versus the step $\Delta\omega$, when $\omega_n = 100\sqrt{2}$ rad/s, $\xi = 1/\sqrt{2}$ and shows how y is evaluated.

3.1 Empirical Relationship

As shown in Section 2.2, families of curves similar to Fig. 5 were obtained for different values of ω_n , and for each curve y was evaluated. This enables Fig. 7 to be plotted, giving y versus ξ for different values of ω_n , from which constant y contours are obtained as shown in Fig. 8. Here, the pseudo-linear region is well defined

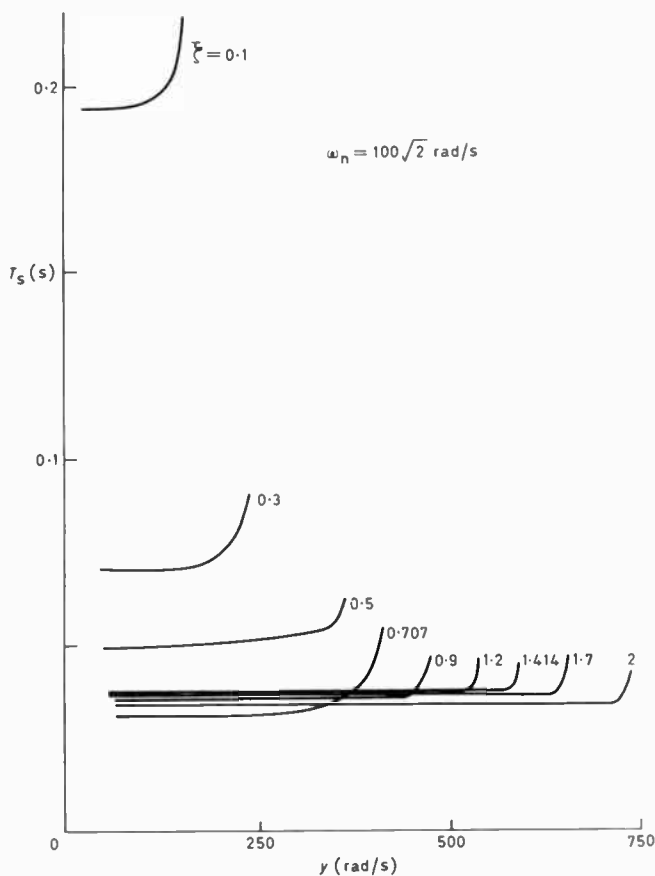


Fig. 5. Plot of the settling time versus the step of input frequency.

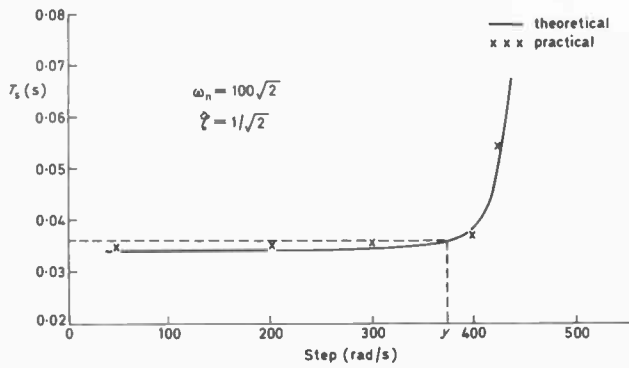


Fig. 6. Determination of input frequency step for pseudo-linear operation (y).

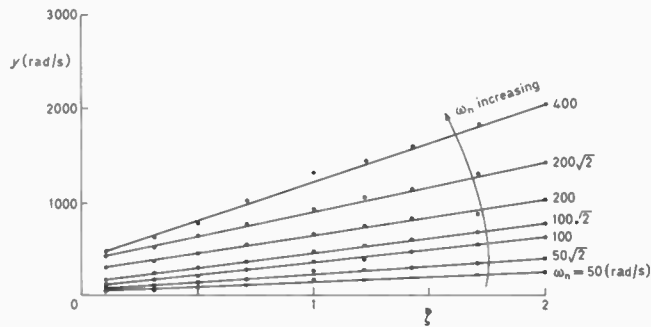


Fig. 7. Plot of y vs. ζ .

and, for a certain value of y , it is the area bounded by the constant y curve away from the origin.

The hyperbolae of Fig. 8 indicate that if y is normalized with respect to ω_n and averaged for all values of ζ , it may be possible to eliminate ω_n and obtain:

$$y_n = \left(\frac{y}{\omega_n} \right)_{\text{averaged over } \zeta} = f(\zeta). \quad (5)$$

When this was carried out, it was found that y/ω_n was fairly constant for any one value of ζ , and hence it was possible to average it to obtain y_n as a function of ζ only. This was plotted in Fig. 9, yielding the linear relationship:

$$y_n = 1.2 + 1.9 \zeta \quad (6)$$

or

$$y = (1.2 + 1.9\zeta)\omega_n. \quad (7)$$

Due to the non-linear differential equation describing the phase-locked loop, it is not possible to justify in an

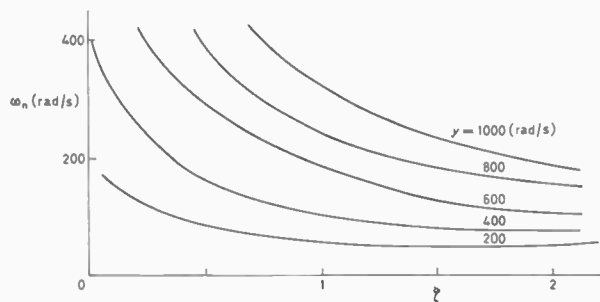


Fig. 8. Constant y contours.

exact manner the relationship given by equations (6) or (7), and as such it is proposed as an empirical relationship valid for the region investigated and shown by the full line in Fig. 9. However, it can be argued intuitively that the relationship is quite reasonable. For very small values of the damping ratio ζ , the step in frequency which the loop can accept, while remaining linear, is directly proportional to the bandwidth of the loop and hence to ω_n . This is the first term of equation (6), which gives the constant of proportionality. As the damping ratio increases, the loop will accept a larger step in frequency, and will have a larger bandwidth. This effectively means that the constant of proportionality increases by a factor proportional to the damping ratio as given by equation (6).

It should be noted that since ζ is defined as $K/2\omega_n$, it can have a value greater than unity, and in fact the results given are up to a value of $\zeta = 2$.

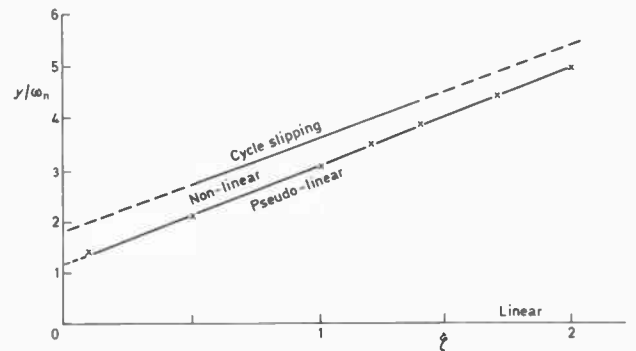


Fig. 9. Operating regions of the p.l.l.

Equations (6) or (7) may now be taken as a definition of the pseudo-linear region, i.e. for any value of ζ and ω_n , y from equation (7) gives the upper bound for the step in input frequency which may be applied, for the loop to behave in essentially a linear fashion. For $\zeta = 1/\sqrt{2}$, which is a very common value to use, equation (7) states that the step in input frequency should not exceed about $2.5\omega_n$. The trajectory corresponding to this is shown by a heavy line in Fig. 4.

3.2 Operating Regions

It is now possible to define the various operating regions of the p.l.l. in a y_n vs. ζ plane as shown in Fig. 9. The x -axis, i.e. $y_n = 0$, is the linear operating region. The area bounded by the x -axis and equation (6) is the pseudo-linear region, where the loop may be approximated to the linear model.

The empirical relationship given by Gardner,⁵ based on Viterbi's results,⁷

$$y_n = 1.8(\zeta + 1) \quad (8)$$

gives the lower bound for cycle slipping. The area between the cycle slipping and the pseudo-linear region, is the non-linear region, where the loop is definitely non-linear. Since T_s rises quite sharply near the cycle slipping

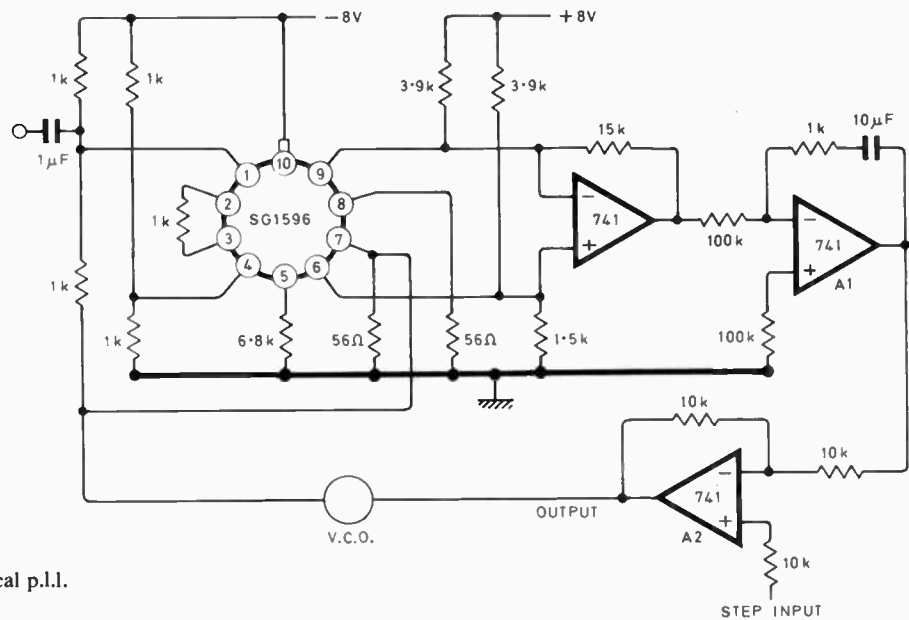


Fig. 10. Circuit diagram of the practical p.l.l.

value of $\Delta\omega$ as shown in Fig. 5, the non-linear region fortunately is quite narrow.

4 Experimental Procedure

A practical phase-locked loop circuit was constructed as shown in Fig. 10 to demonstrate the variation of T_s with $\Delta\omega$. Both the input source and the voltage controlled oscillator (v.c.o.) were synthesized signal generators operating at 150 kHz. The step of input frequency was introduced as a step function to the difference amplifier A2 between the active loop filter and the v.c.o. By writing the equation of the loop, or by inspection, it can be seen that this step of voltage is in effect a step of input frequency. An alternative method is to apply a step to the external f.m. input of input source, if available. The input to the v.c.o. is taken as the output frequency and displayed on a storage oscilloscope, from which T_s may be calculated. Figure 11 shows a trace of the output from the linear p.l.l. for $\omega_n = 50, 100, 200$ and 400 rad/s. The

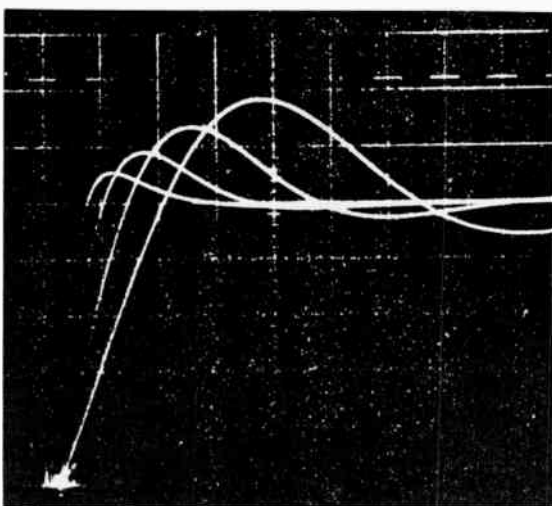


Fig. 11. Trace showing the transient response of the p.l.l.

measured values of T_s at $\omega_n = 100\sqrt{2}$ rad/s are shown in Fig. 3 plotted against K for the linear p.l.l., and at $\omega_n = 100\sqrt{2}$ rad/s and $\xi = 1/\sqrt{2}$ are shown in Fig. 6 plotted against different steps of input frequency. In both plots close agreement with theoretical values is evident.

5 Conclusions

The pseudo-linear region of operation of the phase-locked loop was taken as that where the p.l.l. behaves in essentially a similar manner as the linear model. It was specified from the transient response of the loop as that region of operation where the settling time, after a step in input frequency, does not exceed the settling time of the linear model by more than 10%. By solving the non-linear equation of the p.l.l. on a digital computer, it was possible to map this region in an ω_n versus ξ plane for different values of input steps, y . It was shown that if these input steps are normalized with respect to ω_n , then the normalized value is almost the same for any one value of ξ and, thus it was possible to average the normalized steps over ξ calling it y_n , and obtaining an empirical expression of y_n as a function of ξ only, which turns out to be a linear relationship. This is used as a definition of the upper bound for the pseudo-linear region. It becomes, therefore, possible to specify the maximum step in input frequency which any p.l.l. can accept before the linear analysis breaks down, and how the parameters of the loop (ξ and ω_n) may be modified to increase this region. A practical model was constructed, and showed agreement with the theoretical and digital computer results for the measured value of the settling time. The work is limited to the second-order loop with active filters, which are the types most extensively used, and to which many other types may be approximated. It is hoped that it will stimulate further work to specify the pseudo-linear region for other types of loops.

6 Acknowledgment

The authors would like to express their sincere thanks to the Engineering College Computer Center staff of the University of Baghdad for their great help in completing this work.

7 References

- 1 Viterbi, A. J., 'Acquisition and Tracking Behaviour of Phase-locked Loops', Jet Propulsion Laboratory, External Publication No. 673, July 1959.
- 2 Blanchard, A., 'Phase-locked Loops' (Wiley, New York, 1976).
- 3 Jaffe, R. and Rehtin, E., 'Design and performance of phase-lock circuits capable of near-optimum performance over a wide range of

- input signal and noise levels', *IRE Trans. on Information Theory*, IT-1, pp. 66-76, March 1955.
- 4 Allos, J. E., Al-Araji, S. R., and Ezzet, E., 'Steady state and transient analysis and design of phase-locked loop from the root locus', to be published.
- 5 Gardner, F. M., 'Phase Lock Techniques' (Wiley, New York, 1979).
- 6 D'Azzo, J. and Houpis, H., 'Feedback Control System Analysis and Synthesis' (McGraw-Hill, New York, 1960).
- 7 Viterbi, A. J., 'Principles of Coherent Communication' (McGraw-Hill, New York, 1966).

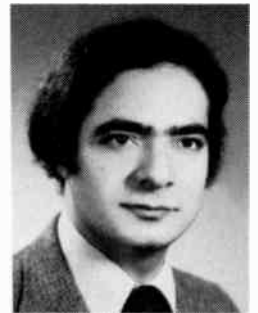
*Manuscript first received by the Institution on 27th May 1980 and in final form on 14th May 1981.
(Paper No. 2005/CC346)*

The Authors

Janan Allos (Fellow 1979) graduated from Battersea College of Technology in 1956 with a B. Sc. (Eng.) degree of the University of London and then spent four years in Daura Refinery, Baghdad. In 1960 he returned to England to study for his Ph.D. degree at Kings College, London and in 1963 went back to Baghdad where he is now Assistant Professor and Computation and Control Research Group Leader. From 1964 until 1978, Dr Allos held positions of Chief Engineer and Technical Director of Forster and Sabbagh Co. (Electronic and Communication Division).



Saleh Al-Araji (Member 1977) was awarded an Iraqi Ministry of Oil Scholarship in 1963, and he gained the B.Sc. and M.Sc. and Ph.D. degrees from the University of Wales in 1968, 1969 and 1972 respectively. After completing his doctorate he participated in the Home Office joint research programme on mobile radio communication at Swansea. He was awarded the Clerk Maxwell premium jointly with Professor W. Gosling in 1976 for a paper entitled 'An automatic clarifier for s.s.b. speech communication'. In 1973 Dr Al-Araji was appointed lecturer at the University of Baghdad where he is now Assistant Professor and Communication and Electronics Research Group Leader.



Ezzett H. Ezzet obtained his B.Sc. and M.Sc. degrees in 1977 and 1979 respectively, from the College of Engineering, University of Baghdad, his M.Sc. work being concerned with the transient response of phase locked loops. He is now an assistant lecturer at the University of Technology in Baghdad.



Optimization of access points for automatic test program generation and fault location in large analogue circuits and systems

M. A. SARRAM, B.Sc., M.Eng., Ph.D.,†

J. HYWEL WILLIAMS, B.Sc.(Tech), Ph.D.,*

Professor D. R. TOWILL, D.Sc., M.Sc.,
B.Sc.(Eng.), C.Eng., M.I.Mech.E., M.I.Prod.E.,
F.I.E.R.E.*

and

K. C. VARGHESE, B.Sc., Ph.D.†

SUMMARY

The paper develops a methodology for the automatic test program generation (ATPG) for a large analogue circuit subject to component drifts. An optimization algorithm developed selects the best set of intermediate access points for a.c. and d.c. tests of the circuit.

During ATPG, faults are simulated by varying each component over a wide range. Voltages measured at all available nodes are thus used in the pre-processing stage of node selection. An optimization procedure based on the discriminating power of measurements and separability between fault signatures is used to select the best set of frequencies applicable for all nodes in a.c. testing. A pre-amplifier and control amplifier of 56 components is chosen as Unit Under Test (UUT) to demonstrate the ATPG. The fault isolation scheme used is based on the nearest neighbour rule.

The relationship between diagnosability and number of test features is shown to follow the customary Pareto type curve. However, four carefully chosen nodes and three carefully chosen test frequencies are shown to give an adequate level of diagnosability. The whole scheme is implemented automatically using a minicomputer interfaced to the UUT.

* Dynamic Analysis Group, University of Wales Institute of Science and Technology, King Edward VII Avenue, Cardiff CF1 3NU.

† Formerly with the Dynamic Analysis Group.

Nomenclature

UUT	Unit Under Test
ATPG	Automatic Test Program Generation
a_{ik}	measurement for k th class at i th feature; also, fault dictionary with $i = 1, 2, \dots M$ features; $k = 1, 2, \dots L$ fault cases
δ	threshold for 'common' attributes
MT	measure of testability
PMT_{dc}	partial measure of testability for d.c.
$R_{nom}(ij)$	nominal response of the UUT, $i = 1, 2, \dots M$ frequencies; $j = 1, 2, \dots N$ nodes
R_{ij}	response of faulty system, $i = 1, 2, \dots M$; $j = 1, 2, \dots N$
Y	measurement vector for an unknown fault
Y_j	deviation vector at j th node
X_{ijk}	recognition matrix, $i = 1, 2, \dots M$ frequencies; $j = 1, 2, \dots N$ nodes; $k = 1, 2, \dots L$ fault cases
X_{ijk}^*	Euclidean normalized matrix of X_{ijk} normalized over i
D_{ij}	discriminatory power of i th frequency at j th node
$d(k_q, k_l)$	separability measure for fault cases k_q and k_l
C_l	confidence level
C_T	total confidence level
C	percentage confidence level
f_{opt}	optimum frequency set
f_{N_1}	test frequency set at node N_1
f^a	frequency set before optimization
d_k	nearest neighbour distance for fault case k
σ	standard deviation of random noise

1 Introduction

The demand for automatic testing and fault isolation in analogue circuits and systems is rapidly increasing in a wide range of industries. This is because substantial cost and time are being expended in manual testing, location, and correction of faults caused by defective material and manufacturing processes. Presently, the desperate shortage of skilled inspectors and repair technicians gives added impetus to the use of ATE to increase workstation throughput, product quality, and productivity generally.

Analogue automatic test program generation (ATPG) should, in principle, provide a software algorithm which receives the circuit or system description as input, and then produces a test program which automatically isolates a failed part.¹ This is a particularly important area of research now that packaging densities of integrated circuits per board are so high that manual test program generation is out of the question.

In fault isolation, there is a tenuous relationship between the provision of access points and increased diagnosability (i.e. the ability to correctly isolate the true fault). Our particular interest is in maintenance testing analogue systems comprising large electro-mechanical and electro-hydraulic components as well as electronic circuits. In some ways testing such systems raises more

severe problems than circuit testing. For example, the provision of additional access points is considerably discouraged, on the grounds that the provision of *any* extra components will degrade reliability.² Also, there is no guarantee that a randomly chosen access point will shed further light on the likely cause of failure. Even a well-chosen access point may be of little value for diagnosis if the noise level is high. Attempts to reduce noise effects by integration will mean a longer test time with consequential increased wear and reduced test station throughput. There is thus a need for the designer to be provided with a means for selecting the minimum number, and indeed, the best set of additional access points. ATPG should be so engineered as to greatly assist this process.

2 Fault Isolation from a Limited Number of Access Points

Over the past few decades a number of approaches for fault isolation in large scale analogue systems from a limited number of measurements have been proposed. These include the use of both time and frequency domain and statistical, non-deterministic and deterministic methods.³⁻⁸ Historical reviews of analogue fault location are available elsewhere^{9,10} and need not be repeated here. In this paper a fault diagnosis scheme which isolates component drift faults via a functional testing approach injecting both d.c. and a.c. signals is used to illustrate how access point selection may be improved.

Catastrophic failures are not considered here. There are a number of schools of thought as to which fault types are most likely to occur, as design, environmental and maintenance crew quality all affect the issue. Our experience is that the uncertainty caused in analogue systems by the combined effects of measurement noise and normal production variances makes drift fault isolation the more complex problem. In contrast, their catastrophic failures are often of such a nature as to rarely require sophisticated test methods.

3 Problem Statement

The problem we seek to solve is: 'given an adequate mathematical model describing an analogue system, including production tolerances and noise levels, what minimum set of test failures should the designer select so as to provide an acceptable level of fault diagnosability?'

In the context of this paper, a test feature is a single measurement data point. Thus at two extremes a four feature set could be four d.c. measurements made at different access points in the system, or gain and phase measurements at two selected frequencies based on single input-output access only. To solve this problem, the designer needs to be provided with ATPG which will provide a numerical measure of the 'worth' of the feature set, so that sufficient confidence can be placed in the test design *before* volume production commences. Additional factors to be considered in ATPG include the most

relevant stimuli for the particular unit under test (UUT), i.e. static testing, swept frequency testing, multi-frequency testing etc., and the test data processing required, both for feature estimation and subsequent fault location.¹¹

In this paper a fault is arbitrarily defined as a change in a component value which results in the system's performance lying outside test gates. Therefore, each component can generate many faults. This definition caters for those system users who believe that an estimate of the value of a failed component is an aid to quality assurance monitoring.

4 Contribution of the Present Paper

The authors feel that the paper will be a useful aid to designers, since it is based on experience gained by a group of engineers on a range of practical systems. The results presented on feature selection using only input-output dynamic measurements have been widely tested by simulation, supplemented where possible by hardware experimentation. There appears to be an acceptable degree of correlation between the diagnosability achieved in large scale simulations, and that predicted *a priori* from data used to select the optimum feature set.

This paper differs fundamentally from some others in the literature in that access points are selected to enhance diagnosability, as distinct from necessarily simplifying computational procedures. It therefore sheds light on the engineering 'worth' of an access point.

D.c. circuits have been less widely studied by the authors, but the UUT considered as an example herein has been implemented in hardware and software form, and considerable experience gained thereon. By choosing a relatively common circuit type, problems of military and commercial confidentiality have been avoided. Although research into test techniques is analogous to hitting a moving target, it is thought that the results will be sufficiently general to withstand at least the immediate effects of galloping obsolescence.

Insofar as the ultimate testing and fault diagnosis of hardware is concerned, we have concentrated on techniques suitable for mini/microcomputer implementation. The same constraint has not been applied at this stage to software developed to provide simulation data for access point optimization. This inefficiency is accepted, and the approach will be refined at a later date.

5 Unit Under Test

The circuit selected as the UUT to demonstrate the access point selection technique developed later in the paper is a pre-amplifier and control amplifier circuit of 56 components. The circuit is shown in Fig. 1 and the component values in Table 1, and it can be used for many applications depending upon the input selector which precedes the pre-amplifier. Together with

additional switching inside the feedback loop the latter is capable of coping with both high and low level signals.^{12,13} The circuit can therefore be optionally matched to any normal input source by selection of fixed resistors and/or equalization networks.

6 Check-out Tolerances

In fault diagnosis, we must first define the demarcation line between 'healthy', i.e. systems in a state of operational readiness, and 'sick', or failed systems. Whereas within digital systems the issue is clear cut (0 or 1), there is a surprisingly wide band of acceptable performance to allow for production tolerances in analogue systems.¹⁴ In contrast to the usual case of assuming parameter independence, we have set check-out tolerances at each node using the worst case method.¹⁵ Circuit analysis is used to determine which end of the tolerance range of a component will cause the worst performance.

After the nominal node voltages have been calculated, the sensitivities of all node voltages with respect to all circuit parameters are estimated. Subsequently (+) indicates that worst high performance is achieved by selecting the component at the upper tolerance limit, whereas (-) indicates that worst-case high performance is achieved by selecting the component at the lower tolerance limit part. Each component value is set at its worst-case performance limit, and the equations are solved with this unique set of parameters to determine worst-case performance.

A unique set of parameters is required for each performance characteristic for the 'worst-case high' and 'worst-case low' situations. This method has been used to set up nodal voltage limits due to component tolerances typically set at 5%.

7 D.C. Modelling

D.c. fault classification concerns only the d.c. level setting part of the circuit. Hochwald and Bastian¹⁶ report a method of fault location using only a d.c. analysis of electronic circuits. However, they have to relate all failures to their d.c. effect and they indicate the need to additionally use a.c. analysis for complex systems. Current measurements have not been used because of the associated complexity of terminal disconnections, particularly on sub-networks which have to be isolated by special electronic partitioning devices such as those described in Reference 17.

A 24 V external supply is needed to set the levels in the circuit in Fig. 1, while the levels in the control amplifier are set by 18 V through the diode Z1. Therefore the whole circuit is considered as two independent subcircuits, d.c. models of which are shown in Fig. 2 in which the nodes are numbered sequentially. This partitioning reduces the modelling task. Also fault isolation on both circuits can be implemented separately if required.

Note:
For component values refer to Table 1

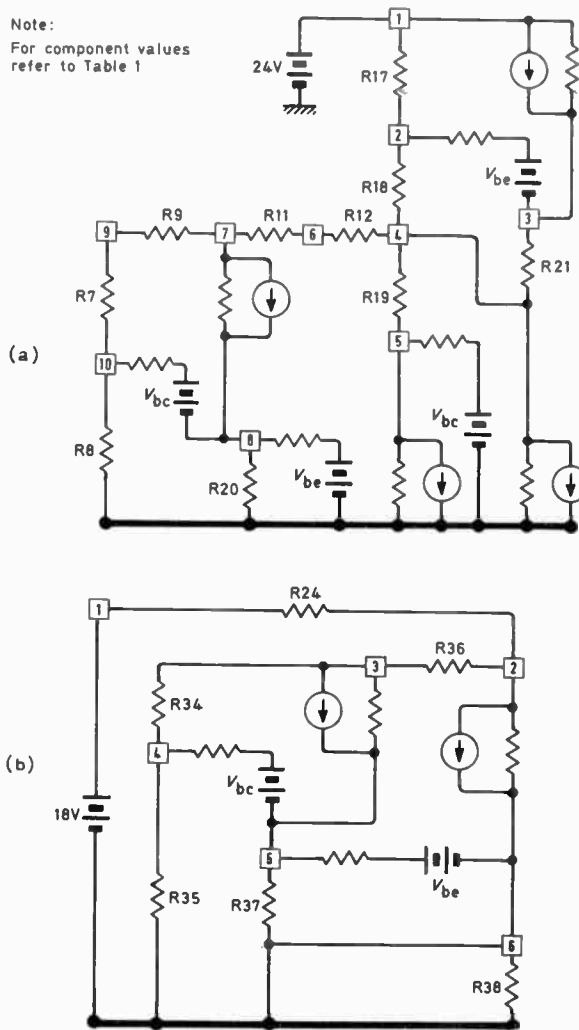


Fig. 2. D.c. models of UUT.

8 Selecting Access Points Using the D.C. Model

It is desirable that the number of access points is kept to a minimum so as to reduce the amount of software, hardware, test time and cost needed. However, for adequate diagnosability, it is not only essential that all likely faults in the circuit be propagated to one or more of the access points, but also their unique fault representation must be maximized. Therefore, it is the amount of discriminatory information between the faults which is of prime importance in selecting the best set of access points.

Suppose we make a measurement of the *i*th feature, for a system with fault *k*, and then with fault (*k* + 1). Then a 'distance measure' showing the separation between these two fault cases is $|a_{ik} - a_{i(k+1)}|$ where *a* is a general symbol or 'attribute' for a measurement of a specific condition. If,

$$|a_{ik} - a_{i(k+1)}| \leq \delta \tag{1}$$

we cannot distinguish the two cases and additional features are required for diagnosis. The threshold δ is

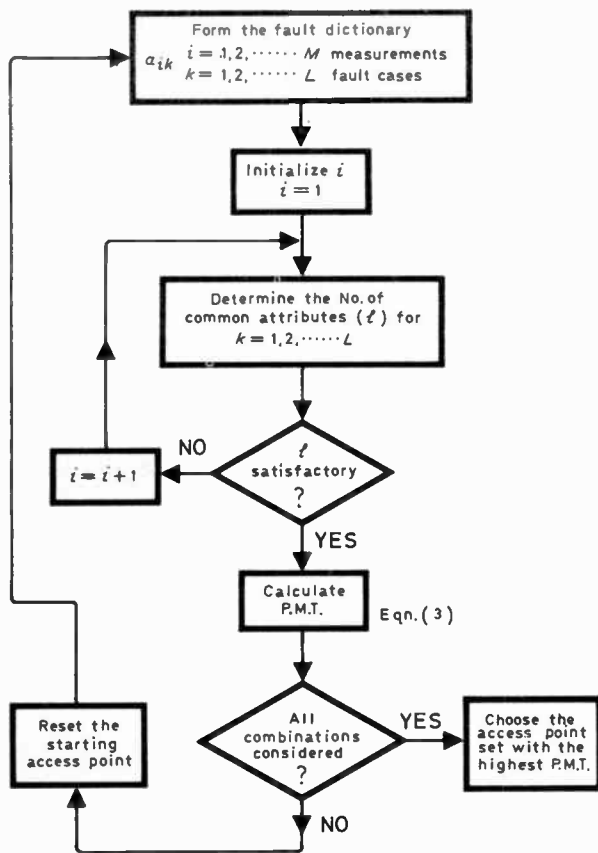


Fig. 3. Flow chart for the selection of access points for d.c. analysis

preset and can be varied, based on the data and required classification level. Also δ can be related to measurement noise and permitted production variation of system components, decreasing with signal-to-noise ratio and increasing for large permissible parameter variations.

A general flow chart for the selection of access points is given in Fig. 3. The fault dictionary indicated is simply a matrix relating the measurements (M in total), to the number of fault cases deemed likely (L in total).

A 'quality factor' or 'performance index' based on testability is incorporated into the access point selection algorithm. Here testability is defined as the characteristic of a design which allows the status (operable or inoperable) of a system or of its subsystems to be confidently determined in a timely fashion.¹⁸ This definition implies satisfactory determination of probable failures and measurements of the likelihood of test success (the correct determination of failed status). One simple measure of testability (MT) is defined as:¹⁹

$$MT = \left[\frac{\text{total number of fault cases propagated by ATPG}}{\text{total number of possible fault cases}} \right] \quad (2)$$

However, in the context of fault diagnosis it is necessary to maximize unique fault representation thereby maximizing the discriminatory information between the fault signatures using d.c. and a.c. approaches. So, to take account of this, the measure of testability in equation (2) is modified and termed partial measure of testability (PMT) defined²⁰ by

$$PMT_{d.c.} = \frac{(\text{total number of fault signatures generated}) - (\text{total number of common fault signatures})}{\text{total number of fault signatures generated}} \quad (3)$$

which is bounded as $0 \leq PMT_{d.c.} \leq 1.0$. This measure is equally applicable to a.c. analysis. The total measure of testability (TMT) is arbitrarily chosen to be the average of the two PMT separately obtained for d.c. and a.c. testing.

9 A.C. Analysis

The a.c. fault isolation scheme for the circuit, the a.c. model for which is shown in Fig. 4, is applied after the d.c. fault analysis phase and directed at those components which are not present in the d.c. analysis.

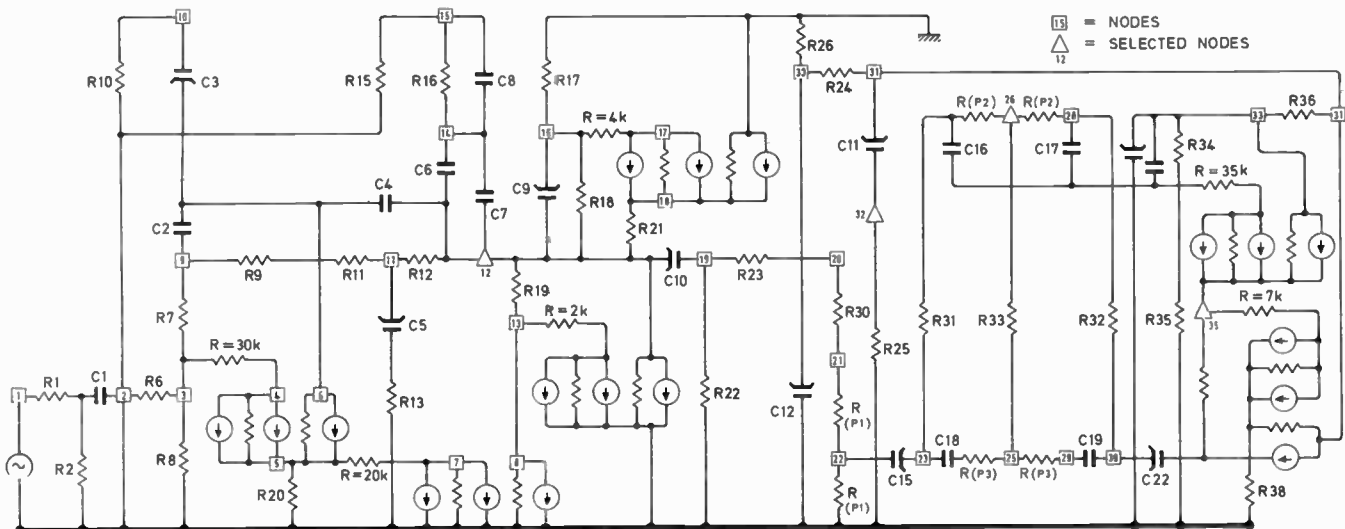


Fig. 4. A.c. model of UUT showing selected access points

The a.c. analysis uses the steady state response of the circuit subjected to sinusoidal excitations carried out at different frequencies over the dynamic range of the circuit.

Although the classical approach of measuring the response of a system to completely define its transfer function is very time consuming for large scale circuits, the a.c. approach, using more than one frequency, does contribute information which much reduces the number of access points needed. Hence, it is important that the number of test frequencies should also be a minimum, and chosen for their discriminatory power between various fault cases. Conversely, the independence of some components to frequency effects inhibits their fault location from input-output dynamic tests, and therefore the need for additional access points is indicated.

10 Setting-up the Recognition Matrix

A recently reported computer-assisted optimization technique for feature selection²¹ is used in the present study for the selection of the best set of test features. For the same purpose, Tinaztepe and Prywes,²² using a program which generates ATLAS coding for the UUT, apply a fault approach to optimize the number of tests. This program is time consuming, and requires engineering expertise in its operation. Although fault location in a specific system is frequently possible, using only input-output frequency domain measurements,²³ for the present paper as the multi-test point approach is required, *the combined set of access points and frequencies chosen must be optimized.*

Let the nominal response of the UUT be

$$R_{nom}(i, j); \begin{matrix} i = 1, 2, \dots M \text{ frequencies} \\ j = 1, 2, \dots N \text{ nodes} \end{matrix} \quad (4)$$

and the response of a faulty UUT be R_{ij} . Then the deviation vectors for the j th access point will be

$$Y_j = (R_j - R_{nom}(j)) \quad (5)$$

For a given fault case k , the deviation vectors are

$$X_{jk} = (R_{jk} - R_{nom}(j)), \quad j = 1, 2, \dots N \quad (6)$$

The deviation vectors for all known fault cases $k = 1, 2, \dots L$ are grouped to form a matrix termed recognition matrix (X_{ijk}) for

$$\begin{matrix} i = 1, 2, \dots M \text{ frequencies} \\ j = 1, 2, \dots N \text{ nodes} \\ k = 1, 2, \dots L \text{ fault cases} \end{matrix} \quad (7)$$

which is considered as the *a priori* information of the UUT for test frequency selection. (X_{ijk}) will be an $(MN) \times L$ matrix.

11 Discrimination between Faults

Optimization in this context is the minimization of the number of frequencies and nodes without losing discriminatory information between fault signatures. A

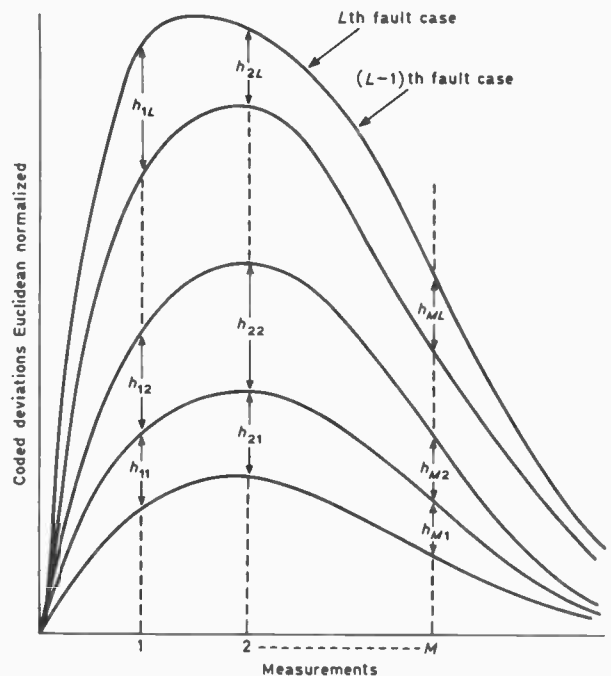


Fig. 5. Calculation of discriminatory information

Discriminatory information given by:

$$D_i = [h_{i1}^2 + h_{i2}^2 + \dots + h_{iM}^2]^{\frac{1}{2}} \quad i = 1, 2, \dots M$$

(see eqn. (8))

Not all combinations are used

'distance' measure for the discriminatory information of the fault signatures in the recognition matrix is one of the criteria used in the optimization algorithm and is defined as

$$D_{ij} = \left[\sum_{k=1}^{L-1} (X_{ijk}^* - X_{ij(k+1)}^*)^2 \right]^{\frac{1}{2}} \quad \text{for } i = 1, 2, \dots M \quad (8) \\ j = 1, 2, \dots N$$

where X_{ijk}^* is the Euclidean normalized matrix of X_{ijk} over i . Normalization is necessary in order to ensure that all quantities are non-dimensionalized and properly scaled. Equation (8) does *not* imply an exhaustive search over all possible combinations of faults, frequencies, and nodes. It is a much restricted definition which considerably reduces computation time during ATPG, but which has been found adequate for feature selection. Figure 5 is a diagrammatic illustration of the calculation of the discriminatory information.

12 Separability and Confidence Level

The separability measure used is a distance measure for calculating information on the separability of fault cases k_q and k_l at each node as follows:

$$d(k_q, k_l) = \left[\sum_{i=1}^M (X_{ik_q}^* - X_{ik_l}^*)^2 \right]^{\frac{1}{2}} \quad (9)$$

There are $L(L-1)/2$ such 'distances' for L fault cases at each node. For the sake of clarity, the calculation of separability measure is illustrated in Fig. 6. Due to

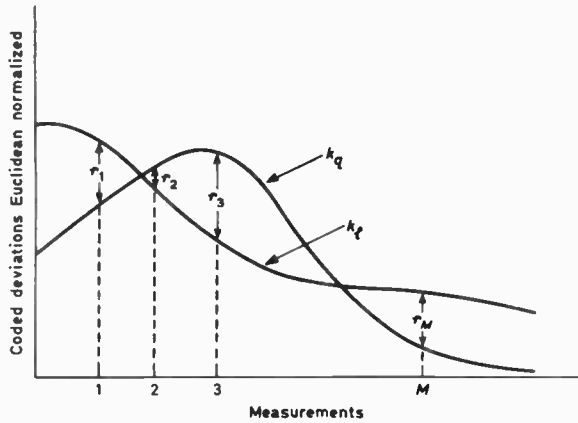


Fig. 6. Separability measure between two fault cases K_q and K_l given by:

$$d(K_q, K_l) = \left[\sum_{i=1}^M (x_{ik_q}^* - x_{ik_l}^*)^2 \right]^{1/2} = [r_1^2 + r_2^2 + \dots + r_M^2]^{1/2}$$

(see eqn. (9))

Euclidean normalization, the range of the separability measure is bounded and is

$$0 < d(k_q, k_l) \leq 2 \quad (10)$$

If for the fault cases k_q and k_l equation (9) becomes zero, the chosen test frequency set is unable to discriminate between those two cases. To complete the frequency selection algorithm of Fig. 7, a confidence level is defined which limits to unity those combinations of fault cases with a high separability measure. The confidence level,

$$C_i = 1 \text{ if } d(k_q, k_l) \geq 1 \\ = d(k_q, k_l) \text{ otherwise} \quad (11)$$

If C_T is the total confidence level for all combinations of fault cases at a node, the percentage confidence level for L fault cases is,

$$C = \left(\frac{C_T}{L(L-1)/2} \right) \times 100 \quad (12)$$

Suppose $N_j, j = 1, 2, \dots, n$ nodes are considered and f_{N_j} represents the optimum set of test frequencies at N_j node, then the optimum set of test frequencies for all nodes is defined for the present study as

$$f_{opt} = [f_{N_1}, f_{N_2}, \dots, f_{N_n}]^T \quad (13)$$

i.e. the optimum set is defined as the selected test frequencies which are common for all nodes considered.

13 Test Point Selection in the A.C. Approach

Having selected the optimum set of test frequencies it is necessary to minimize the number of nodes required to be monitored for the fault diagnosis scheme. An algorithm similar to the d.c. approach is used to select the best set of test points. However, the a.c. analysis has the additional information from the application of various test frequencies and therefore the modification to

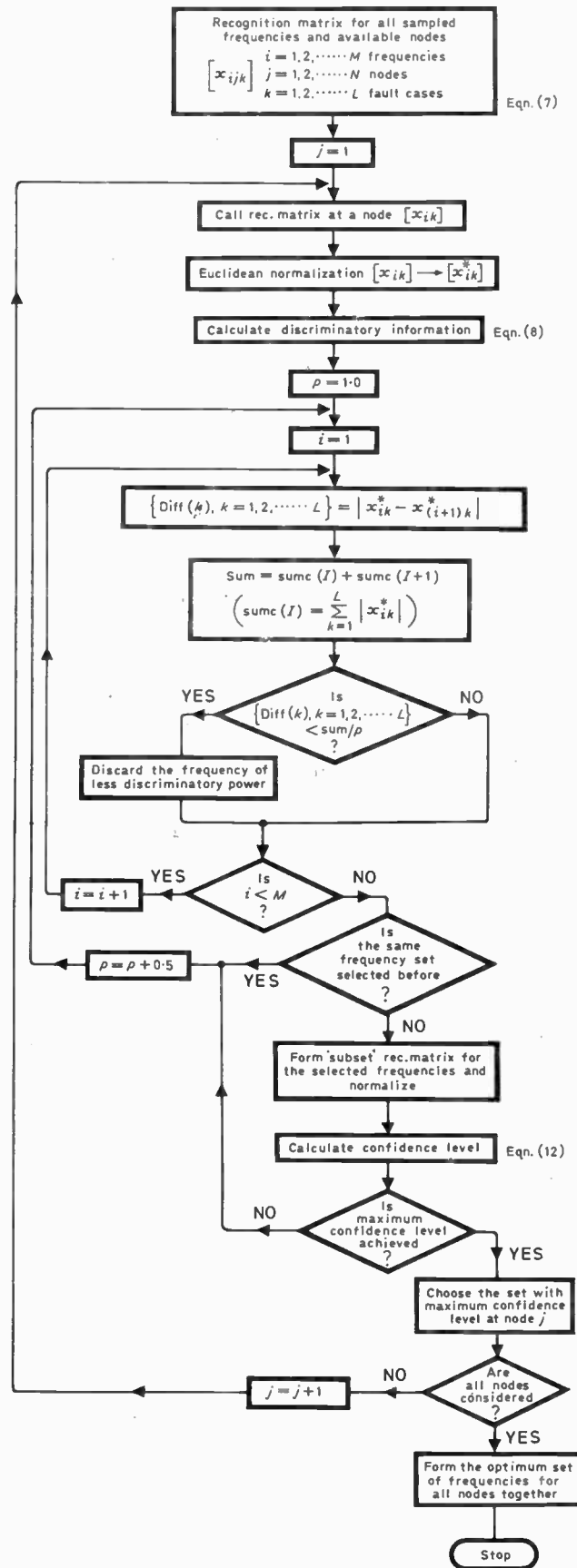


Fig. 7. Flow chart for the optimization of test frequencies

Fig. 3 is that nodes are added only after determining 'common' attributes based on all optimum test frequencies.

14 Test Point Selection for the Pre/Control Amplifier

An ECAP software package²⁴ has been used to calculate the node voltages. This package enables the d.c. and a.c. nodal voltages of a given circuit to be calculated. The user can also increment any parameter and sample from a given statistical defined population. Jagodnick and Wolfson²⁵ have reported a development of ISPICE which gives the operator the opportunity of building in a constraint on the changes in a particular parameter. However, the development is restricted to simulating fault nodal voltages and not their selection. Although the pre-amplifier and control amplifier are not separable in the a.c. analysis, due to the independency of d.c. supply voltage requirements they are considered as two independent subcircuits for d.c. analysis as shown in Figs. 2(a) and (b). In the d.c. approach, the computer simulation of both circuits is carried out in parallel. The selection of the best set of test nodes is based on the sensitivity analysis (fault simulation) of components in the circuit. For the present study the fault dictionary so formed is a grouping of a coded version of the node voltages for known component faults imposed. To provide an accurate software/hardware comparison, each component value has been varied from -90% to +90% of its nominal value in increments of 10%.

This fault dictionary, although large, would enable the designer to consider all likely drift faults. In this simulation, each parameter has 18 fault cases resulting in 18 features, but those drift faults which do not produce response deviations and/or whose deviations in response do not vary from others are eliminated, which reduces some of the redundancy in the matrix. The maximum and minimum voltages at each node are noted from the matrix and the interval is subdivided and coded sequentially.

It is not essential that the sub-intervals for coding be equal but the number of sub-intervals is important. Although increasing the number of sub-intervals increases the cost of software, selection of small intervals provides a better chance of creating unique fault signatures. In this study, if the deviation in response is near the nominal response, a sub-interval is created and coded for every deviation range of approximately 2% of the nominal response value. For a larger response deviation, a sub-interval is formed only for a deviation range of 10% from the nominal response value. This variable range assists detection of fault cases causing similar deviations to have unique representation due to small drifts in component values.

A coded fault dictionary for the pre-amplifier and control amplifier using voltage measurements at 9 and 6 nodes respectively is formed. The fault dictionary has 79

coded fault signatures for the pre-amplifier and 72 for the control amplifier. Note that for d.c. analysis the pre-amplifier has 8 components considered while the control amplifier has 6 components which originally gave 144 (8 × 18) and 108 (6 × 18) fault signatures simulated as explained earlier. Redundant signatures for each component are eliminated to give the reduced number of signatures.

The algorithm described in Fig. 3 is applied to the fault dictionaries and selects various sets of nodes.

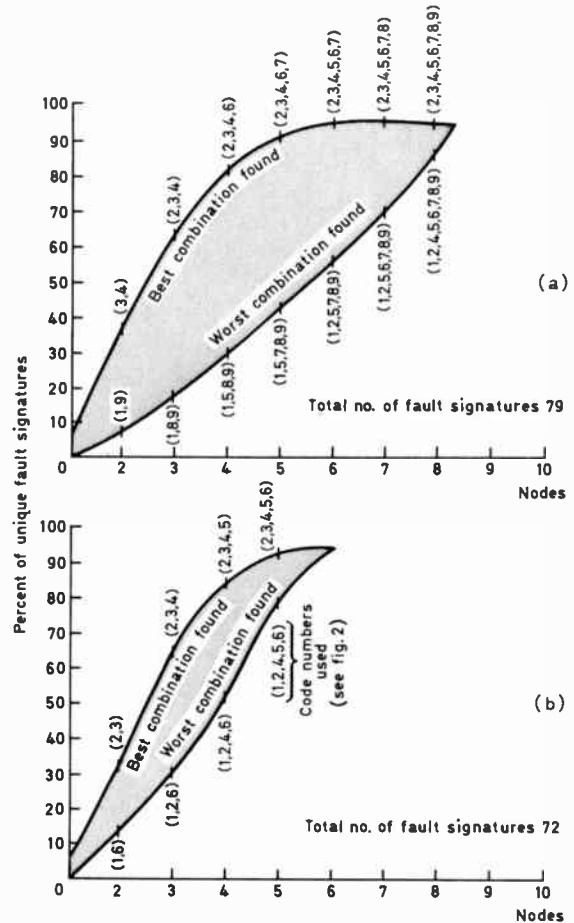


Fig. 8. Percentage of unique fault signatures achieved in d.c. analysis

During use the algorithm considers all combinations of the nodes and the $PMT_{d.c.}$ calculated is used to select the best set of access points. Figure 8 shows the percentage of unique fault signatures achieved and the effect of choosing the best or worst node combinations. Graphs of Fig. 8(a) and (b) follow similar shapes. In both cases, the percentage of unique fault signatures levelled off at 5 nodes for the best combination found during the search algorithm. Nodes (2, 3, 4, 6 and 7) for the pre-amplifier and nodes (2, 3, 4, 5 and 6) for the control amplifier from Fig. 2, are chosen as the best combinations. A reduction of 4 nodes is achieved for the pre-amplifier while the number of nodes required for fault diagnosis of the control amplifier is reduced by one only from the original 6 nodes. One of the advantages of the approach for node

selection adopted here is that nodes can be chosen for a specified percentage of unique fault signatures. For example, if slightly in excess of 80% of unique fault signatures is considered satisfactory for the ATPG of the preamplifier, 4 nodes are sufficient.

15 Frequency Selection

The application of the a.c. approach on the UUT involves test frequency optimization and node selection. The a.c. model of the circuit is shown in Fig. 4 with the nodes numbered sequentially. It is essential to consider the pre-amplifier and control amplifier together.

The nominal frequency response of the pre-amplifier and control amplifier is reasonably flat over the specified frequency range of 20 Hz to 25 kHz. The large amount of computer time needed to calculate the response at many frequencies restricts the number which can be selected even before the optimization. Eight frequencies are chosen to demonstrate the optimization algorithm and are represented by the vector

$$f^a = [20, 100, 300 \text{ Hz}, 1, 3, 5, 10, 25 \text{ kHz}]^T \quad (14)$$

16 An Example of Setting Up the Recognition Matrix

In order to illustrate the formation of the recognition matrix and subsequent fault diagnosis, components R10, R13, R23, R25, R30, R31, R32, C15, C16, C17, C18, C19 and C20 are varied by $\pm 50\%$ while the other components are held at their nominal values. The deviation of the then faulty system response from the nominal response is evaluated at all nodes for the above eight frequencies. Only the amplitude ratio information has been used here, although phase information can also be added to enhance diagnosability.

The deviation vectors evaluated are grouped to form the recognition matrix. Similar matrices are formed for

all nodes. The optimization algorithm shown in Fig. 7 is applied to each matrix and the final optimum set

$$f_{opt} = [300 \text{ Hz}, 1000 \text{ Hz}, 10 \text{ kHz}]^T \quad (15)$$

selected according to equation (13).

17 Node Minimization—A.C. Approach

The minimization of nodes is carried out in the same way as the d.c. approach outlined in Section 8. Figure 9 shows the percentage of unique fault signatures for the best and worst combinations of nodes. Nodes 12, 26, 32 and 35 with three frequencies of equation (15) are selected for the application of fault diagnosis giving a total confidence level of 92%.

It can be seen from Fig. 9(c) corresponding to the best combination of access points and test frequencies, that an increase of the number of access points from 4 to 8 did not give any noticeable increase in the percentage of unique fault signatures, thus obeying a typical 'Pareto' law, i.e. a large increase in resources does not result in a corresponding increase in effectiveness. Also, the asymptotic level in the percentage of unique fault signatures may well be achieved only for the best combination of access points and test frequencies.

18 Fault Diagnosis Results

To show that the selected 4 node, 3 frequency test is satisfactory, 7 components are considered faulty in turn and a pattern recognition approach is used to achieve diagnosis. We proceed as follows; if

$$y = [y_1, y_2, \dots, y_M]^T \quad (16)$$

is a measurement vector due to an unknown fault and

$$a_{ik} \quad \begin{matrix} i = 1, 2, \dots, M \text{ measurements} \\ k = 1, 2, \dots, L \text{ faults} \end{matrix} \quad (17)$$

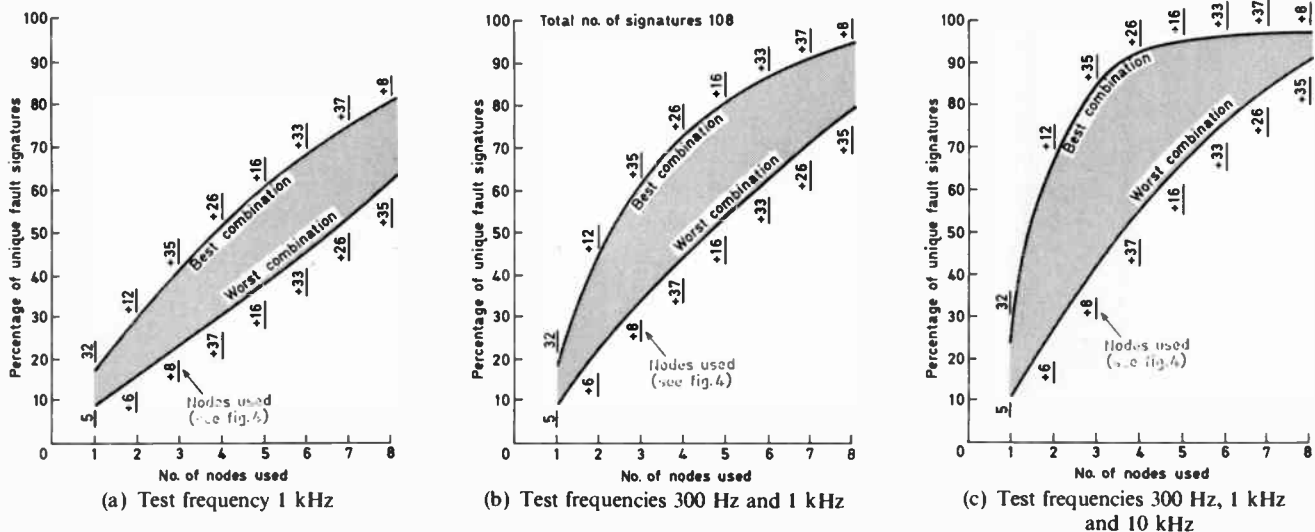


Fig. 9. Percentage of unique fault signatures obtained for best and worst combinations of access points

is a matrix formed by grouping measurement vectors of known faults, then 'distances' between the unknown fault and the known faults are formulated as

$$d_k = \left[\sum_{i=1}^M (x_{ik} - y_i)^2 \right]^{1/2}, \quad k = 1, 2, \dots, L \quad (18)$$

Using the nearest neighbour rule the most likely fault is that with minimum d_k .

The verification of the procedure is carried out by imposing typical faults on the actual circuit of the pre-and control amplifier. In the d.c. approach faults were imposed on R17, R11, R20 and R18 for the pre-amplifier and R37, R36 and R38 for the control amplifier. The coded fault dictionary at the selected nodes is *a priori* formed and nearest neighbour distances calculated for the coded measurement vector due to the imposed fault. All faults imposed on the pre-amplifier and R37 and R38 on the control amplifier were correctly classified based on the minimum distance. However, the 'distance' calculated for the measurement vector due to the imposed fault on R36 was found to be the same for representative vectors in the dictionary for R36 and R37.

A similar procedure was employed for the verification of the a.c. approach and the results are tabulated in Table 2. Fault dictionaries for the four selected nodes and at each of the three chosen frequencies are formed and coded. If d_{k_1} , d_{k_2} and d_{k_3} are the nearest neighbour distances for faults at frequencies f_1 , f_2 and f_3 respectively then

$$d_k = (d_{k_1} + d_{k_2} + d_{k_3}) \text{ for } k = 1, 2, \dots, L \text{ fault cases} \quad (19)$$

The most likely fault is the one for which d_k is a minimum.

19 Effect of Measurement Noise on Diagnosability

In order to study the effect of measurement noise on diagnosability, random noise of varying levels is imposed on node voltage measurements and this fault isolation

Table 2

Some fault diagnosis results using a.c. test measurements on actual hardware

Faults Imposed	Diagnosis Obtained
R30	correct
C18	within group† {C18; R31; R32}
C19	correct
R25	correct
C20	correct
R10	within group† {R13; R10}
R13	within group† {R13; R10}
R32	correct

† Equal minimum distance to each fault case

technique applied. Random noise with nominal node voltage as mean, with standard deviation (σ) equal to 1%, 2% and 3% of nominal is imposed. One hundred simulations were carried out for each fault imposed at each level of noise and the diagnosability (i.e. percentage of correct diagnosis) calculated. For example, a fault in R30 is simulated and the voltages at the selected nodes are calculated. Measurement noise is imposed on these voltages by sampling measurement noise of standard deviation σ from a normal population. Fault diagnosis is now carried out. This is repeated 100 times (note that the imposed fault on R30 is the same) and diagnosability calculated as a percentage, which is (correct diagnosis/no. of simulations) \times 100, as listed in Table 3.

Table 3

Effect of measurement noise on diagnosability via simulation

Faults Imposed	Standard Deviation of Measurement Noise σ		
	1%	2%	3%
R30	80%	73%	58%
R15	100%	98%	97%
R13	100%	85%	67%
C20	100%	88%	75%
R10	100%	83%	78%
R31	97%	89%	70%
C18	76%	69%	49%
C19	75%	66%	46%
R32	97%	85%	87%
C17	98%	78%	69%
C16	100%	69%	53%
R23	100%	80%	79%

20 Ambiguity Groups

In any large analogue circuit there can be many components, the effect of whose variations on performance is indistinguishable from each other. Prior to setting up a fault diagnosis procedure, it is useful to identify and group such components to form ambiguity groups which could then be used to enhance diagnosability. Complex grouping criteria have been discussed in the literature.²⁶ Application of these techniques to the present UUT is under further investigation.

21 Automation of On-line Computer Implementation of Fault Diagnosis Scheme

The fault isolation procedure for the pre-amplifier and control amplifier has been implemented at an automatic test station using a minicomputer. This necessitated the design of special interface units.²⁰ A block diagram of the whole procedure is shown in Fig. 10. The computer program for access point selection, test frequency selection, and fault isolation procedure were written in FORTRAN. Additional to the main program, a sub-routine was written in MACRO²⁷ to read the measured

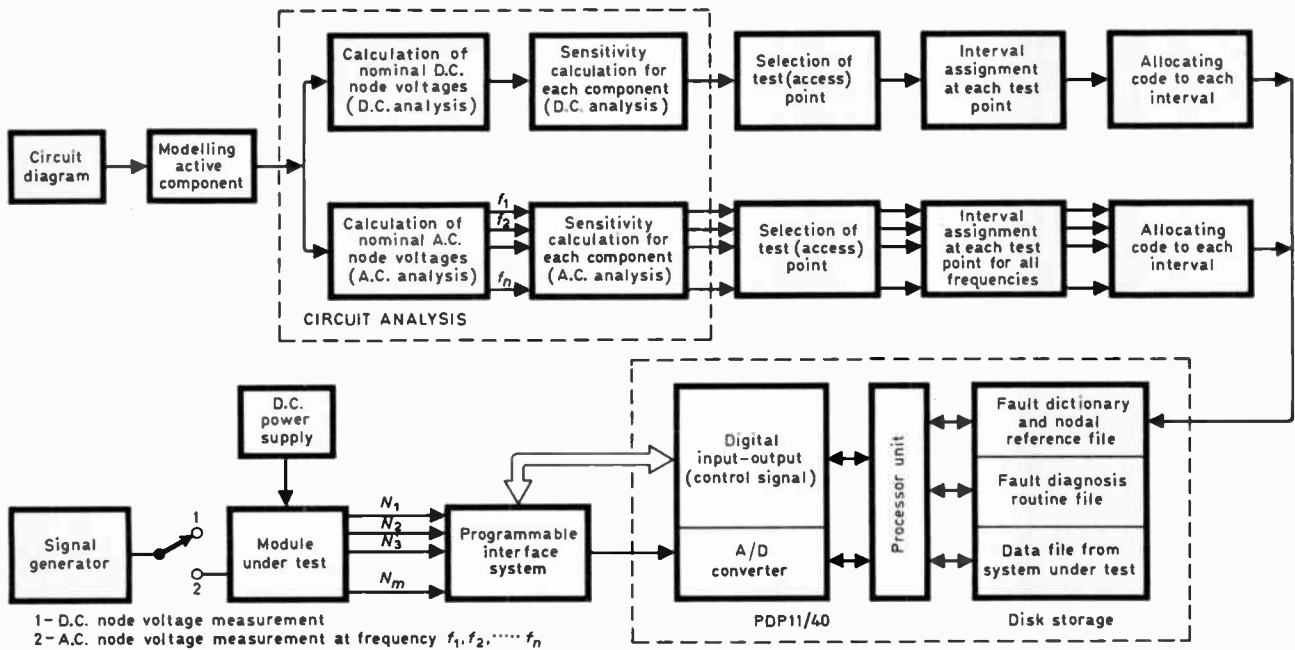


Fig. 10. Minicomputer-based automatic fault diagnosis facility

analogue and digital data from the laboratory peripheral system to the main program. Automatic fault location is implemented in two phases, namely d.c. and a.c. approaches. If the first phase of the testing does not identify the fault, then the second phase of the test is implemented.

The interface is a fundamental requirement of a fully automatic fault location scheme. Node voltages of the circuit are measured in sequence using software controlled digital outputs of the computer addressing an analogue multiplexer. In addition the gain setting of the output voltage from the interface is monitored automatically.

22 Conclusions

A fault diagnosis scheme for large-scale analogue circuits has been developed, based on a limited number of node voltage measurements to isolate drift faults to component level. Procedures for the selection of the best set of test points for d.c. and a.c. approaches have been developed and an optimization algorithm for the selection of test frequencies has been successfully applied. The techniques developed were applied to a hardware amplifier and control amplifier circuit and the whole procedure was automated using a minicomputer.

23 References

- Plice, W. A., 'Automatic generation of fault isolation tests for analog circuit boards—a survey', presented at ATEX EAST '78, Boston, MA, September 1978.
- Garzia, R. F., 'Fault isolation computer methods', NASA Contractor Report CR-1758, February 1971.
- Sriyananda, H., Towill, D. R. and Williams, J. H., 'Voting techniques for fault diagnosis from frequency domain test data', *IEEE Trans. on Reliability*, R-24, no. 4, pp. 260-7, October 1975.
- Sriyananda, H. and Towill, D. R., 'Fault diagnosis using time domain measurements', *The Radio and Electronic Engineer*, 43, no. 9, pp. 523-33, September 1973.
- Varghese, K. C., 'Optimization of feature selection and fault diagnosis in analogue systems', M.Eng. Dissertation, UWIST, Cardiff, 1977.
- Trick, T. M., Mayede, W. and Sakla, A. A., 'Calculation of parameter values from node voltage measurements', *IEEE Trans. on Circuits and Systems*, CAS-26, no. 7, pp. 466-74, July 1979.
- Schreiber, H. H., 'A state space approach to analog automatic test generation', Proc. 1977 National Aerospace Electronics Conf., IEEE No. 77, CH 1203-9 NAECON.
- Lee, J. and Bedrosian, S. D., 'Fault isolation algorithm for analog electronic systems using the fuzzy concept', *IEEE Trans.*, CAS-26, no. 7, pp. 518-22, July 1979.
- Towill, D. R. and Varghese, K. C., 'Analogue system fault location—past, present and future', Proc. Automatic Testing, Brighton, England, December 1979.
- Duhamel, P. and Rault, J. C., 'Automatic test generation techniques for analog circuits and systems: a review', *IEEE Trans.*, CAS-26, no. 7, pp. 411-40, July 1979.
- Schreiber, H. H., 'AATPG classification and recommendations for development ground rules', Proc. Analog Automatic Test Program Generation Workshop, IEEE Circuits Systems Society, 1977.
- Uzunoglu, V., 'Feedback and impedance level in transistor circuits', *Electronic Equipment Engineering*, pp. 42-3, July 1962.
- Blackman, R. B., 'Effect of feedback in impedance', *Bell Syst. Tech. J.*, 22, no. 3, pp. 269-77, October 1943.
- Payne, P. A., Towill, D. R. and Baker, K. J., 'Predicting servomechanism dynamic performance variation from limited production test data', *The Radio and Electronic Engineer*, 40, no. 8, pp. 275-88, December 1970.
- The 1620 Electronic Circuit Analysis Program (1620-EE-02X) User's Manual, White Plains, N.Y., International Business Machines Corp., 1965, pp. 160-5.
- Hochwald, M. and Bastian, J. D., 'A d.c. approach to analog fault dictionary determination', *IEEE Trans.*, CAS-26, no. 7, pp. 523-9, July 1979.
- Zielonko, R., Kralikowski, B. and Hodge, J., 'Fault identification in analogue electronic modules with measurement at external terminals', Proc. VII IMEKO Conf., 1965, pp. AQC 122-1 to 122-10.

- 18 Dejke, W. J., 'A review of measures of testability for analogue systems', Proc. 1977 AUTOTESTCON, November 1977, pp. 279-84.
- 19 Temes, G., 'Large-change sensitivities for linear digital networks', 20th Midwest Symposium on Circuits and Systems, August 1977, Texas Tech. University.
- 20 Sarram, M. A., 'Fault diagnosis in large scale analogue circuits', Ph.D. Thesis, UWIST, Cardiff, 1978.
- 21 Varghese, K. C., Williams, J. H. and Towill, D. R., 'Computer aided feature selection for enhanced analog system fault location', *Pattern Recognition*, 10, no. 4, pp. 265-80, 1978.
- 22 Tinaztepe, C. and Prywes, N. S., 'Generation of software for computer controlled test equipment for testing analog circuits', *IEEE Trans.*, CAS-26, no. 7, pp. 537-48, July 1979.
- 23 Varghese, K. C., Towill, D. R. and Williams, J. H., 'ATPG for an analog pitch rate compensation unit using only input-output frequency domain measurements', Proc. 1979 AUTOTESTCON, Minneapolis, MN. September 1979.
- 24 Jensen, R. W. and Liberman, M. D. 'IBM Electronic Circuit Analysis Program Technique and Applications', pp. 1-5, (Prentice-Hall, Englewood Cliffs, N.J., 1968).
- 25 Jagodnik, J. E. and Wolfson, M. S., 'Systematic fault simulation in an analog simulator', *IEEE Trans.*, CAS-26, no. 7, pp. 549-57, July 1979.
- 26 Varghese, K. C., Williams, J. H. and Towill, D. R., 'Simplified ATPG and analog fault location via a clustering and separability technique', *IEEE Trans.*, CAS-26, no. 7, pp. 496-505, July 1979.
- 27 RT-11 System Reference Manual, 'MACRO Assembler', Digital Equipment Corporation, Maynard, MA. Chapter 5.

*Manuscript first received by the Institution on 4th February 1980 and in final form on 26th January 1981.
(Paper No. 2006/M122)*

min m.i.s. Schottky barrier solar cells—a review

Y. W. LAM, B.Sc., Ph.D., F.Inst.P.,
C.Eng., F.I.E.E.*

SUMMARY

Problems inherent in conventional p-n junction solar cells are discussed. The principle of operation of min m.i.s. solar cells is then described. Among other advantages it is shown that the min m.i.s. solar cells are capable of giving a much higher V_{oc} compared to the p-n junction solar cells. Problems associated with the min m.i.s. solar cells are also discussed. These include the incompatibility of light transmission and conductivity properties of the metal contact in the case of the contact covering the whole of the top surface, the contact linewidth/space ratio in the case of grating cells, resistivity dependence of V_{oc} and degradation of cell performance in time.

1 Introduction

Various methods exist for the conversion of solar energy to electricity, but the one that holds the best promise is the photovoltaic cell, usually known as the solar cell. The solar cell is a semiconductor junction device which converts sunlight directly to electricity. The semiconductor mostly used is single-crystal silicon, and the type of solar cell that has so far received the most attention is the p-n junction. Other semiconductors currently studied for solar cell fabrication include GaAs and CdS. Work is also in progress on polycrystalline and amorphous solar cells. Recently, very high efficiency (18.3%) has been obtained for the grating type minority carrier metal-insulator-semiconductor (min m.i.s.) solar cell. This paper discusses the principle of operation and properties of min m.i.s. solar cells as contenders to the conventional p-n-junction solar cells.

2 p-n-Junction Solar Cell

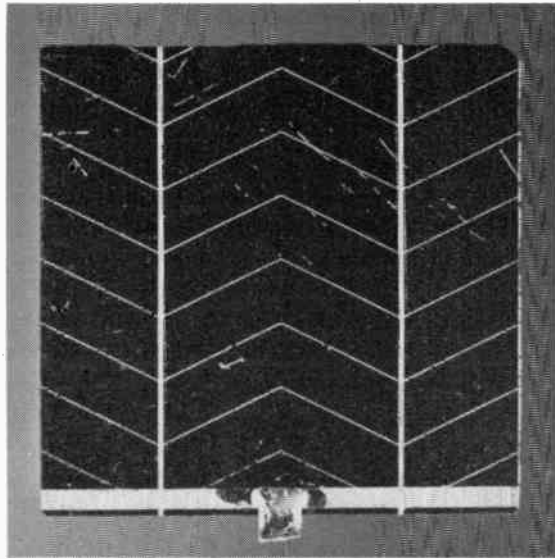
Figure 1(a) shows a p-n-junction solar cell. A metal grid on the top surface helps lower the series resistance and forms one of the two output contacts; the entire metallized bottom surface forms the other contact. This cell measures 2 cm × 2 cm and has an open-circuit voltage of 0.56 V and a short-circuit current of about 120 mA under AM1† conditions of illumination. Figure 1(b) shows a cross-sectional diagram of the cell. The top n-diffused layer is very thin, typically 0.3 μm and phosphorus-doped, so that the junction is formed very close to the surface. Since the generation rate of electron-hole pairs falls off exponentially as a function of distance from the surface due to absorption and the effective carrier collection is about a diffusion length on either side of the junction depletion layer, a junction close to the surface will ensure maximum efficiency of operation.

However, making the junction shallow increases the series resistance of the cell since the current generated has to flow to the grid contact through the n-type diffused layer. In order to reduce this series resistance an alternative to having a relatively deep junction is to increase the doping of the top layer. This, unfortunately, increases the recombination rate and thus lowers the carrier lifetime in this very important top region¹ and creates what is normally known as a 'dead layer'. As this is a region of maximum carrier generation, the existence of the dead layer greatly lowers the carrier collection efficiency and reduces the short-circuit current I_{sc} . The large recombination rate in the top layer also lowers the open-circuit voltage, V_{oc} , through the increase in the saturation current, I_0 . Another factor that causes an increase in saturation current is the narrowing of the semiconductor bandgap due to excessive doping.

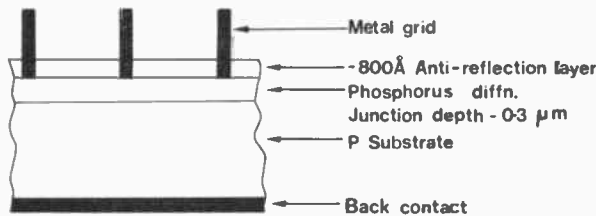
Another problem associated with p-n junction solar cells is the preferential diffusion of dopants through grain

* Department of Electronics, The Chinese University of Hong Kong, Shatin, N.T., Hong Kong

† AM1: Sea level at noon on the equator. In practice the conditions are established by reference to a secondary standard.



(a) A p-n-junction solar cell



(b) Cross-sectional diagram of the solar cell.
Fig. 1.

boundaries when polycrystalline materials are used. This preferential diffusion has the tendency of short-circuiting the junction formed and results in a low V_{oc} .

It is thus clear that there are problems inherent in the p-n-junction structure that are not easily resolved. The m.i.s. solar cell, to be discussed in the following Section, can in principle overcome some of the problems mentioned above and provide additional advantages such as simplicity of fabrication.

3 Min M.I.S. Solar Cell

In the m.i.s. solar cell I is a thin insulator of SiO_2 ($< 20 \text{ \AA}$). The development of the m.i.s. solar cell originated from the Schottky-barrier solar cell.²⁻⁴

A Schottky barrier is a metal-semiconductor contact with rectifying properties. Because the high-temperature diffusion step is not required, the process is particularly suited to polycrystalline solar cell fabrication which has proved to be difficult in conventional p-n junctions due to junction shorting by preferential diffusion of impurities through grain boundaries. Figure 2 shows the $I-V$ characteristics of a Schottky barrier in the dark and under illumination. Ideally the illuminated characteristics are those in the dark displaced downwards. In the same diagram the characteristics of a p-n junction in the dark as well as under illumination are also shown. In comparing the two sets of characteristics it may be seen that the Schottky barrier gives a lower I_{sc}

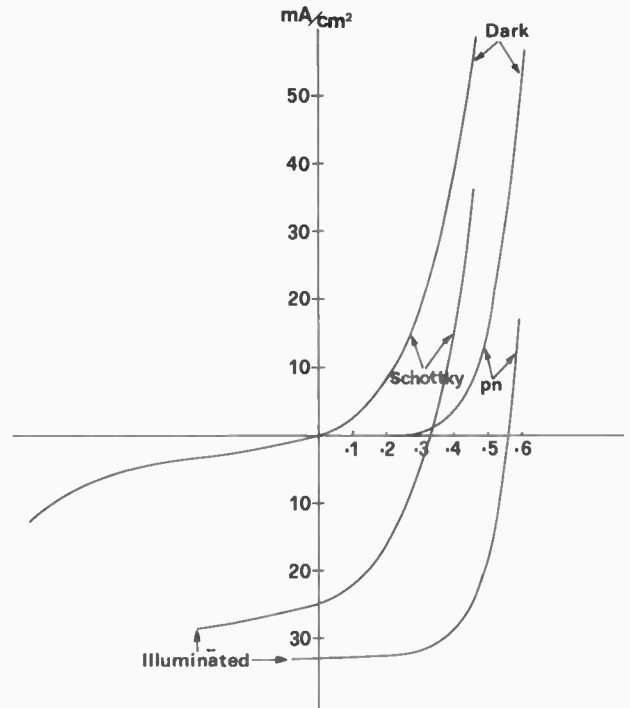


Fig. 2. $I-V$ characteristics of a Schottky barrier and a p-n-junction solar cell in the dark and under illumination.

and a considerably smaller V_{oc} . The lower I_{sc} is due mainly to the absorption of light by the semitransparent metal layer which forms the Schottky barrier (Fig. 3), and to surface states at the metal-semiconductor interface. The low V_{oc} is attributed to the basic operation principle of the Schottky barrier as a majority-carrier device.

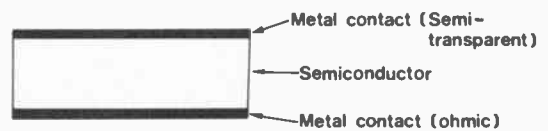


Fig. 3. A Schottky-barrier solar cell.

The incorporation of a thin insulating layer between the metal and semiconductor seems to have multiple effects towards the improvement of V_{oc} .⁵⁻⁷ First, as shown in Fig. 4 the insulating layer introduces an extra voltage drop $\Delta\phi$ and therefore reduces I_0 . The open-circuit voltage is given by

$$V_{oc} = \frac{nkT}{q} \ln \left\{ \left(\frac{I_{sc}}{I_0} \right) + 1 \right\} \quad (1)$$

Thus, reducing I_0 increases V_{oc} .

Secondly, the existence of the insulating layer markedly reduces the forward-bias dark current of the cell. This is illustrated in Fig. 5. The forward-bias current is mainly a majority current whose transport through the junction is strongly affected by the transport properties of the insulating layer. There is a small minority current

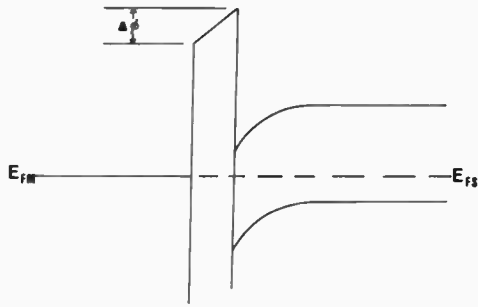


Fig. 4. Band diagram of an m.i.s. cell.

component, however, that is controlled mainly by diffusion. Until the oxide is over a certain thickness, about 20 Å, the diffusion mechanism remains the controlling factor for the transport of minority carriers; above this critical thickness tunnelling becomes an important controlling factor. Hence the introduction of the insulator can substantially reduce the majority-carrier component of the current and if the thickness of the insulator is less than, say, 20 Å the minority-carrier current is relatively unaffected.

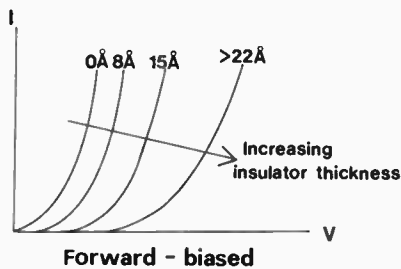


Fig. 5. Dark forward-biased IV characteristics of an m.i.s. cell as a function of insulator thickness.

Thirdly, it is well known that a Schottky barrier often measures the same barrier height irrespective of the metal work function. This is because the Fermi level is pinned (stabilized) to a fixed level at the semiconductor surface by the high density of interface states between the metal and semiconductor.⁸ It is also well known that an oxide layer provides anchorage for some of the dangling bonds and thus effectively frees the Fermi level which can then take up a position as determined by the relative magnitudes of the metal and semiconductor work functions.

Finally, the Fermi level having been freed from the pinning effect of the interface states, a metal with an appropriate work function may be chosen so as to create an inversion at the semiconductor surface. This further reduces the majority-carrier component of the current and converts a principally majority-current Schottky

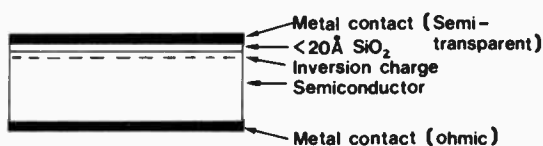


Fig. 6. An m.i.s. solar cell.

device into a minority-current (min) m.i.s. device. The junction in this device is an induced one, as shown in Fig. 6. Since it is now a minority-current device it behaves in almost every respect as a conventional p-n junction, and as such it is expected to give the same efficiency of energy conversion.

Figure 4 shows the band diagram of such a junction for a p-type semiconductor. A little consideration will show that for maximum inversion of the semiconductor surface a low work-function metal must be used with p-type semiconductors and a high work-function metal with n-type semiconductors. Candidates for metals in p-Si m.i.s. are Mg, Al and Ti, and for metals in n-Si m.i.s., Au, Ni and Pd.

3.1 The Metal Contact

In principle an m.i.s. solar cell should have the contact metal covering the entire surface of the cell. To let sufficient light through to the semiconductor the metal must be made very thin (< 100 Å). However, such a thin metal film will have a high sheet resistance, and to make a metal film with good conductivity and reasonable transmission properties would require very critical control of its thickness and purity of the metal. At a thickness of less than 100 Å the reproducibility can be a problem. Furthermore, unless well passivated, it does not take long for the metal to become oxidized right through the film.

3.2 Transparent-oxide Heterojunction

An alternative to the use of a metal top contact is a transparent oxide such as SnO₂.⁹ The electron affinity of SnO₂ is about 4.85 eV and should be sufficient to invert the surface of n-type silicon as shown in Fig. 7.

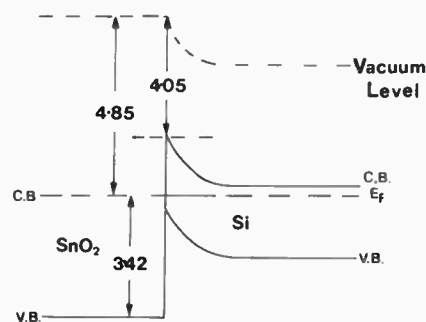


Fig. 7. Band diagram of an SnO₂-Si heterojunction.

Experience has shown, however, that SnO₂ alone does not give sufficiently low sheet resistance and to improve the situation the film is often doped with indium. Unfortunately, like metal films, conductivity and transmission are incompatible properties, i.e. a high conductivity invariably means low transmission and vice-versa, and in practice a compromise has to be accepted. The SnO₂ film, with a refractive index of 1.9–2.2, is itself an ideal antireflection layer between air and silicon and thus represents the saving of one step in the fabrication process.

3.3 Grating M.I.S. Cell

An alternative to having the metal over the entire surface is the grating structure shown in Fig. 8. Underneath the metal grating inversion results as a consequence of the metal work function. The metal grating has a thickness of 1–4 μm and thus will absorb all the light falling upon it. Its function here, therefore, only serves to create an induced p-n junction for carrier collection. The active part of the cell where carriers are actually generated is the area between the grating lines. Means must be

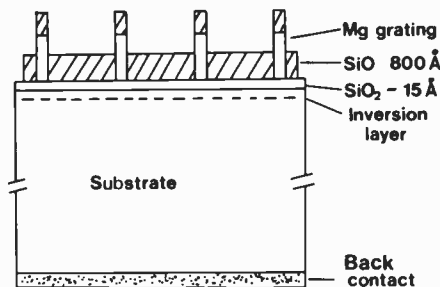


Fig. 8. An m.i.s. grating structure.

provided, therefore, for the semiconductor in this area to be inverted. A convenient way to do this is to select an insulator to cover the semiconductor surface; the insulator chosen must have the right refractive index so as to serve as an antireflection layer and contain the right kind of charge so as to invert the semiconductor surface underneath.^{10,11} SiO seems to serve the purpose well. It can be evaporated in vacuum and if the rate of evaporation is low the resulting SiO layer is found to contain sufficient positive charge which is required for the semiconductor surface inversion. SiO is by no means the only insulator suitable for this application, but because of its refractive index of 1.9 which is ideal as an antireflection layer of the λ/4 type, and the fact that it can easily be deposited by evaporation it becomes the immediate candidate for such a purpose. Other insulators, for example, SiO₂, may serve just as well.

It may be mentioned, in passing, that a grating metallization on top of the transparent oxide SnO₂ will also help to reduce the series resistance of the heterojunction cell.

3.4 Grating Size

Assuming that the surface is inverted in the area between grating lines, the field that exists in the space-charge region will direct electrons generated to flow perpendicularly to the inversion layer. Once they are in the inversion layer they flow laterally to the collecting contact lines of the metal grating as indicated in Fig. 9. Power loss occurs mainly as a result of resistive effects in the inversion layer. Recombination with holes and trapping by surface states can also occur in the electron journey to the grating lines particularly if inversion of the surface is insufficient. Note that the lateral flow of

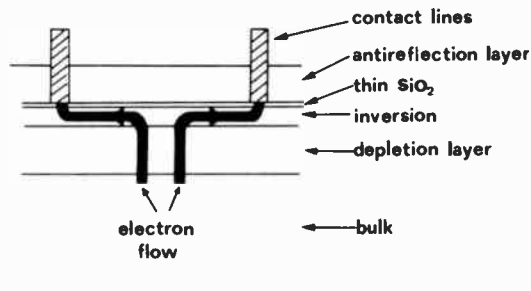


Fig. 9. Electron flow paths to contact lines.

electrons increases linearly from the centre towards the grating lines.

Most published results on m.i.s. solar cells give active-area efficiency. This is the efficiency of the solar cell which would be obtained in the absence of contact lines which only act as current collecting electrodes. These lines block the transmission of sunlight and are a source of power loss. The wider these contact lines are in relation to the spacing between them the lower is the ratio of generated power to available solar power. On the other hand increasing the spacing increases the resistive loss. A simple calculation shows that for a minimum power loss the spacing should be¹²

$$\delta = \left(\frac{6WV_{mp}}{\rho_s J_{mp}} \right)^{1/3} \quad (2)$$

where W is the width of the contact lines, ρ_s is the sheet resistivity of the inversion layer in Ω/square, and V_{mp} and J_{mp} are the generated voltage and current density under maximum power conditions. If $W = 10 \mu\text{m}$, $\rho_s = 5 \times 10^4 \Omega/\text{square}$, $V_{mp} = 450 \text{ mV}$ and $J_{mp} = 30 \text{ mA/cm}^2$, $\delta = 121 \mu\text{m}$, which is about that presently used for m.i.s. grating cells (order of 100 μm).

3.5 Antireflection Coating

Most semiconductors have a refractive index greater than 3, and therefore a high reflectance. An antireflection layer is usually formed by depositing over the semiconductor surface a coating of material which is transparent to sunlight in the spectrum of interest and which has a refractive index n_1 such that $n_0 < n_1 < n$. It may be shown that the reflectance is a minimum if

$$n_1^2 = n_0 n \quad (3)$$

Equation (3) is the condition for λ/4 matching, and the thickness t_1 of the antireflection layer is given by

$$n_1 t_1 = \lambda/4 \quad (4)$$

To match silicon ($n = 3.6$) to air ($n_0 = 1$), n_1 should be about 1.9. Equation (4) gives a thickness of about 79 nm, taking 600 nm as the midpoint of the useful spectrum. The reflectance over the spectrum of such a system is shown in Fig. 10.¹³

Better results can be obtained if two antireflection coatings are used. The result is also shown in Fig. 10 for a particular combination of two antireflection layers.

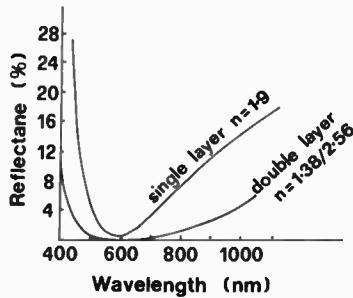


Fig. 10. Reduction of reflectance by antireflection layers.

For use in the m.i.s. grating solar cell the antireflection coating has the additional responsibility of inducing inversion on the semiconductor surface. SiO has been found to be suitable for p-type material, i.e. it will induce an n-type surface, while Al₂O₃ is suitable for n-type material, i.e. it will induce a p-type surface. SiO can be deposited by evaporation in vacuum while Al₂O₃ can be formed by anodization of aluminium deposited also by evaporation in vacuum.

3.6 Textured Cells

Another way to reduce the reflectance is by texturing the semiconductor surface.^{14,15} This is done by a preferential etch which etches silicon more rapidly in one crystallographic direction. As a result pyramids are formed and light undergoes multiple reflections as shown in Fig. 11. Together with an antireflection coating the loss of light due to reflection can be kept below 3%. Furthermore, light enters the surface at an angle and is therefore absorbed close to the surface. This should improve the carrier collection efficiency, particularly for light of longer wavelengths. This is an advantage especially for the m.i.s. solar cell since the 'dead layer' as found in the conventional p-n junction cell has been eliminated.

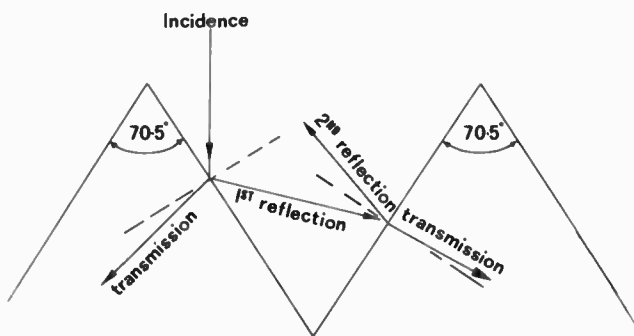


Fig. 11. Transmission and reflection of light at a textured surface.

The texturing, however, means an additional processing step which requires careful handling and thus increases the processing cost. Furthermore, because of the textured surface contact grating lines become longer by a factor of $\sqrt{3}$. This increases the series resistance of the cell unless the grating lines are made correspondingly thicker or wider.

3.7 Effects of Substrate Resistivity on V_{oc}

Figure 12 shows the highest V_{oc} so far attained.¹⁶ The considerably higher V_{oc} obtained in m.i.s. cells is a consequence of the elimination of the 'dead layer' that exists in p-n junction solar cells.

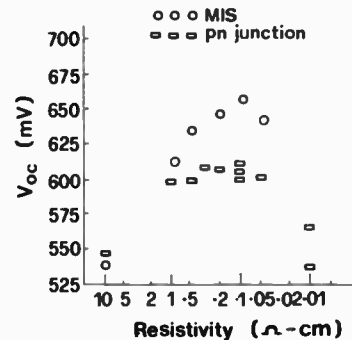


Fig. 12. V_{oc} as a function of substrate resistivity.

In general, since the saturation reverse current I_0 is given by

$$I_0 = \frac{qAD_n n_i^2}{L_n N_A} \tag{5}$$

where A is the area of the cell, D_n the diffusion constant for electrons, n_i the intrinsic concentration, N_A the substrate doping concentration and L_n the electron diffusion length, increasing N_A decreases I_0 . Therefore, as seen from equation (1), V_{oc} increases with N_A . However, the lifetime of minority electrons falls rapidly if N_A is increased beyond a certain limit, and I_0 will increase. Figure 12 shows that maximum V_{oc} occurs at a substrate resistivity of about 0.1 Ω cm, corresponding to $N_A \approx 5 \times 10^{17} \text{ cm}^{-3}$.

Another factor that limits V_{oc} in min m.i.s. solar cells is the degree of inversion that may be obtained with a given substrate resistivity. The inversion charge Q_n is given by¹⁷

$$Q_n = Q_{ss} - (4q\epsilon_s\epsilon_0 N_A \phi_{FP})^{1/2} \tag{6}$$

where Q_{ss} is the fixed positive oxide charge responsible for the inversion, and ϕ_{FP} is the Fermi potential given by

$$\phi_{FP} = \frac{kT}{q} \ln \frac{N_A}{n_i} \tag{7}$$

Therefore, the higher N_A is, the lower is Q_n and hence I_{sc} , the short-circuit current. Again, as seen from equation (1), a decrease in I_{sc} will also result in a decrease in V_{oc} . In addition, a high N_A means a narrow depletion width, leading to a poor response for the long wavelengths, unless a back surface field (b.s.f.) is incorporated.

3.8 Efficiency η

As explained in Section 2, the main problem with the conventional p-n junction solar cell is the existence of the 'dead layer' which is associated with the heavy doping of the front emitter region. The min m.i.s. solar cell, on the

other hand, eliminates this heavily-doped layer. Instead, an inversion layer exists immediately at the surface of the semiconductor. The induced junction is electronically identical to the ideal p-n junction and thus should have similar properties.^{6,7} However, compared with the practical p-n junction the elimination of the 'dead layer' in the min m.i.s. solar cell greatly enhances the carrier collection efficiency leading to an increase in I_{sc} . It also lowers the saturation current, I_0 , leading to an increase in V_{oc} . Since the induced junction is actually at the surface, there is a marked improvement in the short-wavelength response as compared to a p-n-junction cell¹¹ (approximately 85% increase in response is obtained at 370 nm).

Another factor that helps increase the efficiency of the min m.i.s. solar cell is the elimination of the diffusion step in the fabrication process. This saves the cell from being subjected to high-temperature treatment which is known to cause deterioration in carrier lifetime.¹⁸

Recent experimental results¹⁶ give an active-area efficiency of 18.3% for the min m.i.s. solar cell without any back surface field. This compares very favourably with that of the more complicated black cell¹⁹ whose active-area efficiency is 18.5% or the $p^+ - n - n^+$ b.s.f. cell²⁰ whose active-area efficiency is estimated as 18.6%. It is worth noting the very high V_{oc} obtainable from the min m.i.s. solar cell. At very high V_{oc} (> 650 mV), surface states become important as they cause excessive surface recombination. There are thus prospects for further increase of efficiency in the min m.i.s. cell, for example, by incorporating a back surface field in the base region, and by proper surface treatment. These effects are presently being investigated.

3.9 Degradation Problems

Figure 13 shows the characteristics of a min m.i.s. solar cell with magnesium contact lines immediately after fabrication and a week later. The contact-line spacing of this cell has been deliberately made very wide (about 2.6 mm) in order to reveal specifically some degradation effects. It is clear that in the period of one week severe degradation has taken place.

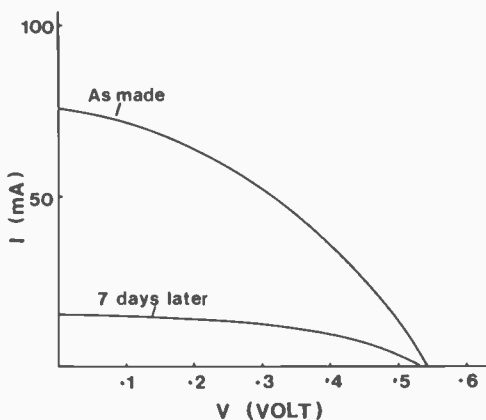


Fig. 13. I/V characteristics of a coarse-grating cell.

A possible mechanism leading to the degradation is that of the m.i.s. contact-line structure. This is due to the reduction of the thin oxide layer by the overlying metal contact. High-temperature life-testing of Al/SiO_x/p-Si solar cells²¹ has shown that below 200°C this mechanism proceeds at a negligible rate. Mg/SiO_x/p-Si solar cells are presently under investigation and preliminary results seem to suggest that the problem is not serious.

Another possible mechanism for degradation is caused by the ageing effect of the insulator-semiconductor interface leading to an increase in surface-state density.

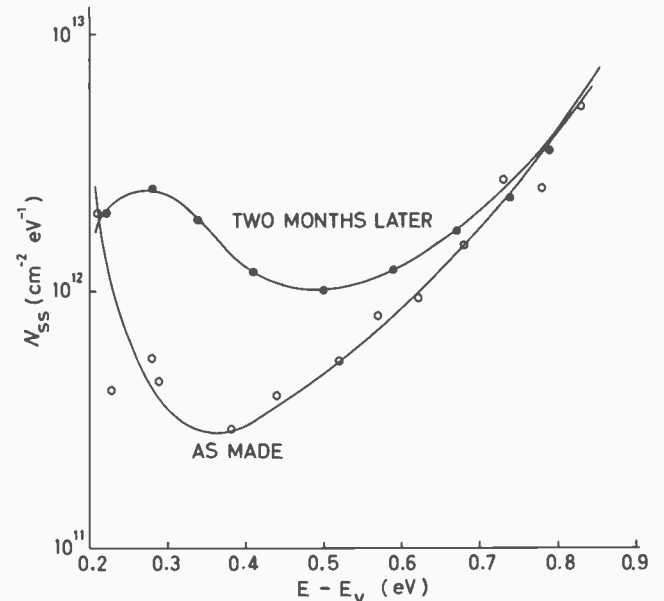


Fig. 14. N_{ss} curves of an Al-SiO-Si structure.

Measurements on some m.i.s. capacitors with SiO as the insulator have shown that in a period of two months an order of magnitude increase in surface-state density is possible (Fig. 14). However, if the semiconductor surface is inverted most of the surface states will be occupied under steady-state conditions and unable to cause degradation on a magnitude as shown in Fig. 13.

The most likely mechanism leading to degradation originates from the weakening of the inversion layer at the semiconductor surface underneath the SiO in between contact lines. This inversion layer assists the collection of minority electrons in at least three ways. First, the inversion layer provides a path of low resistance for the lateral movement of electrons. Secondly, immediately below the inversion layer is the depletion region whose width is a maximum at strong inversion with the associated large electric field. A large electric field is essential for the separation of the electrons from the holes and for driving the former towards the semiconductor surface. Thirdly, electrons from the inversion layer help immunize the effects of surface states present at the insulator-semiconductor interface, which otherwise would capture the optically-generated

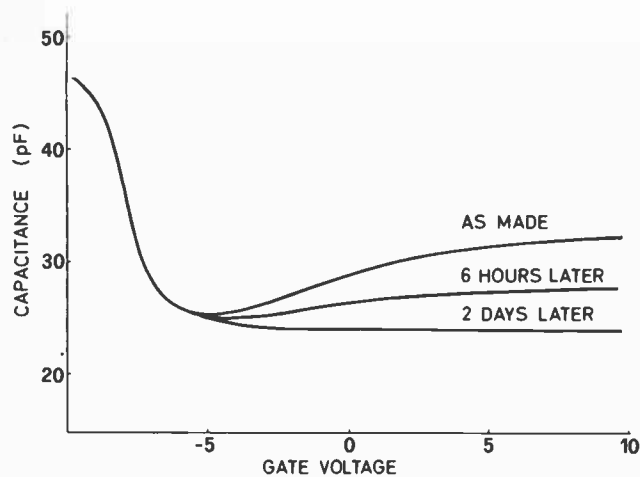


Fig. 15. H.f. CV characteristics of an M-SiO-Si capacitance.

minority electrons. If for any reason inversion disappears altogether, leaving behind only the depletion layer, electrons arriving at the semiconductor surface under the depletion-layer field will suffer serious resistive loss in their lateral movement to the contact lines due to recombination at the surface states as well as low electron concentration at the surface. The collection of minority electrons may then be limited to regions within a diffusion length on either side of the contact lines. Evidence of the disappearance of the inversion layer on either side of a contact line is clearly shown in Fig. 15 where CV curves of an m.i.s. capacitor are shown with time elapsed after fabrication. The insulator of the m.i.s. capacitor is SiO₂ of about 800 Å in thickness. The frequency of measurement is 1 MHz. Low-frequency CV characteristics are evidence of the existence of an inversion layer in regions of the semiconductor surrounding the metal contact, the so-called a.c. conductance effect.²² It can be seen that in about two days after fabrication the CV characteristics have changed from the low-frequency type to the high-frequency type, indicating a considerable weakening of the inversion layer surrounding the contact. Unless this problem can be overcome line spacing should be made less than a diffusion length. In top-grade silicon a diffusion length in the region of 130–180 μm may be expected. This compares favourably with the line spacing of about 100 μm presently used for m.i.s. solar cell contact grating. For wider spacings degradation may be expected in time as the inversion layer weakens.

The weakening or disappearance of the inversion layer may be caused by the neutralization of the positive charge in the antireflection coating or the accumulation of negative charge on the top surface of this coating. Experiments have shown that the accumulation of negative charge is the main reason responsible for the degradation.²³ The problem, however, may be overcome by appropriate passivation.²⁴ One of the methods tried is to cover the cell with a layer of concentrated non-ionic

surfactant C0630.† This is a colourless and very viscous liquid. Experiments on C0630-passivated fine-grating cells showed that over a period of three months, I_{sc} remained practically constant at its maximum value while for the unpassivated cell, I_{sc} fell by at least 5%. C0630-passivated coarse-grating cells showed a variation in I_{sc} of about $\pm 10\%$ in a period of 8 months while in the unpassivated cell I_{sc} fell to about 20% of its starting value. Other non-ionic surfactants may also give acceptable results. For example, C0990, a solid non-ionic surfactant at room temperature, may be applied to the surface of the cell by heating and spinning. However, because C0990 is an off-white wax it causes some loss of efficiency in photovoltaic operation due to light absorption. It has also been found possible to use mixtures of C0630 and C0990 which retain good transmission properties while still remaining a solid at room temperature. Research is at present directed to finding an insulator or combination of insulators which would serve the combined purposes of antireflection, inversion charge inducement and passivation. It may be mentioned, in passing, that problems associated with this type of degradation will also occur in other solar cells which use antireflection coatings as charge inducing layers¹⁰ so that similar considerations will apply.

4 Conclusions

In conclusion it is useful to summarize the advantages and disadvantages of the min m.i.s. solar cells as compared to the conventional p-n-junction solar cells.

1. The min m.i.s. solar cell is a relatively simple structure to fabricate and economic studies²⁵ have shown lower cell processing costs.

2. Elimination of the heavily doped top layer removes the 'dead-layer' that exists in the conventional p-n-junction, thus increasing the carrier lifetime and collection efficiency in the surface region of the cell where the generation rate is a maximum, especially for the ultra-violet end of the spectrum. In addition, the potential barrier of the min m.i.s. cell is right at the semiconductor surface and this further improves the collection efficiency of carriers generated by light of short wavelengths. The combined effect is an increase in I_{sc} and V_{oc} .

3. Elimination of the diffusion step in the fabrication process saves the cell from being subjected to high-temperature treatment which is known to cause deterioration in carrier lifetime. This should further help improve the efficiency of the min m.i.s. solar cell.

4. Elimination of the diffusion step makes the min m.i.s. cell an ideal structure for polycrystalline materials since there is no problem of preferential diffusion of dopants through grain boundaries which tends to short circuit the junction. The use of

† Surfactant C0630: trade name Antarox, manufactured by GAF.

polycrystalline materials should result in a reduction of cost.

5. Min m.i.s. solar cells are faced with the problem of finding a top contact material that is sufficiently transparent and at the same time has a high conductivity. The grating min m.i.s. solar cell, on the other hand, tends to be more susceptible to degradation. Three degradation mechanisms have been identified. The principal mechanism found to be responsible for the degradation is the accumulation of negative charge on the outer surface of the antireflection coating. However, recent research to overcome this problem seems very promising, and it may be concluded that when this problem is entirely solved, the grating min m.i.s. solar cell will be a real contender to the conventional p-n-junction solar cell for the direct conversion of solar energy into electricity.

5 References

- 1 Redfield, D., 'Mechanism of performance limitations in heavily doped silicon devices', *Appl. Phys. Letters*, **33**, no. 6, pp. 531-3, 1978.
- 2 Anderson, W. A. and Delahoy, A. E., 'Schottky barrier diodes for solar energy conversion', *Proc. IEEE*, **60**, pp. 1457-8, 1972.
- 3 Purlfrey, D. L. and McQuat, R. F., 'Schottky-barrier solar-cell calculations', *Appl. Phys. Letters*, **24**, pp. 167-9, 1974.
- 4 Anderson, W. A., Delahoy, A. E. and Milano, R. A., 'An 8% efficient layered Schottky-barrier solar-cell', *J. Appl. Phys.*, **45**, pp. 3913-5, 1974.
- 5 Card, H. C. and Yang, E. S., 'MIS-Schottky theory under conditions of optical carrier generation in solar cells', *Appl. Phys. Letters*, **29**, pp. 51-3, 1976.
- 6 Green, M. A. and Godfrey, R. B., 'MIS solar cell—general theory and new experimental results for silicon', *Appl. Phys. Letters*, **29**, pp. 610-2, 1976.
- 7 Tarr, N. G. and Purlfrey, D. L., 'New experimental evidence for minority-carrier MIS diodes', *Appl. Phys. Letters*, **34**, no. 4, pp. 295-7, 1979.
- 8 Bardeen, J., 'Surface states and rectification at a metal semiconductor contact', *Phys. Rev.*, **71**, 717-27, 1947.
- 9 Ghosh, A. K., Fishman, C. and Feng, T., 'SnO₂/Si solar cells—heterostructure or Schottky-barrier or MIS-type device', *J. Appl. Phys.*, **49**, pp. 3490-98, 1978.
- 10 Salter, G. C. and Thomas, R. E., 'Induced junction silicon solar cells', *Conf. Rec., 11th Photovoltaic Specialists Conf.*, pp. 364-70, 1975.
- 11 Godfrey, R. B. and Green, M. A., '655 mV open-circuit voltage, 17.6% efficient silicon MIS solar cells', *Appl. Phys. Letters*, **34**, no. 11, pp. 790-3, 1979.
- 12 Lam, Y. W., unpublished.
- 13 Hovel, H. J., 'Solar cells', *Semiconductors and Semimetals*, **11**, pp. 204-6, 1975.
- 14 Chitre, S. R., 'A high volume cost efficient production macrostructuring process', *Conf. Rec., 13th Photovoltaic Specialists Conf.*, pp. 152-4, 1978.
- 15 Bae, M. S., 'Schottky effect and photovoltaic devices on the textured surfaces', *Conf. Rec., 13th Photovoltaic Specialists Conf.*, pp. 1337-41, 1978.
- 16 Green, M. A., Godfrey, R. B., Willison, M. R. and Blakers, A. W., 'High efficiency (> 18% active area, AM1) silicon min MIS solar cells', *Conf. Rec., 14th Photovoltaic Specialists Conf.*, pp. 684-7, 1980.
- 17 Grove, A. S., 'Physics and Technology of Semiconductor Devices' (Wiley, New York, 1967).
- 18 Graff, K., 'Semiconductor Silicon 1973', p. 170 (Electrochemical Society, New York, 1973).
- 19 Haynos, J., Allison, J., Arndt, R. and Meulenberg, A., *Proc. Int. Conf. Photovoltaic Power Generation (Hamburg)*, p. 487., 1974.
- 20 Fossum, J. G. and Burgess, E. L., 'High-efficiency p⁺-n-n⁺ back-surface-field silicon solar cell', *Phys. Letters*, **33**, no. 3, 238-40, 1978.
- 21 Godfrey, R. B. and Green, M. A., 'High temperature life testing of Al/SiO_x/p-Si contacts for MIS solar cells', *Appl. Phys. Letters*, **34**, pp. 860-1, 1979.
- 22 Nicollian, E. H. and Goetzberger, A., 'Lateral a.c. current flow model for metal-insulator-semiconductor capacitors', *IEEE Trans. on Electron Devices*, **ED-12**, pp. 108-17, 1965.
- 23 Lam, Y. W., Green, M. A. and Davies, L. W., 'Electrostatic effects in inversion layer MIS solar cells' *Appl. Phys. Letters*, **37**, pp. 1087-9, 1980.
- 24 Lam, Y. W., Green, M. A. and Davies, L. W., 'Surface passivation of inversion layer MIS solar cells', *Electronics Letters*, **16**, pp. 707-8, 1980.
- 25 Rajkanan, K. and Singh, R., 'An outlook for automated CIS solar cell factory', *Conf. Rec., 14th IEEE Photovoltaic Specialists Conf.*, pp. 970-3, 1980.

*Manuscript first received by the Institution on 1st September 1980 and in final form on 18th November 1980
(Paper No. 2007/CC347)*

The Author

Yat-Wah Lam received his B.Sc. from the University of London, his Master's degree from the University of Birmingham, and his Doctorate from the University of Manchester. Having spent about eight years in the electronics industry in the UK, Dr Lam took up teaching at the University of Birmingham in 1963; from 1969 to 1971 he was the Mullard Research Fellow at UMIST. Dr Lam returned to Hong Kong in 1971 to join the Chinese University where he is now Reader in Electronics, his current research interest being in the field of semiconductor physics and devices.



Detection processes for a 9600 bit/s modem

A. P. CLARK, M.A., Ph.D.,
D.I.C., C.Eng., M.I.E.R.E.*

and

M. J. FAIRFIELD, M.Sc.*

SUMMARY

The paper describes various detection processes for a modem that has been designed for operation at 9600 bit/s over the public switched telephone network. The modem is a synchronous serial system, using a 16-point q.a.m. signal, with near-maximum-likelihood detection at the receiver. The detection processes are modifications of a technique that has recently been developed for use with severely distorted digital signals, the modifications leading to much simpler implementation. Results of computer-simulation tests are presented, comparing the tolerances of the various detectors to additive white Gaussian noise, when the data are transmitted over different telephone circuits. The effects, on the tolerance to noise of a detector, of inaccuracies in the estimates of the level and carrier phase of the received signal are also studied.

*Department of Electronic and Electrical Engineering, University of Technology, Loughborough, Leicestershire LE11 3TU

1 Introduction

A telephone circuit in the switched telephone network may have any one of a very wide range of attenuation-frequency characteristics and any one of a correspondingly wide range of group-delay frequency characteristics, giving an available (or usable) bandwidth that may lie anywhere in the range from about 1500 Hz to 3000 Hz.¹ It is evident therefore that for the satisfactory transmission of data at a rate as high as 9600 bits/second over the switched telephone network, the receiver must be adaptive in the sense that it takes full account of the distortion introduced into the received data signal. The conventional approach to this problem is to use an adaptive non-linear (decision-feedback) equalizer that is adjusted to minimize the mean-square error in the equalized signal.²⁻⁵ Such systems are known to operate satisfactorily over telephone circuits at rates of up to 4800 bits/second. At higher transmission rates, however, satisfactory operation is not always obtained over the poorer telephone circuits.

An alternative approach that has recently been considered is the use of the Viterbi-algorithm detector.⁵⁻⁷ This selects as the detected message the possible sequence of transmitted data-symbols (signal-element values) for which there is the minimum mean-square difference between the samples of the corresponding received data signal, for the given signal distortion but in the absence of noise, and the samples of the signal actually received. When the data signal is received in the presence of stationary additive white Gaussian noise, giving statistically independent Gaussian noise samples at the detector input, this is a process of maximum-likelihood detection; when the transmitted data-symbols are statistically independent and equally likely to have any of their possible values, the detection process minimizes the probability of error in the detection of the received message.⁵ It is assumed here that the received signal is sampled at the Nyquist rate, so that the corresponding samples contain all the information in this signal.

Unfortunately, when the sampled impulse-response of the channel contains a large number of components (non-zero samples), which is the case in the particular application considered here, the Viterbi-algorithm involves both an excessive amount of storage and an excessive number of operations per received data symbol. One approach for overcoming this difficulty is to use a linear feedforward transversal filter at the detector input to reduce the number of components in the channel sampled-impulse-response. The filter is adjusted adaptively to give a 'desired' sampled impulse-response for the channel and filter, which has a given small number of components and may or may not be fixed.⁸⁻¹¹ The disadvantage of this arrangement is that, for some telephone circuits, the linear filter may equalize some of the amplitude distortion introduced by the telephone

circuit and under these conditions maximum-likelihood detection is no longer achieved, leading to an inferior performance.⁵ The linear filter should ideally perform the function of a 'whitened matched-filter',^{6,14} which ensures that true maximum-likelihood detection is achieved by the Viterbi-algorithm detector. This filter contains a linear filter matched to the channel, followed by a transversal filter, the two filters being separated by a sampler. The sampler samples the output signal from the matched filter, once per data symbol, the sampling phase being appropriately adjusted to maximize the signal/noise ratio in the samples. The zeros (roots) of the z transform of the sampled impulse-response of the channel and matched filter occur in complex-conjugate reciprocal pairs, and it is assumed here that there are no zeros exactly on the unit circle in the z plane (that is, have an absolute value of unity). The samples are fed to a linear feedforward transversal filter which removes all zeros of the z transform of the channel and matched filter that lie outside the unit circle, leaving the remaining zeros unchanged. Thus the z transform of the channel and whitened matched filter has no zeros outside the unit circle.

In the ideal arrangement, where the highest possible transmission rate is required over a baseband channel which is bandlimited and introduces stationary additive white Gaussian noise at its output, the real-valued baseband data signal is transmitted over the channel at the Nyquist rate. The receiver input filter is now a lowpass filter having a flat amplitude response and linear phase characteristic over the passband and a cut-off frequency (in Hz) at half the signal element rate. The output signal from the lowpass filter is sampled once per data symbol (at the Nyquist rate). The samples of the data signal contain all the information in the data-signal waveform and the corresponding noise samples are statistically independent Gaussian random variables with zero mean and fixed variance.

Under these conditions the linear matched filter and sampler that form the first part of the whitened matched filter can be replaced by the given receiver input filter and sampler, followed by a linear feedforward transversal filter, which is such that the resultant sampled impulse-response (for the receiver filter, sampler and transversal filter) is the same as that of the original matched filter and sampler. Since the receiver input filter and sampler introduce no information loss (there being also no bandlimiting of the data signal by the receiver filter), they may now be considered as part of the channel, whose sampled impulse-response (for a given sampling phase) remains unchanged. The transversal filter therefore becomes the matched filter for this channel. The sampled impulse-response of the transversal filter is just the time reverse of that of the channel, and, in the more general case with complex-valued signals, it becomes the complex conjugate of the time reverse. The zeros of the z

transform of the matched filter are the complex conjugates of the reciprocals of the zeros of the z transform of the channel. Thus, for every zero of the channel z -transform, the matched filter adds another zero at the complex conjugate of the reciprocal value of z , such that the zeros of the resultant z transform occur in complex-conjugate reciprocal pairs.

Following the transversal matched filter just described is the linear feedforward transversal filter previously mentioned, that removes all zeros of the z transform of the channel and matched filter that lie outside the unit circle. The two transversal filters operate with the same sampling interval and phase and can clearly be combined to give a single linear feedforward transversal filter. It can be seen that this filter must be such that, in the z transform of the sampled impulse-response of the channel and filter, all zeros of the z transform of the channel, that lie outside the unit circle in the z plane, are replaced by the complex conjugates of their reciprocals, all remaining zeros being left unchanged. Thus all zeros of the z transform of the channel and filter lie inside the unit circle. It has been shown that this filter is an all-pass network (with a flat amplitude response) that performs an orthogonal transformation on the received signal.⁵ The filter removes all phase distortion introduced by the channel and then processes the signal, without changing the amplitude distortion introduced by the channel, in such a way as to place all zeros of the z transform of the channel and filter inside the unit circle. Thus, whenever the channel introduces any amplitude distortion, the channel and filter introduce the same amplitude distortion together with some phase distortion, the latter being determined entirely by the amplitude distortion.

The linear transversal filter of the whitened matched-filter just described is identically the same as the linear feedforward transversal filter that forms the first part of a conventional non-linear (decision-feedback) equalizer, where this is fed with the given sampled signal and is adjusted to minimize the mean-square error (and hence maximize the signal/noise ratio) in its output signal, subject to the exact equalization of the channel.⁵ It follows that the linear transversal filter of the whitened matched filter may be adaptively adjusted for the channel to give approximately the required response, at least at high signal/noise ratios (where near perfect equalization of the channel is achieved by the corresponding adaptive equalizer), using basically the same simple arrangement as that involved in a conventional adaptive non-linear equalizer.⁵ The signal at the output of the linear filter is fed to the maximum-likelihood detector, and the feedback filter gives an estimate of the sampled impulse-response of the channel and linear filter, which is required by the detector. The details of the arrangement will be described later. In practice, the linear filter usually introduces some constant gain or attenuation, which however has the

same effect on the noise as on the data signal, and so does not change in any way the statistical relationship between the noise and data signal. Furthermore, when an allowance has been made for the change in level, the noise components at the filter output have the same statistical properties as those at its input, being therefore statistically independent and with a fixed variance. This means that a Viterbi-algorithm detector operating at the output of the filter has the same tolerance to the Gaussian noise as the appropriate Viterbi-algorithm detector operating at its input, although generally involving much less complex equipment. Unfortunately, since the linear filter does not now remove any of the amplitude distortion introduced by the channel, it does not always, or even in general, achieve a sufficient reduction in the number of components of the resultant sampled impulse-response, to permit the practical use of a conventional Viterbi-algorithm detector at its output.

It follows that the Viterbi-algorithm detector must be replaced here by a near-maximum-likelihood detector that uses very much less storage and requires far fewer operations per received data-symbol, for the given number of components in the sampled impulse-response of the channel. Various systems of this type have been developed and tested by computer simulation, with very promising results.^{5, 12, 13}

An alternative approach that has recently been studied is to discard the linear filter altogether, so that the near-maximum-likelihood detector operates directly on the original sampled signal, at the output of the sampler.¹⁴ An estimator is, of course, required here to determine the sampled impulse-response of the channel, but this can be implemented relatively simply, requiring a transversal filter with only as many taps as there are components in the sampled impulse-response of the channel.^{15, 16} However, computer-simulation tests (whose results have

not been published) have shown that in the presence of very severe phase distortion, such as can occur over the poorer switched telephone circuits, these systems require a considerable amount of storage and a large number of operations per received data-symbol, in order to achieve near-maximum-likelihood detection. The most cost-effective arrangement for the given application is therefore to use an adaptive linear filter of the type previously described, connected between the sampler and detector and acting as a whitened matched filter. The adaptive filter has the important property that it (at least approximately) removes all the phase distortion introduced by the channel and then adjusts the sampled impulse-response of the channel and filter into a form that is ideally suited to a near-maximum-likelihood detector of the type considered here.^{5, 13}

The paper describes the application of the methods involved in some recently developed detection processes to the design of a q.a.m. (quadrature amplitude modulated) system operating at 9600 bits/second with a 16-point q.a.m. signal. Details are given here of some novel detection processes that avoid the high complexity involved with a 16-point signal in the previously described processes. Results of computer-simulation tests are then presented, comparing the performances of the various systems, when operating over different telephone circuits, and showing also the effects of inaccuracies in the estimates of the level and carrier phase of the received signal.

2 Model of Data Transmission System

The model of the data-transmission system is shown in Fig. 1. This is a synchronous serial 16-point q.a.m. system. The information to be transmitted is carried by the data-symbols $\{s_i\}$, where

$$s_i = \pm \alpha \pm j\beta \tag{1}$$

and $j = \sqrt{-1}$, $\alpha = 1$ or 3 and $\beta = 1$ or 3 . The $\{s_i\}$ are

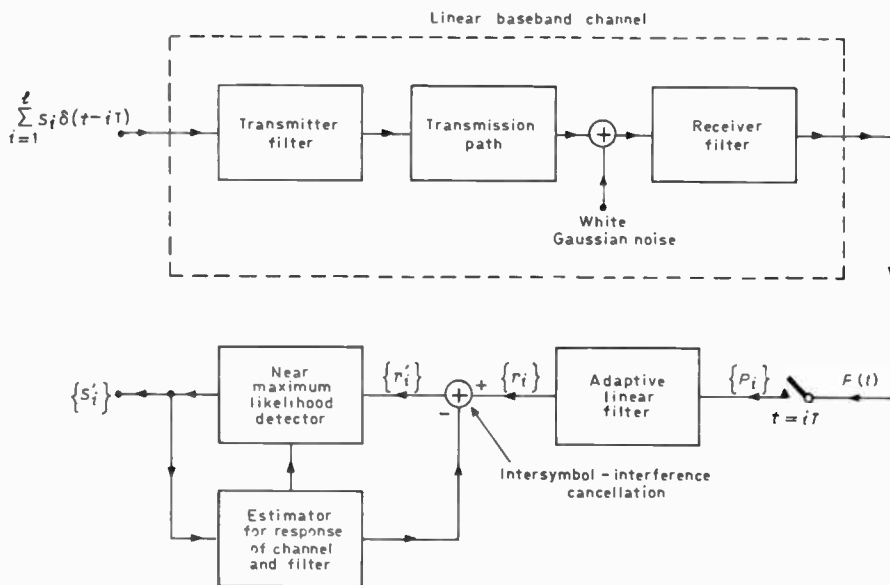


Fig. 1. Data-transmission system.

statistically independent and equally likely to have any of their 16 possible values. It is assumed that $s_i = 0$ for $i \leq 0$, so that $s_i \delta(t - iT)$ is the i th signal element at the input to the transmitter filter. The transmission path is a linear baseband channel that includes a telephone circuit together with a linear q.a.m. modulator at the transmitter and a linear q.a.m. demodulator at the receiver. The basic structure of the modulator and demodulator has been described elsewhere.¹⁷ The signals transmitted over the 'in-phase' channel of the q.a.m. system are represented by real-valued quantities, and the signals over the 'quadrature' channel by imaginary-valued quantities, to give a resultant complex-valued baseband signal at both the input and output of the transmission path in Fig. 1. The carriers of the transmitted signals in the in-phase and quadrature channels are taken to be $\sqrt{2} \cos 2\pi f_c t$ and $-\sqrt{2} \sin 2\pi f_c t$, respectively, where $f_c = 1800$.¹⁷ The transmitter filter, transmission path and receiver filter together form a linear baseband channel whose impulse response is the complex-valued function $q(t)$, with an effective duration of less than $(g + 1)T$ seconds, where g is the appropriate integer. It is assumed for the purpose of this study that $q(t)$ is time invariant over any one transmission. The various types of additive and multiplicative noise normally introduced by telephone circuits are neglected here, and it is assumed that the only noise is stationary white Gaussian noise with complex values, zero mean and a flat (frequency independent) power spectral density, which is added to the data signal at the output of the transmission path, to give the complex-valued Gaussian noise waveform $v(t)$ at the output of the receiver filter. Although telephone circuits do not normally introduce significant levels of Gaussian noise, the relative tolerance of different data-

transmission systems to white Gaussian noise is a good measure of their relative overall tolerance to the additive noise actually experienced over telephone circuits.¹

The waveform at the output of the receiver filter is the complex-valued signal

$$p(t) = \sum_{i=1}^l s_i q(t - iT) + v(t) \tag{2}$$

where l is some large positive integer. The waveform $p(t)$ is sampled once per data symbol at the time instants $\{iT\}$ to give the received samples $\{p_i\}$, which are fed to the adaptive linear filter (Fig. 1). This filter is taken to have been adjusted exactly as previously described so that it acts as a whitened matched filter, the only difference being that the filter now operates with complex-valued samples in place of the real-valued samples previously assumed. Thus the sampled impulse-response of the linear baseband channel and adaptive linear filter (Fig. 1) is given by the $(g + 1)$ -component vector

$$Y = y_0 y_1 \dots y_g \tag{3}$$

which has complex-valued components and a z transform with all its zeros inside or on the unit circle in the z plane. Furthermore, when an allowance has been made for the change in level, the noise components $\{w_i\}$ at the output of the filter have the same statistical properties as the noise components $\{v_i\}$ at its input, where $v_i = v(iT)$. The delay in transmission over the baseband channel and adaptive filter, other than that involved in the time-dispersion of the received signal, is for convenience neglected here, so that $y_0 \neq 0$ and $y_i = 0$ for $i < 0$ and $i > g$. Thus the sample value at the filter output, at time $t = iT$, is the complex-valued quantity

$$r_i = \sum_{h=0}^g s_{i-h} y_h + w_i \tag{4}$$

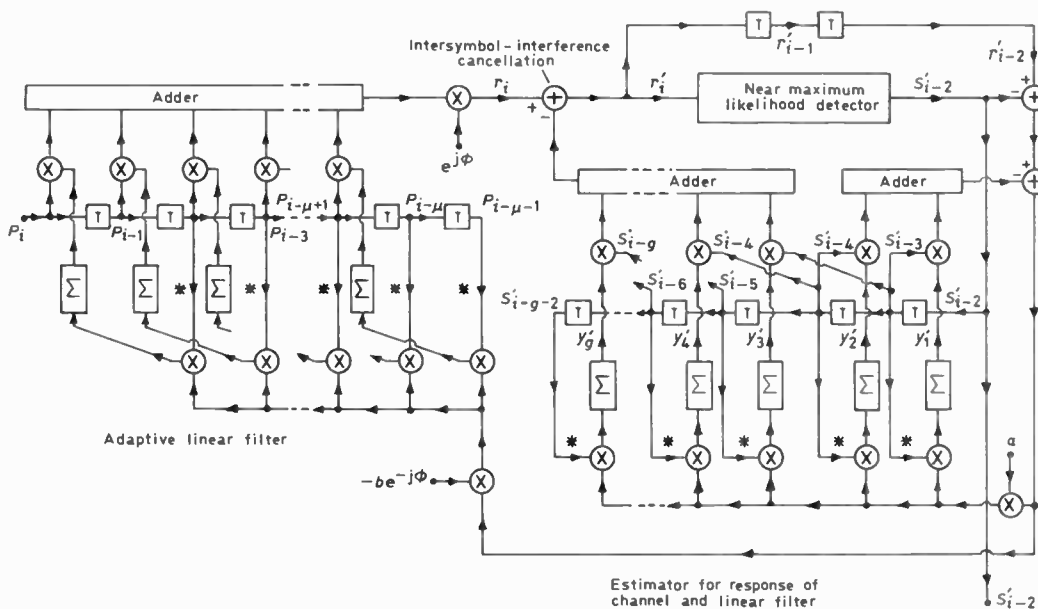


Fig. 2. Adaptive adjustment of linear filter and estimator.

where the real and imaginary parts of the $\{w_i\}$ are statistically independent Gaussian random variables with zero mean and variance σ^2 .

The adjustment of the adaptive linear filter and the estimation of Y is achieved by the arrangement shown in Fig. 2. It can be seen that this is a simple development of a conventional adaptive non-linear (decision-feedback) equalizer for the case where there is a delay in detection (of two sampling intervals in this particular example).⁵ Clearly, when there is no delay in detection, the arrangement degenerates into a conventional equalizer. The main tap of the μ -tap adaptive linear feedforward transversal filter, is close to the last tap, for all channels. A square marked T is a store that holds the corresponding sample value, the stored values being shifted one place in the direction shown during each sampling interval. A square marked Σ is an accumulator that sums the input samples, and * indicates that the corresponding sample value is replaced by its complex conjugate. a and b are small positive constants, and ϕ radians is the carrier phase correction necessitated by a phase error in the coherent demodulator. ϕ is determined by the carrier phase control circuit, which is not shown in Figs. 1 and 2. The adaptive adjustment of ϕ , together with that of the transversal-filter tap-gains in Fig. 2, is arranged to be such that $y_0 = 1$, and the method of adjustment of each transversal filter is the same as that in a conventional equalizer.⁵ Further details of this and of the determination of ϕ are however beyond the scope of the paper.

Except where otherwise stated it will be assumed that the adaptive linear filter is correctly adjusted and that the estimate of Y , which is the sequence y'_0, y'_1, \dots, y'_g stored in the channel estimator, is also correct. The estimate of Y , together with a prior knowledge of the possible values of s_i , are used by the near-maximum-likelihood detector and intersymbol-interference canceller.

The detector (Fig. 1) operates on its input samples $\{r'_i\}$ to give the finally detected data-symbols $\{s'_i\}$, s'_i being determined after the receipt of r'_{i+n} , where $n < g$, so that there is a delay in detection of n sampling intervals. The intersymbol-interference canceller removes from the samples $\{r'_i\}$ estimates (detected values) of all components involving data symbols $\{s_i\}$ whose final detected values $\{s'_i\}$ have already been determined. Thus the intersymbol interference canceller operates on r'_i to give

$$r'_i = r_i - \sum_{h=n+1}^g s'_{i-h} y_h \quad (5)$$

When $s'_{i-h} = s_{i-h}$, for all $\{h\}$, as will be assumed for the present,

$$r'_i = \sum_{h=0}^n s_{i-h} y_h + w_i \quad (6)$$

so that the sampled impulse-response of the channel and

adaptive filter has been reduced from $g+1$ to $n+1$ components, thus greatly simplifying the detection process when $n \ll g$.

Let S_k, R'_k and W_k be the k -component row vectors whose i th components are s_i, r'_i and w_i , respectively, for $i = 1, 2, \dots, k$. Also let X_k, Z_k and U_k be the k -component row-vectors whose i th components are x_i, z_i and u_i , respectively, for $i = 1, 2, \dots, k$, where x_i has one of the 16 possible values of s_i ,

$$z_i = \sum_{h=0}^n x_{i-h} y_h \quad (7)$$

and u_i is the possible value of w_i satisfying

$$r'_i = z_i + u_i \quad (8)$$

In the k -dimensional complex vector space containing the vectors R'_k, Z_k and U_k , the square of the 'unitary' distance between the vectors R'_k and Z_k is

$$|U_k|^2 = |u_1|^2 + |u_2|^2 + \dots + |u_k|^2 \quad (9)$$

where $|u_i|$ is the absolute value (modulus) of u_i .

When all real and imaginary components of the $\{w_i\}$ are statistically independent and with a fixed variance, the maximum-likelihood vector X_k is its possible value such that $|U_k|^2$ is minimized. Under the assumed conditions this X_k is the possible value of S_k most likely to be correct.

3 System A

The detection process used here is a modification of an arrangement previously¹³ referred to as System 2 and it operates as follows. Just prior to the receipt of the sample r'_k at the detector input, the detector holds in store m n -component vectors $\{Q_{k-1}\}$, where m is a multiple of 4,

$$Q_{k-1} = x_{k-n} x_{k-n+1} \dots x_{k-1} \quad (10)$$

and x_i is as previously defined. Each vector Q_{k-1} is associated with the corresponding cost $|U_{k-1}|^2$ (eqn. (9)), in the evaluation of which it is assumed that $s'_i = s_i$ for every i . This implies that the intersymbol interference canceller operates in the ideal manner and means, of course, that there is an inaccuracy in $|U_{k-1}|^2$ whenever one or more of the $\{s'_i\}$ are incorrect.

On the receipt of r'_k , each of the stored vectors $\{Q_{k-1}\}$ is expanded into four $(n+1)$ -component vectors $\{P_k\}$, where

$$P_k = x_{k-n} x_{k-n+1} \dots x_k \quad (11)$$

The first n components of P_k are as in the original vector Q_{k-1} and the last component x_k has the four different values $\pm 2 \pm 2j$. The cost associated with each vector P_k is evaluated as

$$c_k = |U_{k-1}|^2 + |r'_k - \sum_{h=0}^n x_{k-h} y_h|^2 \quad (12)$$

For each of the four possible values of x_k , the detector then selects the $\frac{1}{4}m$ vectors $\{P_k\}$ having the smallest costs

$\{c_k\}$, to give a total of m selected vectors together with their associated costs. Each selected vector \mathbf{P}_k is next expanded into four vectors $\{\mathbf{P}_k\}$ where the first n components are again as in the original vector \mathbf{Q}_{k-1} , and to the given value of the last component x_k (now $\pm 2 \pm 2j$) are added the four different values $\pm 1 \pm j$. The cost associated with each expanded vector is evaluated as

$$|U_k|^2 = |U_{k-1}|^2 + |r'_k - \sum_{b=0}^n x_{k-b} y_b|^2 \quad (13)$$

The detected data-symbol s'_{k-n} is then taken as the value of x_{k-n} in the vector \mathbf{P}_k with the smallest cost, and the first symbol x_{k-n} in each vector \mathbf{P}_k is discarded to give the corresponding vector \mathbf{Q}_k , which is, of course, associated with the same cost $|U_k|^2$. Finally, m vectors $\{\mathbf{Q}_k\}$ are selected from the $4m$ vectors $\{\mathbf{P}_k\}$, as follows. When $m = 32$, the detector selects, for each of the 16 possible values of x_k , the two vectors $\{\mathbf{Q}_k\}$ that have the smallest costs and differ in the value of x_{k-1} . When $m = 16$, the detector selects, for each of the 16 possible values of x_k , the vector \mathbf{Q}_k having the smallest cost. The selected vectors are now stored together with their associated costs. These arrangements can be implemented simply and ensure that all selected vectors are different, thus preventing any 'merging' of the stored vectors.¹³

The technique just described is an arrangement of 'double expansion' in which it is assumed that

$$x_k = x_{a,k} + x_{b,k} \quad (14)$$

where

$$x_{a,k} = \pm 2 \pm 2j \quad (15)$$

and

$$x_{b,k} = \pm 1 \pm j \quad (16)$$

so that x_k is treated as the sum of two separate 4-level data-symbols $x_{a,k}$ and $x_{b,k}$. In the expansion of the m stored vectors $\{\mathbf{Q}_{k-1}\}$, $x_{b,k}$ is set to zero so that x_k is treated as though it were $x_{a,k}$. In the expansion of the m selected vectors $\{\mathbf{P}_k\}$, x_k is taken as $x_{a,k} + x_{b,k}$, the value of $x_{a,k}$ for each vector being, of course, that determined in the first process of expansion and selection.

The arrangement relies on the fact that if some complex number q_k is at a smaller unitary distance from a given one of the 4 possible values of $x_{a,k}$ than from the 3 remaining possible values of $x_{a,k}$, then it is also at a smaller unitary distance from $x_{a,k} + x_{b,k}$, for the given $x_{a,k}$ and for one of the 4 possible values of $x_{b,k}$, than it is from the remaining 15 possible values of $x_{a,k} + x_{b,k}$. This implies that the possible value of x_k closest to q_k may be determined in two successive operations: first the selection of the possible value of $x_{a,k}$ closest to q_k , and then, for the selected value of $x_{a,k}$, the determination of the possible value of $x_{b,k}$ such that $x_{a,k} + x_{b,k}$ is closest to q_k .

4 System B

This is a development of an arrangement previously¹³ referred to as System 1 and it operates as follows. Just prior to the receipt of the sample r'_k at the detector input, the detector holds in store m n -component vectors $\{\mathbf{Q}_{k-1}\}$ together with the associated costs $\{|U_{k-1}|^2\}$ (eqns. (10) and (13)). On the receipt of r'_k the detector expands each vector \mathbf{Q}_{k-1} into the corresponding 16 vectors $\{\mathbf{P}_k\}$ (eqn. (11)) having the 16 possible values of x_k (given by $\pm \alpha \pm j\beta$, for $\alpha = 1$ or 3 and $\beta = 1$ or 3) and it evaluates the cost $|U_k|^2$ for each of the 16 vectors $\{\mathbf{P}_k\}$. It then selects the vector \mathbf{P}_k with the smallest cost and takes the detected data-symbol s'_{k-n} to have the value of x_{k-n} in the selected vector \mathbf{P}_k . All vectors $\{\mathbf{P}_k\}$ for which $x_{k-n} \neq s'_{k-n}$ are now discarded, and the first component of each of the remaining vectors $\{\mathbf{P}_k\}$ is omitted to give the corresponding n -component vectors $\{\mathbf{Q}_k\}$. The one of these vectors derived from the vector \mathbf{P}_k with the smallest cost $|U_k|^2$ is the first selected vector \mathbf{Q}_k . The detector then selects from the remaining vectors $\{\mathbf{Q}_k\}$ the $m-1$ vectors associated with the smallest costs, to give a total of m vectors $\{\mathbf{Q}_k\}$ and their associated costs, which are stored. The discarding of the given vectors $\{\mathbf{P}_k\}$ prevents the merging of the stored vectors, since it ensures that, if these are all different at the start of transmission, no two or more of them can subsequently become the same.

5 System C

The technique of double expansion, applied in System A, is here applied to System B, to give an arrangement involving less storage and a smaller number of operations in a detection process than does System B. Following the expansion of the m stored vectors $\{\mathbf{Q}_{k-1}\}$ into $4m$ vectors $\{\mathbf{P}_k\}$, for which $x_k = \pm 2 \pm 2j$, and the evaluation of the associated costs $\{c_k\}$, as in System A, the detector selects the m vectors $\{\mathbf{P}_k\}$ with the smallest costs, regardless of the values of any of their $\{x_i\}$. Following the expansion of the latter vectors into $4m$ vectors $\{\mathbf{P}_k\}$ and the evaluation of their costs $\{|U_k|^2\}$, again as in System A, the detector selects the vector \mathbf{P}_k with the smallest cost and takes the detected data-symbol s'_{k-n} to have the value of x_{k-n} in the selected vector \mathbf{P}_k . All vectors $\{\mathbf{P}_k\}$ for which $x_{k-n} \neq s'_{k-n}$ are now discarded, and the detection process proceeds as in System B.

6 System D

This is an alternative approach to that in System C towards reducing the amount of storage and the number of operations involved in a detection process of System B. On the receipt of r'_k the detector expands each of the m vectors $\{\mathbf{Q}_{k-1}\}$ into the corresponding four vectors $\{\mathbf{P}_k\}$, where x_k has the four values ± 1 and ± 3 , and the detector evaluates c_k (eqn. (12)) for each of the $4m$ vectors $\{\mathbf{P}_k\}$. The detector also expands each vector \mathbf{Q}_{k-1} into four vectors $\{\mathbf{P}_k\}$, where x_k has the four values

$\pm j$ and $\pm 3j$ ($j = \sqrt{-1}$), and again evaluates c_k for each vector \mathbf{P}_k . The detector then discards from each group of four vectors $\{\mathbf{P}_k\}$ (originating from a single vector \mathbf{Q}_{k-1} via either of the two expansion processes) the vector \mathbf{P}_k with the largest cost c_k , leaving three vectors in each group. Bearing in mind that $y_0 = 1$, this can be done very simply without in fact evaluating c_k for any vector \mathbf{P}_k , but using just the real and imaginary parts of the quantity

$$d_k = r'_k - \sum_{h=0}^n x_{k-h}v_h = \left(r'_k - \sum_{h=1}^n x_{k-h}v_h \right) - x_k \quad (17)$$

in equation (12), for the different possible values of x_k . Thus, from the values of d_k for the six vectors $\{\mathbf{P}_k\}$, in the two groups of three vectors originating from any single vector \mathbf{Q}_{k-1} , the resulting values of d_k for the nine vectors $\{\mathbf{P}_k\}$, given by all combinations of the three real and three imaginary values of x_k in the six vectors, are very easily evaluated, to give the corresponding costs $\{|\mathbf{U}_k|^2\}$ of the nine vectors, computed according to equation (13). x_k is, of course, complex valued in each of these vectors. The detector now has $9m$ vectors $\{\mathbf{P}_k\}$ together with the associated costs. The detector then determines s'_{k-n} from the value of x_{k-n} in the vector \mathbf{P}_k with the smallest cost, and the detection process proceeds exactly as for System B.

7 System E

This is a simple modification of System D in which each of the m stored vectors $\{\mathbf{Q}_{k-1}\}$ is expanded into four vectors $\{\mathbf{P}_k\}$, where x_k has the four values ± 1 and ± 3 , and also into four vectors $\{\mathbf{P}_k\}$, where x_k has the four values $\pm j$ and $\pm 3j$, exactly as before, but now the detector selects from each group of four vectors $\{\mathbf{P}_k\}$ the two vectors with the smallest costs $\{c_k\}$, the basic method of selection being that described for System D. From the four vectors $\{\mathbf{P}_k\}$ derived from any single vector \mathbf{Q}_{k-1} , x_k being real-valued in two of these and imaginary-valued in the other two, the detector forms the four vectors $\{\mathbf{P}_k\}$ having the complex-valued $\{x_k\}$ given by all combinations of the real and imaginary values of x_k in the original four vectors, and evaluates the associated costs $\{|\mathbf{U}_k|^2\}$. The detector now has $4m$ vectors $\{\mathbf{P}_k\}$ together with the associated costs, and proceeds with the detection of s_{k-n} and the selection of m vectors $\{\mathbf{Q}_k\}$ exactly as for System B.

8 System F

This is a simple modification of System E which operates exactly as does System E except that the detector derives only three (rather than four) vectors $\{\mathbf{P}_k\}$ with complex values for x_k , from any single vector \mathbf{Q}_{k-1} , the vectors $\{\mathbf{P}_k\}$ being those with the smallest costs $\{|\mathbf{U}_k|^2\}$ in the corresponding group of four vectors of System E. Again, the selection process for the $\{\mathbf{P}_k\}$ can be implemented very simply, without in fact evaluating the costs, which

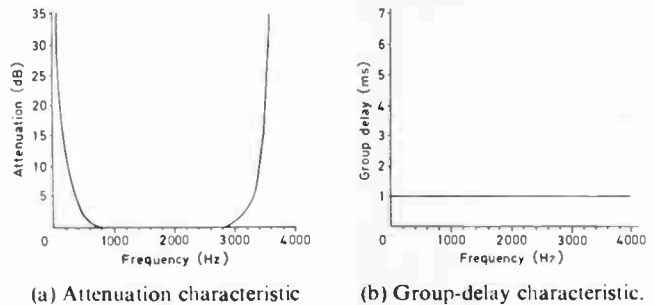


Fig. 3. Telephone-circuit 1.

are determined after the selection process. Thus the detector generates $3m$ vectors $\{\mathbf{P}_k\}$ together with the associated costs $\{|\mathbf{U}_k|^2\}$, and then proceeds with the detection of s_{k-n} and the selection of m vectors $\{\mathbf{Q}_k\}$, exactly as for System B.

9 Computer Simulation Tests

The tolerance to additive white Gaussian noise of the six systems A-F and of a conventional non-linear (decision-feedback) equalizer have been determined by computer simulation over models of four different telephone circuits, using the arrangements shown in Figs. 1 and 2 and described in Sections 1-8. In every case (including that of the equalizer) it is assumed that the adaptive linear filter has an appropriately large number of taps and is accurately adjusted to perform the ideal linear transformation described in Sections 1 and 2.

Figures 3-6 show the attenuation and group-delay characteristics of the four different telephone circuits

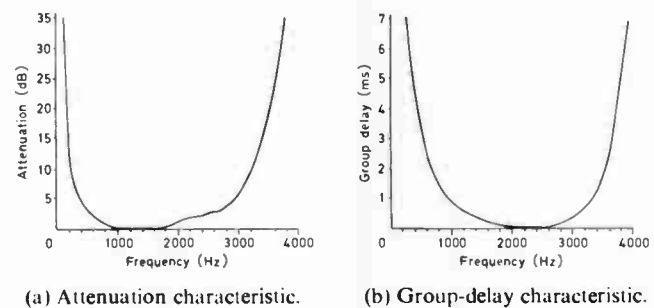


Fig. 4. Telephone-circuit 2.

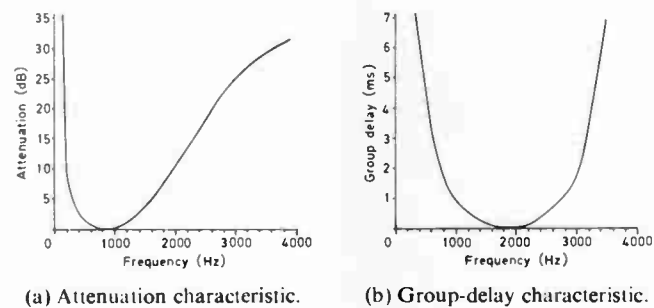


Fig. 5. Telephone-circuit 3.

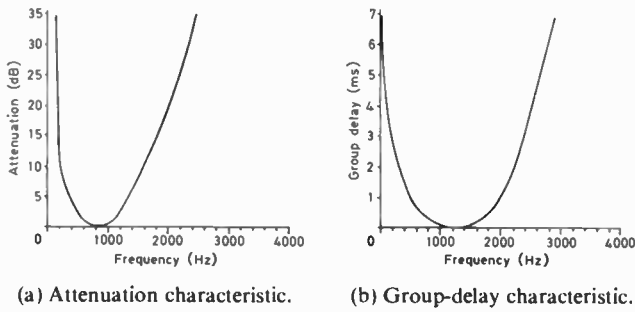


Fig. 6. Telephone-circuit 4.

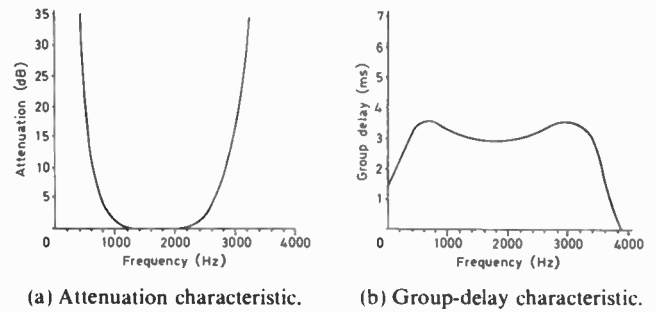


Fig. 7. Combination of transmitter and receiver filters.

used in the tests, the telephone circuit forming a part of the transmission path in Fig. 1. Figure 7 shows the resultant attenuation and group-delay characteristics of the equipment filters, these being here considered as operating on the transmitted bandpass signal, rather than on the baseband signals in the transmitter and receiver as shown in Fig. 1, to demonstrate more clearly the effects of the equipment filters in limiting some of the distortion introduced by the telephone circuit. The equipment filters are taken to include the filtering required to convert the sequence of impulses at the transmitter input (Fig. 1) into the corresponding

rectangular waveform used in an actual modem.

Table 1 shows the sampled impulse-response of the linear baseband channel, sampler and adaptive linear filter in Fig. 1, for each of the four different telephone circuits tested. This gives some idea of the resultant distortion introduced by each channel, bearing in mind that the ideal sampled impulse-response has the first component equal to unity and the remainder all zero. It can be seen from Figs. 3 and 7 that nearly all the signal distortion shown in Table 1 for the telephone circuit 1 is in fact introduced by the equipment filters. The telephone circuits 1 and 2 introduce negligible and

Table 1

Sampled impulse-response of baseband channel and adaptive linear filter in Fig. 1, for each of the four telephone circuits.

TELEPHONE CIRCUIT 1		TELEPHONE CIRCUIT 2		TELEPHONE CIRCUIT 3		TELEPHONE CIRCUIT 4	
REAL PART	IMAGINARY PART						
1.0000	0.0000	1.0000	0.0000	1.0000	0.0000	1.0000	0.0000
0.3412	0.0667	0.5091	0.1960	0.4861	1.0988	0.2544	1.9941
-0.1298	-0.0358	-0.1465	0.0000	-0.5980	0.0703	-1.7394	-0.2019
0.0263	0.0051	0.0323	-0.0171	0.1702	-0.1938	0.6795	-0.8086
0.0015	0.0008	0.0125	0.0200	-0.0245	0.1000	0.0408	0.5113
-0.0019	-0.0016	-0.0099	-0.0109	0.0100	-0.0258	-0.1189	-0.1463
-0.0017	0.0006	0.0046	0.0074	-0.0134	0.0110	0.0343	0.0420
-0.0011	-0.0004	-0.0069	-0.0083	0.0056	-0.0042	-0.0185	-0.0364
0.0018	0.0010	0.0059	0.0076	0.0003	0.0003	0.0139	0.0216
-0.0014	0.0000	-0.0025	-0.0053	-0.0008	0.0041	-0.0102	-0.0009
-0.0008	-0.0004	-0.0013	0.0040	0.0000	-0.0061	-0.0019	-0.0034
-0.0016	-0.0001	0.0024	-0.0028	0.0007	-0.0007	0.0037	-0.0046
-0.0006	0.0001	-0.0009	0.0018	0.0037	0.0002	-0.0028	-0.0006
-0.0006	0.0003	-0.0006	-0.0006	-0.0019	-0.0025	-0.0019	-0.0046
0.0005	-0.0001	0.0001	-0.0003	0.0020	0.0008	0.0083	0.0022
0.0000	0.0004	0.0002	0.0008	0.0005	-0.0002	-0.0056	0.0059
0.0002	-0.0003	0.0000	-0.0006	-0.0022	0.0002	-0.0046	-0.0028
-0.0004	0.0000	-0.0003	-0.0001	0.0007	-0.0005	0.0049	-0.0019
-0.0001	0.0002	-0.0002	0.0003	-0.0008	0.0002	-0.0009	0.0037
0.0004	-0.0001	0.0003	-0.0002	0.0005	0.0005	-0.0009	0.0003
0.0000	0.0000	0.0000	0.0000	0.0000	0.0000	0.0000	0.0000
0.0000	0.0000	0.0000	0.0000	0.0000	0.0000	0.0000	0.0000

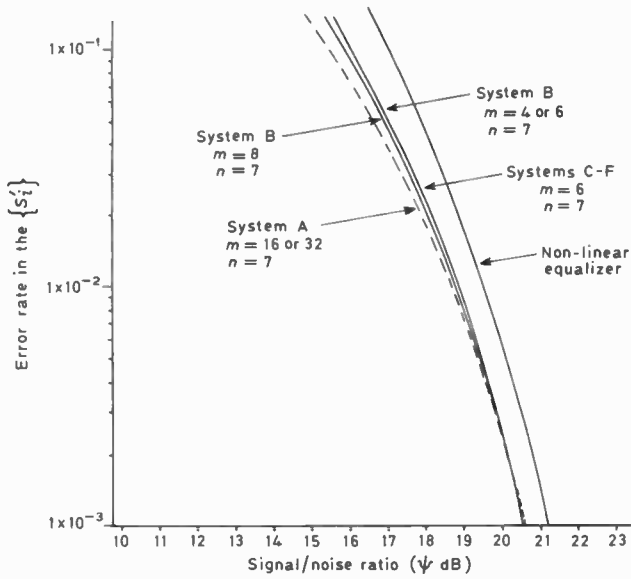
typical levels of distortion, respectively, whereas the circuits 3 and 4 are close to the typical worst circuits normally considered for the transmission of data at 9600 and 600-1200 bits/second, respectively. The telephone circuit 3, which is close to the Post Office network N6, introduces severe group-delay distortion as well as considerable attenuation distortion, and the telephone circuit 4, which is close to the Post Office network N3, introduces very severe attenuation distortion.

Figures 8(a)-(d) show the performances of Systems A-F and of a conventional non-linear equalizer, for the telephone circuits 1-4. The signal/noise ratio is taken to

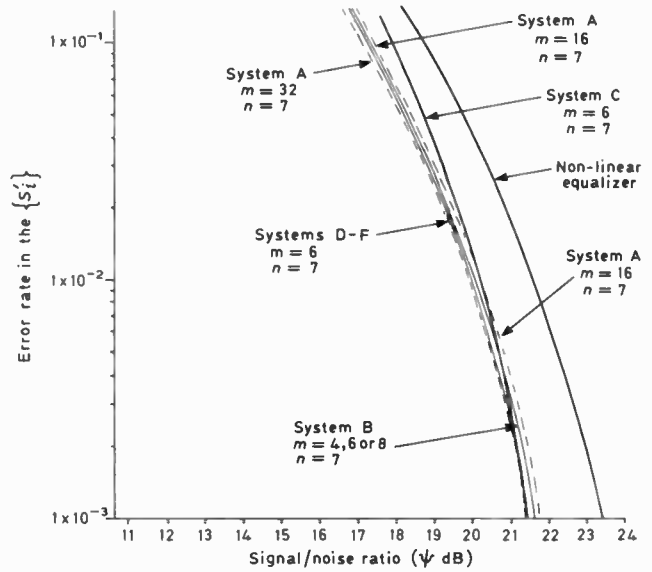
be ψ dB, where

$$\psi = 10 \log_{10} (E/\frac{1}{2}N_0) \quad (18)$$

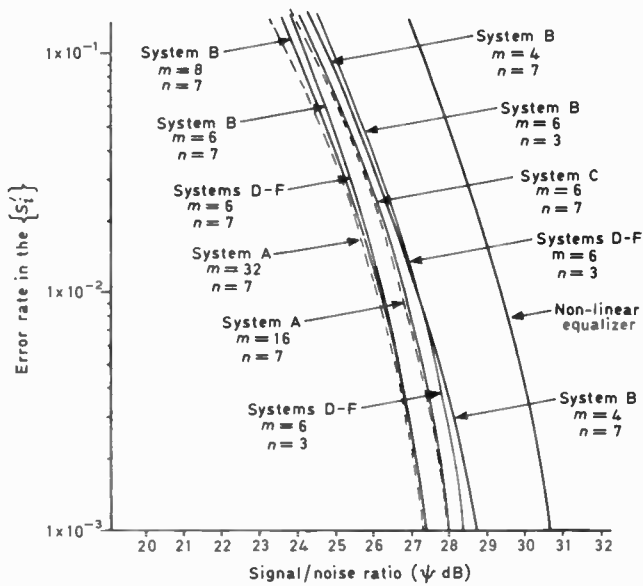
E is here the average transmitted energy per data-symbol s_i , at the input to the transmission path (Fig. 1), and $\frac{1}{2}N_0$ is the two-sided power spectral density of the additive white Gaussian noise at the input to the receiver filter. The 95% confidence limits of the curves in Fig. 8 are generally better than $\pm \frac{1}{2}$ dB. System A has been tested with both $m = 16$ and 32 and with $n = 7$, where m is the number of stored vectors $\{Q_k\}$ and n is the number of components in Q_k . Systems B-F have all been tested with



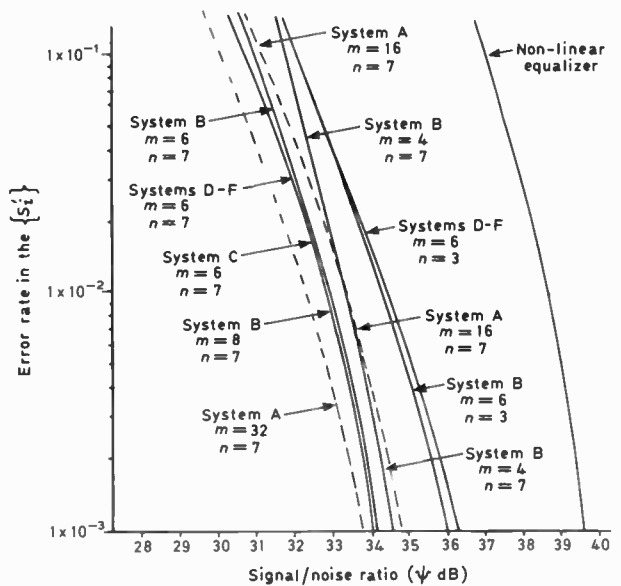
(a) Operating over telephone-circuit 1.



(b) Operating over telephone-circuit 2.



(c) Operating over telephone-circuit 3.



(d) Operating over telephone-circuit 4.

Fig. 8. Variation of error rate with signal/noise ratio for the different systems.

$m = 6$ and with both $n = 3$ and 7 . For the telephone circuits 3 and 4, System B has in addition been tested with both $m = 4$ and 8 and with $n = 7$.

The phase of the sampling instants $\{iT\}$ at the receiver has a much more significant effect on the tolerance to noise of the conventional equalizer than on that of any of the other systems tested. The sampling phase used over each channel has therefore been selected to give a good performance of the conventional equalizer, with a tolerance to noise within about $\frac{1}{2}$ dB of optimum, which is probably as good as would be achieved in practice.

It can be seen from Fig. 8 that the Systems A-F all have a much better overall tolerance to additive white Gaussian noise than the conventional non-linear equalizer. The System A with $m = 32$ (32 stored vectors) and $n = 7$ (a delay in detection of 7 sampling intervals) has the best performance of all systems tested, as would perhaps be expected, but when $m = 16$ and $n = 7$ its tolerance to noise at the lower error rates in the $\{s_{ii}'\}$ becomes inferior to that of the Systems B-F, with $m = 6$ and $n = 7$. The latter arrangements all have a similar

tolerance to noise at the lower error rates, this being significantly better than that with $m = 6$ and $n = 3$, over the telephone circuits 3 and 4. No very useful advantage in the tolerance to noise of the Systems B-F seems likely to be achieved by increasing m to a value greater than 6, but when m is reduced from 6 to 4 there is a noticeable degradation in performance. At error rates around 1 in 10^3 , the Systems B-F, with $m = 6$ and $n = 7$, have an advantage in tolerance to additive white Gaussian noise, over the non-linear equalizer, of approximately $\frac{1}{2}$, $1\frac{1}{2}$, 3 and $5\frac{1}{2}$ dB, for the telephone circuits 1, 2, 3 and 4, respectively.

Figure 9 shows the effects on the error rate in the $\{s_{ii}'\}$ of inaccuracies in the estimates made by the receiver of the level and carrier phase of the received signal, when System E with $m = 6$ and $n = 7$ operates over the telephone circuits 1-4. It can be seen that, over the telephone circuit 3, the system can tolerate an inaccuracy of about $\frac{1}{4}$ dB in the estimate of the received signal level or else an inaccuracy of about 2 degrees in the estimate of the received signal carrier phase, for an increase of two times in the error rate of the $\{s_{ii}'\}$, this representing a reduction of less than $\frac{1}{2}$ dB in tolerance to additive white Gaussian noise. It seems likely therefore that in a well-designed modem and with the correction of the more serious phase jitter in the received signal carrier, no very serious degradation in tolerance to additive noise should be experienced due to the inaccurate estimation of the received signal level or carrier phase.

10 Conclusions

Of the various arrangements tested, Systems E and F with $m = 6$ and $n = 7$ appear to be the most cost-effective. They promise to give a substantial improvement in tolerance to additive noise over the conventional non-linear equalizer, without involving a great increase in equipment complexity. Bearing in mind that the telephone circuit 4 is basically similar to the typical worst telephone circuit likely to be experienced over the switched telephone network in this country, it seems that so long as the accurate convergence of the adaptive linear filter can be achieved and appropriate steps are taken in the design of the modem to combat the effects of carrier-phase jitter, correct operation of the system should be obtained over nearly all circuits on the public switched telephone network.

11 Acknowledgment

The investigation has been sponsored by Plessey Telecommunications Ltd., Beeston, Nottingham, and the authors are grateful for their permission to publish this paper. The detection processes described in the paper are the subject of a British patent application.

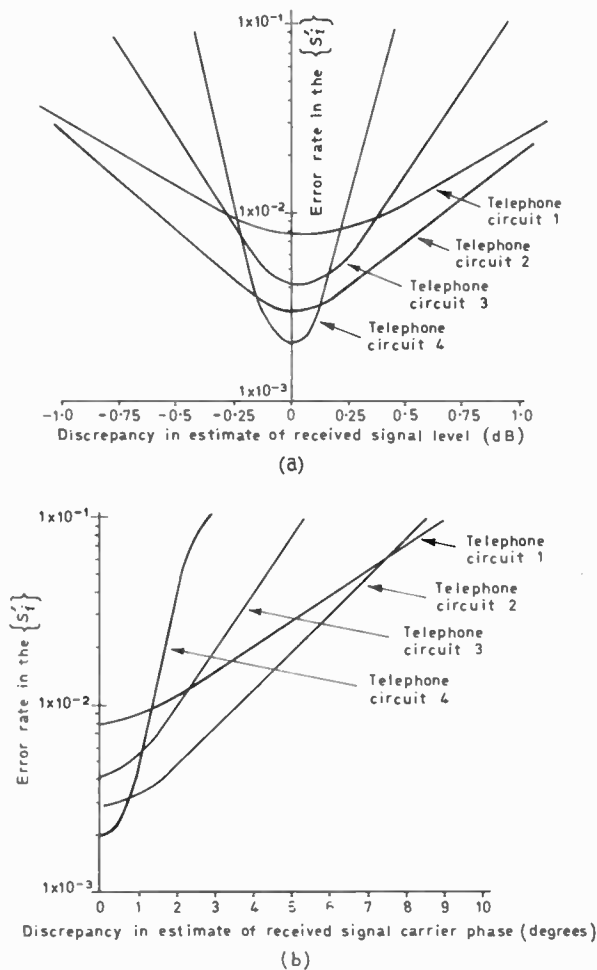


Fig. 9. Variation of error rate with an inaccuracy in the estimate made by the receiver of (a) the level and (b) the carrier phase of the received signal, for the System E with $m = 6$ and $n = 7$ operating over the telephone-circuits 1-4.

12 References

- 1 Clark, A. P., 'Principles of Digital Data Transmission' (Pentech Press, London, 1976).
- 2 Monsen, P., 'Feedback equalization of fading dispersive channels', *IEEE Trans. on Information Theory*, IT-17, pp. 56-64, January 1971.
- 3 Westcott, R. J., 'An experimental adaptively equalized modem for data transmission over the switched telephone network', *The Radio and Electronic Engineer*, 42, pp. 499-507, November 1972.
- 4 Clark, A. P. and Tint, U. S., 'Linear and non-linear transversal equalizers for baseband channels', *The Radio and Electronic Engineer*, 45, pp. 271-83, June 1975.
- 5 Clark, A. P., 'Advanced Data-Transmission Systems' (Pentech Press, London, 1977).
- 6 Forney, G. D., 'Maximum-likelihood sequence estimation of digital sequences in the presence of intersymbol interference', *IEEE Trans.*, IT-18, pp. 363-78, May 1972.
- 7 Forney, G. D., 'The Viterbi algorithm', *Proc. IEEE*, 61, pp. 268-78, March 1973.
- 8 Qureshi, S. U. H. and Newhall, E. E., 'An adaptive receiver for data transmission over time-dispersive channels', *IEEE Trans.*, IT-19, pp. 448-57, July 1973.
- 9 Falconer, D. D. and Magee, F. R., 'Adaptive channel memory truncation for maximum-likelihood sequence estimation', *Bell Syst. Tech. J.*, 52, pp. 1541-62, November 1973.
- 10 Cantoni, A. and Kwong, K., 'Further results on the Viterbi-algorithm equalizer', *IEEE Trans.*, IT 20, pp. 764-7, November 1974.
- 11 Desblache, A.E., 'Optimal short desired impulse response for maximum-likelihood sequence estimation', *IEEE Trans. on Communications*, COM-25, pp. 735-38, July 1977.
- 12 Foschini, G. J., 'A reduced state variant of maximum-likelihood sequence detection attaining optimum performance for high signal-to-noise ratios', *IEEE Trans.*, IT-23, pp. 605-9, September 1977.
- 13 Clark, A. P., Harvey, J. D. and Driscoll, J. P., 'Near-maximum-likelihood detection processes for distorted digital signals', *The Radio and Electronic Engineer*, 48, pp. 301-9, June 1978.
- 14 Clark, A. P., Kwong, C. P. and Harvey, J. D., 'Detection processes for severely distorted digital signals', *IEE J. Electronic Circuits and Systems*, 3, pp. 27-37, January 1979.
- 15 Magee, F. R. and Proakis, J. G., 'Adaptive maximum-likelihood sequence estimation for digital signalling in the presence of intersymbol interference', *IEEE Trans.*, IT-19, pp. 120-4, January 1973.
- 16 Clark, A. P., Kwong, C. P. and McVerry, F., 'Estimation of the sampled impulse-response of a channel', *Signal Processing*, 2, pp. 39-53, January 1980.
- 17 Clark, A. P. and Harvey, J. D., 'Detection of distorted q.a.m. signals', *IEE J. Electronic Circuits and Systems*, 1, pp. 103-9, April 1977.

*Manuscript first received by the Institution on 7th October 1980 and in final form on 10th February 1981
(Paper No. 2008/Comm 324)*

The Authors

Michael Fairfield received a B.Sc. in electrical and electronic engineering from Loughborough University of Technology in 1973. Subsequently he has been employed in research at the University, first as a student in the field of ultrasonic non-destructive testing and measurement, part of the work being submitted for a M.Sc. degree in 1976. This was followed by a single year's research contract studying the applications of ultrasonics to borehole rock structure analysis for the Department of Energy. Since 1977 Mr Fairfield has worked on research contracts for Plessey Telecommunications for the development and design of digital modems for data transmission over voice band circuits.



Adrian Clark (Member 1964) who graduated from the University of Cambridge in 1954, is now a Reader in the Department of Electronic and Electrical Engineering at Loughborough University of Technology. Before joining the University in 1970, Dr Clark spent 12 years in industry at Plessey Telecommunications Research, Taplow, working on various aspects of digital communication systems; this period was interrupted for three years when Dr Clark held an Industrial Fellowship at Imperial College, London, as a result of which he was awarded his doctorate. He has numerous papers in the Institution's Journal and conferences to his credit and has published two books on Data Transmission. Dr Clark is a member of the Communications Group Committee and has also served on conference organizing committees.



Contributors to this issue*

Robert Simpson obtained his B.Tech. and M.Sc. degrees from Loughborough University of Technology and his Ph.D. from the University of Salford. After working in industry for English Electric and B.A.C., he joined the staff of Preston Polytechnic where he is now Head of Systems and Instrumentation Division. He spent the 1979/80 academic year as visiting Professor at Oregon State University. Dr Simpson has written 25 technical papers and is co-author of a book on Dynamics and Control. His current research interests are digital control and digital signal processing.



Trevor Terrell studied at the Harris College (now Preston Polytechnic), obtaining an H.N.D. in electrical engineering in 1965, at the completion of a five-year engineering apprenticeship. From 1964 to 1967 he was employed as an engineer by the Post Office Engineering Department working on the design and implementation of telecommunication networks. In 1967 he joined Mullard Magnetic Components as an Electronic Development Engineer, working on the design and development of electronic measuring instruments and digital systems. Two years later he attended a one-year M.Sc. course in digital electronics at UMIST and obtained his degree in 1970. For the following two years he worked at UMIST on the design and implementation of a digital simulator for computer-controlled traffic studies, resulting in the award of a Ph.D. degree in 1972. In September 1973 Dr Terrell was appointed as a Lecturer in the Electrical Engineering Department of Preston Polytechnic, in 1974, he was promoted to Senior Lecturer and since September 1978 he has been Principal Lecturer. His research interests are microprocessor systems and digital signal processing. Dr Terrell has written more than a dozen papers and articles and is the author of a book on Digital Filters.



Mehdi Sarram graduated from Ayra-Mehra Technical University of Tehran in industrial engineering in 1974. The same year he was accepted for the M.Eng. Course in system test technology at the Dynamic Analysis Group at UWIST and was awarded the Ph.D. degree in January 1979. He is now working with Kaavian Heavy Rolling Mill in Ahwaz, Iran as automation engineer.



J. Hywel Williams is a Lecturer in Engineering Production and Deputy Head of the Dynamic Analysis Group at the University of Wales Institute of Science and Technology. Prior to joining UWIST he was a Development Engineer with Teddington Aircraft Controls, and B.S.A. Electrics. From 1971 to 1976 he was a Research Associate with the Dynamic Analysis Group sponsored by the Electrical Quality Directorate, Ministry of Defence, and he has continued as a consultant to MoD. He holds the degree of B.Sc.(Tech). in mathematics and obtained his Ph.D. from the University of Wales in 1977 on the topic of 'Probabilistic models for quality assurance'. Dr Williams was one of the architects in the setting up of the UWIST/Hoover Teaching Company Programme and is currently a member of the Management Committee which administers the Scheme.



Denis Towill (Fellow 1970) is Professor of Engineering Production and Head of the Dynamic Analysis Group at the University of Wales Institute of Science and Technology (UWIST), Cardiff. He holds the degree of B.Sc. (Eng.) from the University of Bristol, and the degrees of M.Sc. and D.Sc. from the University of Birmingham. Prior to taking up his present appointment he was a Senior Lecturer in Automatic Control at the Royal Military College of Science, a Consulting Engineer, and a Dynamic Analyst with the British Aircraft Corporation. He is the author of the textbook 'Transfer Function Techniques for Control Engineers' and the research monograph 'Coefficient Plane Models for Analysis and Design'. On six occasions he has been awarded IERE premiums for outstanding papers in the Journal. He has undertaken lecture tours in the United States and the Far East, and was recently commissioned to prepare a NATO AGARD-ograph on the Dynamic Testing of Avionic Systems.



Kadamula Varghese received his B.Sc. from Kerala University in 1971, and his M.Eng. degree in system test technology from the University of Wales Institute of Science and Technology (UWIST) in 1977. He obtained his Ph.D. from the University of Wales in 1981 for a thesis on 'Testing and fault location in analogue systems via pattern recognition techniques'. From 1971 to 1975 Mr Varghese was the head of the Department of Mathematics of a senior secondary school in Sierra Leone, West Africa. He joined the Dynamic Analysis Group, UWIST, in 1977 and was a member of the teaching staff in the Department of Mechanical Engineering and Engineering Production until September 1980. He is currently with Plessey Radar, Weybridge, Surrey.



*See also pages 434, 454 and 465.